

# Renormalization in Open Quantum Field theory I: Scalar field theory

---

Avinash<sup>a</sup>, Chandan Jana<sup>b</sup>, R. Loganayagam<sup>b</sup>, Arnab Rudra<sup>c</sup>

<sup>a</sup>*Indian Institute of Science,*

*C.V. Raman Avenue, Bangalore 560012, India.*

<sup>b</sup>*International Centre for Theoretical Sciences (ICTS-TIFR)*

*Shivakote, Hesarahatta Hobli, Bengaluru 560089, India.*

<sup>c</sup>*Center for Quantum Mathematics and Physics (QMAP)*

*Department of Physics, University of California, Davis, CA 95616 USA*

*E-mail: [baidyaavinash@gmail.com](mailto:baidyaavinash@gmail.com), [chandan.jana@icts.res.in](mailto:chandan.jana@icts.res.in),  
[nayagam@gmail.com](mailto:nayagam@gmail.com), [rudra.arnab@gmail.com](mailto:rudra.arnab@gmail.com)*

ABSTRACT: While the notion of open quantum systems is itself old, most of the existing studies deal with quantum mechanical systems rather than quantum field theories. After a brief review of field theoretical/path integral tools currently available to deal with open quantum field theories, we go on to apply these tools to an open version of  $\phi^3 + \phi^4$  theory in four spacetime dimensions and demonstrate its one loop renormalizability (including the renormalizability of the Lindblad structure).

---

# Contents

<b>1</b>	<b>Introduction and Motivation</b>	<b>1</b>
1.1	Basics of Schwinger-Keldysh theory	6
1.2	Basics of Lindblad theory and Effective theory	7
<b>2</b>	<b>Introduction to Open effective theory</b>	<b>9</b>
2.1	Lindblad condition	9
2.2	Exact propagators	11
2.3	Feynman rules	12
2.4	Lindblad condition from tree level correlators	13
<b>3</b>	<b>One loop beta function</b>	<b>14</b>
3.1	One loop beta function for $m^2$	15
3.2	One loop beta function for $m_\Delta^2$	18
3.3	Checking Lindblad condition for mass renormalization	18
3.4	One loop beta function for $\lambda_3$	19
3.5	One loop beta function for $\sigma_3$	20
3.6	Checking Lindblad condition at the level of cubic couplings	23
3.7	One loop beta function for $\lambda_4$	23
3.8	One loop beta function for $\sigma_4$	27
3.9	One loop beta function for $\lambda_\Delta$	27
3.10	Checking Lindblad condition for quartic couplings	29
3.11	Summary of the results	30
<b>4</b>	<b>Computation in the average-difference basis</b>	<b>31</b>
4.1	Action in the average-difference basis	31
4.2	One loop computations	32
4.3	Lindblad condition is never violated by perturbative corrections	34
<b>5</b>	<b>Running of the coupling constants and physical meaning</b>	<b>37</b>
5.1	Linearized analysis around the fixed point	39
5.2	Numerical analysis of RG equations	41
<b>6</b>	<b>Conclusion and Future directions</b>	<b>42</b>
<b>A</b>	<b>Notations and Conventions</b>	<b>47</b>
A.1	Most commonly used acronyms	47
A.2	Conventions for Feynman integrals	47

<b>B</b>	<b>Evaluating Passarino-Veltman Loop Integrals for open <math>\phi^3 + \phi^4</math> theory</b>	<b>50</b>
B.1	Passarino-Veltman $A$ type integrals	50
B.2	Integrals $B_{PM}(k)$ and $B_{MP}(k)$	51
B.3	Integrals $B_{PP}(k)$ and $B_{MM}(k)$	52
B.4	Reduction of divergent integrals to $B_{RP}(k)$	56
B.5	Evaluation of $B_{RP}(k)$	62
B.6	UV divergences and symmetry factors	65
<b>C</b>	<b>Passarino-Veltman diagrams in the average-difference basis</b>	<b>66</b>
C.1	Passarino-Veltman $A$ type integral in the average-difference basis	67
C.2	Passarino-Veltman $B$ type integral in the average-difference basis	67
<b>D</b>	<b>Computations in the average-difference basis</b>	<b>69</b>
D.1	Beta functions for the mass terms	70
D.2	Beta functions for the cubic couplings	72
D.3	Beta functions for the quartic couplings	75
<b>E</b>	<b>Tadpoles</b>	<b>78</b>
	<b>References</b>	<b>80</b>

---

## 1 Introduction and Motivation

Effective field theories are one of the great success stories of theoretical physics. From our understanding of elementary particles of the standard model to current cosmological models of evolution of the universe, from the theory of critical phenomena to polymer physics, the range and success of effective field theories is wide and diverse. The concept and the techniques of renormalisation, in particular have become textbook material and essential tools in the toolkit of many a theoretical physicist. Over the past few decades, String theory has further enriched this structure with its system of dualities, including the shocking suggestion that many theories of quantum gravity are really large  $N$  quantum field theories in disguise.

Despite all these successes, there are a variety of phenomena which still resist a clear understanding from the standard effective field theory viewpoint. A large class of them involve dissipation and information loss in evolution. It may be because the systems are open quantum systems in contact with an environment. Or the system might effectively behave like an open system because coarse-graining has traced out some degrees of freedom into which the system dissipates. To tackle these systems, one needs to develop a quantum field theory of *mixed states* where we can trace out degrees of freedom, run on a renormalisation flow and study dualities.

This is not a new question. Two of the founders of quantum field theory - Schwinger and Feynman addressed these questions early on and made seminal contributions to the quantum field theories of density matrices. These are the notions of a Schwinger-Keldysh path integral [1, 2] and the Feynman-Vernon influence functionals [3, 4] - the first addressing how to set up

the path-integral for unitary evolution of density matrices by doubling the fields and the second addressing how coarse-graining in a free theory leads to a density matrix path-integral with non-unitary evolution.

The third classic result in this direction is by Veltman who, in the quest to give diagrammatic proofs of Cutkosky's cutting rules [5], effectively reinvented the Schwinger-Keldysh path integral and proved that the corresponding correlators obey the largest time equation [6, 7]. The fourth important advance towards the effective theory of mixed states is the discovery of the quantum master equation by Gorini-Kossakowski-Sudarshan [8] and Lindblad [9]. The quantum master equation prescribes a specific form for the Feynman-Vernon influence functional [3, 4] using the constraints that evolution should preserve the trace of the density matrix (trace-preserving) as well as keep the eigenvalues of the density matrix stably non-negative (complete positivity). We will review these ideas and their inter-relations in due turn. Our goal here is to construct a simple relativistic field theory which elucidates these ideas.

Before we move on to the subject of the paper, let us remind the reader of the broader motivations which drive this work. First of all, the theory of open quantum systems is a field with many recent advancements and is of experimental relevance to fields like quantum optics, cold atom physics, non-equilibrium driven systems and quantum information. (See [10–14] for textbook treatments of the subject.) It makes logical sense to test these ideas against relativistic QFTs and how they change under Wilsonian renormalisation.<sup>1</sup> Second, open relativistic QFTs are very relevant by themselves in heavy ion physics and cosmology [17–20]. Third motivation is to better understand the apparently non-unitary evolution engendered by black holes and to give a quantitative characterization of the information loss. In particular, AdS/CFT suggests that exterior of black holes is naturally dual to open conformal field theories. Hence, it is reasonable to expect that developing the theory of open conformal field theories would tell us how to think about horizons in quantum gravity.

In this work, we take a modest step towards answering these questions by setting up and studying the simplest looking open quantum field theory : the open version of scalar  $\phi^3 + \phi^4$  in  $d = 4$  space-time dimensions. One can characterise the effective theory of density matrix of  $\phi^3 + \phi^4$  theory by a Schwinger-Keldysh (SK) effective action. This action involves the ket field  $\phi_R$  as well as the bra field  $\phi_L$  describing the two side evolution of the density matrix. It takes the form

$$\begin{aligned}
S_\phi = & - \int d^d x \left[ \frac{1}{2} z (\partial\phi_R)^2 + \frac{1}{2} m^2 \phi_R^2 + \frac{\lambda_3}{3!} \phi_R^3 + \frac{\lambda_4}{4!} \phi_R^4 + \frac{\sigma_3}{2!} \phi_R^2 \phi_L + \frac{\sigma_4}{3!} \phi_R^3 \phi_L \right] \\
& + \int d^d x \left[ \frac{1}{2} z^* (\partial\phi_L)^2 + \frac{1}{2} m^{2*} \phi_L^2 + \frac{\lambda_3^*}{3!} \phi_L^3 + \frac{\lambda_4^*}{4!} \phi_L^4 + \frac{\sigma_3^*}{2!} \phi_L^2 \phi_R + \frac{\sigma_4^*}{3!} \phi_L^3 \phi_R \right] \\
& + i \int d^d x \left[ z_\Delta (\partial\phi_R) \cdot (\partial\phi_L) + m_\Delta^2 \phi_R \phi_L + \frac{\lambda_\Delta}{2!2!} \phi_R^2 \phi_L^2 \right]
\end{aligned} \tag{1.1}$$

---

<sup>1</sup>We should mention that in the non-relativistic context, various interacting models and their 1-loop renormalisation have already been studied. We will refer the reader to chapter 8 of [15] for textbook examples of 1-loop renormalisation in non-relativistic non-unitary QFTs. The examples include Hohenberg-Halperin classification of dynamics near classical critical points, reaction diffusion models, their critical behavior/scaling and surface growth models including the famous KPZ equations. A more detailed exposition is available in [16].

This is the most general local, power-counting renormalisable, Lorentz invariant and CPT invariant action that could be written down involving  $\phi_R$  and  $\phi_L$ . Note that CPT acts as an anti-linear, anti-unitary symmetry exchanging  $\phi_R$  and  $\phi_L$  and taking  $i \mapsto (-i)$ . It can be easily checked that, under this anti-linear, anti-unitary flip  $e^{iS}$  remains invariant provided the couplings appearing in the last line of action  $\{z_\Delta, m_\Delta^2, \lambda_\Delta\}$  are real. This action along with a future boundary condition identifying  $\phi_R$  and  $\phi_L$  at future infinity defines the SK effective theory which we will study in this paper.

There are two features of the above action which makes it distinct from the SK effective action of the unitary  $\phi^3 + \phi^4$  theory. First, there are interaction terms which couple the ket field  $\phi_R$  with the bra field  $\phi_L$ . Such cross couplings necessarily violate unitarity and indicate the breakdown of the usual Cutkosky cutting rules. They are also necessarily a part of ‘influence functionals’ as defined by Feynman and Vernon and are generated only when a part of the system is traced out [3, 4]. A more obvious way the above action violates unitarity is due to the fact that  $S$  is not purely real. If we turn off all cross couplings between  $\phi_R$  and  $\phi_L$  and set to zero all imaginary couplings in  $S$ , we recover the SK effective action of the unitary  $\phi^4$  theory :

$$S_{\phi, \text{Unitary}} = - \int d^d x \left[ \frac{1}{2} z (\partial \phi_R)^2 + \frac{1}{2} m^2 \phi_R^2 + \frac{\lambda_3}{3!} \phi_R^3 + \frac{\lambda_4}{4!} \phi_R^4 \right] + \int d^d x \left[ \frac{1}{2} z (\partial \phi_L)^2 + \frac{1}{2} m^2 \phi_L^2 + \frac{\lambda_3}{3!} \phi_L^3 + \frac{\lambda_4}{4!} \phi_L^4 \right] \quad (1.2)$$

where all couplings are taken to be real. Our aim is to deform  $\phi^4$  theory away from this familiar unitary limit and study the theory defined in (1.1) via perturbation theory.

The first question one could ask is whether this theory is renormalisable in perturbation theory, i.e., whether, away from unitary limit, the one-loop divergences in this theory can be absorbed into counter terms of the same form. We answer this in affirmative in this work and compute the 1-loop beta functions to be

$$\begin{aligned} \frac{dm^2}{d \ln \mu} &= \frac{1}{(4\pi)^2} (\lambda_3 + \sigma_3^*) (\lambda_3 + 2\sigma_3 - \sigma_3^*) + \frac{m^2}{(4\pi)^2} \left[ \lambda_4 + 2\sigma_4 - i\lambda_\Delta \right] \\ \frac{dm_\Delta^2}{d \ln \mu} &= -\frac{4}{(4\pi)^2} \text{Im } \sigma_3 (\text{Re } \lambda_3 + \text{Re } \sigma_3) + \frac{2}{(4\pi)^2} \text{Re} \left[ m^2 (\lambda_\Delta + i\sigma_4) \right] \end{aligned} \quad (1.3)$$

for the mass terms,

$$\begin{aligned} \frac{d\lambda_3}{d \ln \mu} &= \frac{3}{(4\pi)^2} \left[ \lambda_4 (\lambda_3 + \sigma_3) + \sigma_4 (\lambda_3 + \sigma_3^*) + i\lambda_\Delta (\sigma_3 - \sigma_3^*) \right] \\ \frac{d\sigma_3}{d \ln \mu} &= \frac{1}{(4\pi)^2} \left[ (\lambda_4 + 2\sigma_4^*) (\sigma_3 - \sigma_3^*) + \sigma_4 (\lambda_3^* + 2\lambda_3 + 3\sigma_3) - i\lambda_\Delta (\lambda_3^* + 2\lambda_3 + 3\sigma_3^*) \right] \end{aligned} \quad (1.4)$$

for the cubic couplings, and

$$\begin{aligned} \frac{d\lambda_4}{d \ln \mu} &= \frac{3}{(4\pi)^2} (\lambda_4 + 2\sigma_4 - i\lambda_\Delta) (\lambda_4 + i\lambda_\Delta) \\ \frac{d\sigma_4}{d \ln \mu} &= \frac{3}{(4\pi)^2} (\lambda_4 + \sigma_4 + \sigma_4^* + i\lambda_\Delta) (\sigma_4 - i\lambda_\Delta) \\ \frac{d\lambda_\Delta}{d \ln \mu} &= \frac{1}{(4\pi)^2} i \left[ (\lambda_4 + 2\sigma_4^*) (\sigma_4^* + i\lambda_\Delta) + 3i\sigma_4 \lambda_\Delta - c.c. \right] \end{aligned} \quad (1.5)$$

for the quartic couplings. Note that at 1-loop level we can set  $z = 1$  and  $z_\Delta = 0$  since there is no field renormalisation. These equations constitute the central result of this paper.

The above set of  $\beta$  functions have a remarkable property which is made evident by deriving the 1-loop renormalisation running of certain combinations of couplings :

$$\begin{aligned}
\frac{d}{d \ln \mu} (\text{Im } m^2 - m_\Delta^2) &= \frac{2}{(4\pi)^2} \left[ (\text{Im } \lambda_3 + 3 \text{Im } \sigma_3)(\text{Re } \lambda_3 + \text{Re } \sigma_3) \right. \\
&\quad \left. + (\text{Im } \lambda_4 + 4 \text{Im } \sigma_4 - 3\lambda_\Delta)(\text{Re } m^2) \right] \\
\frac{d}{d \ln \mu} (\text{Im } \lambda_3 + 3 \text{Im } \sigma_3) &= \frac{3}{(4\pi)^2} \left[ (\text{Re } \lambda_4 + 2 \text{Re } \sigma_4)(\text{Im } \lambda_3 + 3 \text{Im } \sigma_3) \right. \\
&\quad \left. + (\text{Re } \lambda_3 + \text{Re } \sigma_3)(\text{Im } \lambda_4 + 4 \text{Im } \sigma_4 - 3\lambda_\Delta) \right] \\
\frac{d}{d \ln \mu} (\text{Im } \lambda_4 + 4 \text{Im } \sigma_4 - 3\lambda_\Delta) &= \frac{6}{(4\pi)^2} (\text{Im } \lambda_4 + 4 \text{Im } \sigma_4 - 3\lambda_\Delta)(\text{Re } \lambda_4 + 2 \text{Re } \sigma_4)
\end{aligned} \tag{1.6}$$

These equations show that the conditions

$$\text{Im } z - z_\Delta = 0, \quad \text{Im } m^2 - m_\Delta^2 = 0, \quad \text{Im } \lambda_3 + 3 \text{Im } \sigma_3 = 0, \quad \text{Im } \lambda_4 + 4 \text{Im } \sigma_4 - 3\lambda_\Delta = 0, \tag{1.7}$$

are preserved under renormalisation! We will prove a non-renormalisation theorem at all orders in perturbation theory to prove that the above conditions are never corrected at any order in loops. One can think of this as violating Gell-Mann's totalitarian principle [21] that "Everything not forbidden is compulsory" (or as there being new principles in open quantum field theory which forbid some combinations from appearing in perturbation theory). This kind of fine-tuning of couplings which are still protected under renormalisation is a hallmark of open quantum field theories and is a signature of microscopic unitarity [22].

We will now move to briefly describe the significance of the above conditions. We will give three related derivations of the conditions above in this work:

1. In the Schwinger-Keldysh formalism, the microscopic unitarity demands that difference operators (i.e., operators of the form  $O_R - O_L$ ) have trivial correlators. This, as a statement about correlation functions, should hold even in the coarse-grained open effective field theory. The decoupling of difference operators then naturally lead to the conditions above.
2. Relatedly, while the open EFT is non-unitary, one can demand that a certain weaker version of Veltman's largest time equation be obeyed. This then leads to the conditions above.
3. The trace preserving and the complete positivity of the evolution demands that the Feynman-Vernon influence functional be of the Lindblad form. Insisting that the dynamics of the open EFT be of the Lindblad form naturally leads to the conditions above.

Thus, a certain weak form of unitarity still holds in the open EFT and is explicitly realized by the conditions above. And once these conditions are satisfied, the structure is robust against perturbative renormalisation.

There is a fourth way of deriving the same conditions, whose deeper significance we will leave for our future work. Say one adds to the above action for the open EFT two Grassmann odd ghost fields  $g$  and  $\bar{g}$  and demand that the following Grassmann odd symmetry hold for the entire theory :

$$\delta\phi_R = \delta\phi_L = \bar{\epsilon}g + \epsilon\bar{g} , \quad \delta g = \epsilon(\phi_R - \phi_L) , \quad \delta\bar{g} = -\bar{\epsilon}(\phi_R - \phi_L) . \quad (1.8)$$

This symmetry then fixes the  $\phi$  self-couplings to obey equation (1.7). Further, the ghost action is completely fixed to be

$$S_g = - \int d^d x \left[ z_g (\partial\bar{g}) \cdot (\partial g) + \left( m_g^2 + \mathcal{Y}_3\phi_R + \mathcal{Y}_3^*\phi_L + \frac{1}{2!}(\mathcal{Y}_4\phi_R^2 + \mathcal{Y}_\Delta\phi_R\phi_L + \mathcal{Y}_4^*\phi_L^2) \right) \bar{g}g \right] \quad (1.9)$$

where

$$\begin{aligned} z_g &= \text{Re } z , & m_g^2 &= \text{Re } m^2 , \\ \mathcal{Y}_3 &= \frac{1}{3}(\text{Re } \lambda_3 + \text{Re } \sigma_3) + \frac{i}{4}(\text{Im } \lambda_3 - \text{Im } \sigma_3) , \\ \mathcal{Y}_4 &= \frac{1}{3}(\text{Re } \lambda_4 + \text{Re } \sigma_4) + \frac{i}{4}(\text{Im } \lambda_4 + \lambda_\Delta) , \\ \mathcal{Y}_\Delta &= \frac{1}{3}(\text{Re } \lambda_4 + 4 \text{Re } \sigma_4) \end{aligned} \quad (1.10)$$

If the boundary conditions/initial states are chosen such that the ghosts do not propagate, our computations of the beta functions still hold. We will leave a detailed examination of these issues to the future work. We will also not address in this work various other crucial questions on the derivation of a open EFT : first is the problem of infrared divergences in the unitary theory which need to be tackled correctly to yield a sensible open EFT. Second is the related question of the appropriate initial states and dealing with various transient effects. The third question we will comment on but leave out a detailed discussion of, is the modification of the cutting rules in the open EFT. We hope to return to these questions in the future.

**Organization of the paper** The rest of the paper is organized as follows. In the rest of the introduction, we will very briefly review the relevant background for our work. This includes the concepts of Schwinger-Keldysh path integrals, their relation to Veltman's cutting rules, Feynman-Vernon influence functionals for open EFTs and the Lindblad form for the evolution. The readers who are familiar with these concepts are encouraged to skim through these subsections in order to familiarize themselves with our notation.

In section 2 we will write down the action for the open EFT and set up the propagators and Feynman rules. We will also discuss the conditions under which the evolution density matrix of the theory is of Lindblad form. In section 3 we compute the one loop beta function for various coupling constants. The result of the section is summarized in 3.11. In section 4, we rewrite the theory in average-difference basis and we illustrate the great simplification that happens in this basis. The details of the computation in this basis can be found in appendix D. In section 4.3, we present a proof that the Lindblad condition is never violated under perturbative corrections. Section 6 consists of the conclusion of our analysis and various future directions. Appendix A describes some of our notations and conventions. Computation of the various one

loop Passarino-Veltman integrals required for open EFT can be found in appendix B and in appendix C.

### 1.1 Basics of Schwinger-Keldysh theory

The Schwinger-Keldysh(SK) path integrals have been reviewed in [15, 20, 23–26]. Here we will mention some key features : given a unitary QFT and a initial density matrix  $\rho(t = t_i) = \rho_i$ , we define the SK path integral via

$$\mathcal{Z}_{SK}[J_R, J_L] \equiv \text{Tr} \left\{ U[J_R] \rho_i (U[J_L])^\dagger \right\} \quad (1.11)$$

Here,  $U[J]$  is the unitary evolution operator of the quantum field theory deformed by sources  $J$  for some operators of the theory. This path integral is a generator of all correlation functions with at most one time-ordering violation. This should be contrasted with the Feynman path-integral which can compute only completely time-ordered correlators.

One could in principle consider the generating functions for correlators with arbitrary number of time-ordering violations [27] (for example, the correlator used to obtain the Lyapunov exponent involves two time-ordering violations [28]) but, in this work, we will limit ourselves to just the usual SK path-integral. The Schwinger-Keldysh path integral gives a convenient way to access the evolution of the most general mixed state in quantum field theory including the real time dynamics at finite temperature. It is an essential tool in the non-equilibrium description of QFTs which is directly defined in Lorentzian signature without any need for analytic continuation from the Euclidean description.

Given an action  $S[\phi, J]$  of the unitary QFT, we can give a path-integral representation of  $\mathcal{Z}_{SK}[J_R, J_L]$  by introducing a ket field  $\phi_R$  and a bra field  $\phi_L$  :

$$\mathcal{Z}_{SK}[J_R, J_L] \equiv \int_{\rho_i(\phi_R, \phi_L)}^{\phi_R(t=\infty)=\phi_L(t=\infty)} [d\phi_R][d\phi_L] e^{iS[\phi_R, J_R] - iS[\phi_L, J_L]} \quad (1.12)$$

The lower limit is the statement that near  $t = t_i$  the boundary condition for the path-integral is weighed by the initial density matrix  $\rho_i$ . The upper limit is the statement that the bra and the ket fields should be set equal at far future and summed over in order to correctly reproduce the trace. The factors  $e^{iS[\phi_R, J_R]}$  and  $e^{-iS[\phi_L, J_L]}$  correctly reproduce the evolution operators  $U[J_R]$  and  $(U[J_L])^\dagger$  respectively.

If the unitary QFT is in a perturbative regime, the above path integral can be used to set up the Feynman rules [15, 23].

1. In a unitary QFT, there are no vertices coupling the bra and the ket fields. The bra vertices are complex conjugates of ket vertices.
2. The ket propagator is time-ordered while the bra propagator is anti-time-ordered. In addition to these, SK boundary conditions also induce a bra-ket propagator which is the on-shell propagator (obtained by putting the exchanged particle on-shell). We will term these propagators as *cut propagators*. The terminology here is borrowed from the discussion of Cutkosky cutting rules where one thinks of the dividing lines between the bra and ket parts of the diagram as a ‘cut’ of the diagram where particles go on-shell.



We will call these rules as Veltman rules after Veltman who re-derived these rules in his study of unitarity [6, 7]. To reiterate, a fundamental feature of Veltman rules is the fact that in a unitary theory, bra and ket fields talk only via cut propagators but not via cut vertices. As we will see in the following, this ceases to be true in an open QFT where, as Feynman and Vernon [3, 4] showed, there are novel cut vertices which signal non-unitarity.

One of the fundamental features of the Veltman rules is a statement called the largest time equation which is fundamental to Veltman’s approach to proving perturbative unitarity and cutting rules. The largest time equation is a direct consequence of the definition of SK path integral in equation (1.11) as reviewed in [24]. We will briefly summarise below the argument for the largest time equation and its relation to SK formalism. We will refer the reader to [29] or [24] for more details.

In the SK path integral, consider the case where the sources obey  $J_R = J_L = J(x)$  beyond a particular point of time  $t = t_f$ . One can then argue that the path-integral is in fact independent of the source  $J(x)$  in the future of  $t_f$ . This follows from unitarity : the contributions of  $U[J_R]$  and  $U[J_L]^\dagger$  have to cancel each other in  $\mathcal{Z}_{SK}$  if  $J_R = J_L$  by unitarity.

To convert the above observation into a statement about correlators, we begin by noting that the source  $J(x)$  couples to difference operators  $O_R - O_L$  in the SK path integral. If we differentiate the path-integral (1.12) with respect to the common source  $J(x)$ , it follows that one is basically computing a correlator with the difference operators  $O_R - O_L$  placed in the future of  $t_f$ . The independence of  $\mathcal{Z}_{SK}$  on  $J(x)$  then implies the vanishing of the correlators with the future-most (or the largest time) operators as difference operators  $O_R - O_L$ .

Microscopic unitarity thus requires that correlators of purely difference operators are trivial and any macroscopic open EFT should faithfully reproduce this condition. One of the main motivations of this work is to understand how these conditions get renormalized and the relation of these conditions to the Lindbladian form studied in open quantum system context.

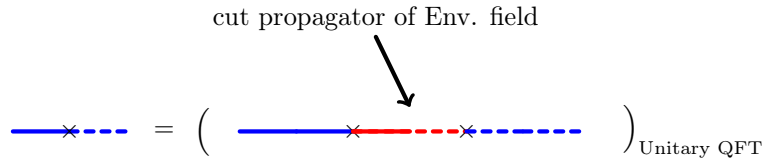
## 1.2 Basics of Lindblad theory and Effective theory

Following Feynman-Vernon [3, 4], we can integrate out the ‘environment’ fields in the Schwinger-Keldysh path integral and obtain an effective path integral for the quantum system under question. This inevitably induces a coupling between the bra and ket fields (called Feynman-Vernon(FV) coupling in the following) as shown schematically in the figure 1. Here the red-line represents the ‘environment’ fields of Feynman-Vernon which couples to the system field via a linear coupling. These ‘environment’ fields when traced/integrated out induce the unitarity violating FV coupling for the fields describing the open quantum field theory.

Note that the propagator that induces FV coupling is necessarily a cut propagator of the environment which means that the FV coupling is only induced in the regime where the ‘environment’ fields go on-shell. This also explains why, in usual QFT where we integrate out heavy fields that can never go on-shell in vacuum, no FV coupling or effective non-unitarity is induced by Wilsonian RG.<sup>2</sup> We will assume that the open QFT that we are studying in this paper arises from some hitherto unspecified microscopic theory à la Feynman-Vernon.

---

<sup>2</sup>Note that this is true about dilute states which are near vacuum state. A counterexample is at finite temperature where thermal fluctuations of the environment can and do contribute to the influence functional.



**Figure 1:** Feynman-Vernon vertex of an open QFT

The FV couplings induced by integrating out environment fields need not always be local. A local description for the resultant open QFT is often accomplished by working with a limit where the time scales in the environment are assumed to be very fast compared to the rate at which the information flows from the system to the environment. In this approximation (often termed Born-Markov approximation), one expects a nice local non-unitary EFT and our intent here is to study renormalisation in such an EFT. In the context of open quantum mechanical systems, under a clear separation of timescales, one can derive the Lindblad equation (or the quantum master equation) [8–10] for the reduced density matrix of the form

$$i\hbar \frac{d\rho}{dt} = [H, \rho] + i \sum_{\alpha, \beta} \Gamma_{\alpha\beta} \left( L_{\beta} \rho L_{\alpha}^{\dagger} - \frac{1}{2} L_{\alpha}^{\dagger} L_{\beta} \rho - \frac{1}{2} \rho L_{\alpha}^{\dagger} L_{\beta} \right). \quad (1.13)$$

Here,  $H$  is the Hamiltonian of the system leading to the unitary part of the evolution, whereas the non-unitary (Feynman-Vernon) part of the evolution comes from rest of the terms in RHS. The non-unitarity is captured by a set of operators  $L_{\alpha}$  and a set of couplings  $\Gamma_{\alpha\beta}$  of the system. It is easily checked that the form above implies

$$\frac{d}{dt} \text{tr} \rho = 0 \quad ,$$

i.e., it is trace-preserving. Further, if  $\Gamma_{\alpha\beta}$  is a positive matrix, one can show that the above equation describes a dissipative system which keeps the eigenvalues of  $\rho$  non-negative. These two properties (along with linearity in  $\rho$ ) qualify Lindblad form of evolution as a physically sensible dynamics describing an open quantum system. The above equation in Schrödinger picture has an equivalent Heisenberg picture description via an evolution equation for operators :

$$i\hbar \frac{d\mathcal{A}}{dt} = [\mathcal{A}, H] + i \sum_{\alpha, \beta} \Gamma_{\alpha\beta} \left( L_{\alpha}^{\dagger} \mathcal{A} L_{\beta} - \frac{1}{2} L_{\alpha}^{\dagger} L_{\beta} \mathcal{A} - \frac{1}{2} \mathcal{A} L_{\alpha}^{\dagger} L_{\beta} \right). \quad (1.14)$$

Equivalently, one can obtain a path-integral description by adding to the Schwinger-Keldysh action of the system, an influence functional term of the form [26]

$$S_{FV} = i \int \sum_{\alpha, \beta} \Gamma_{\alpha\beta} \left( L_{\alpha}^{\dagger}[\phi_R] L_{\beta}[\phi_L] - \frac{1}{2} L_{\alpha}^{\dagger}[\phi_R] L_{\beta}[\phi_R] - \frac{1}{2} L_{\alpha}^{\dagger}[\phi_L] L_{\beta}[\phi_L] \right) \quad (1.15)$$

where we have indicated the way the action should be written in terms of the bra and ket fields in order to correctly reproduce Lindblad dynamics. We note that the Lindblad form of

the influence functional has a particular structure which relates the  $\phi_R$ - $\phi_L$  cross-terms with the imaginary parts of both the  $\phi_R$  action and  $\phi_L$  action.

Let us note some important features of the above expression. If we set  $\phi_R = \phi_L$  in the action above, it vanishes. It is clear that this is exactly the calculation done few lines above in the Schrödinger picture to show that Lindblad evolution is trace-preserving. This is also related to the difference operator decoupling mentioned in the last subsection in the context of Schwinger-Keldysh path integrals. Thus, trace preserving property in the Schrödinger picture becomes difference operator decoupling at the level of SK path integral for the EFT.

We also note that if we take one of the Lindblad operators say  $L_\beta$  to be an identity operator, the Lindblad form then becomes a difference operator, i.e., it can be written as a difference between an operator made of ket fields and the same operator evaluated over the bra fields. This is the form of SK action for a unitary QFT (c.f. equation (1.12)) and it merely shifts the system action. But when both Lindblad operators are not identity, one gets various cross terms and associated imaginary contributions to the pure  $\phi_R$  and the pure  $\phi_L$  action. Thus, once the cross couplings are determined, one can use the Lindblad form to determine all imaginary couplings. This is the route we will take to write down the Lindblad conditions like the ones in equation (1.7).

Having finished this brief review of the necessary ideas, let us turn to the open  $\phi^4$  theory whose renormalisation we want to study. We will begin by describing in detail the effective action and the associated Feynman rules in the next section.

## 2 Introduction to Open effective theory

Let us begin by writing down the action for the most general open quantum field theory, consisting of a real scalar which can interact via cubic and quartic interactions, given in (2.1). The most general action, taking into account CPT symmetry (See for example, [24]) and SK boundary conditions, is given by

$$\begin{aligned}
S = & - \int d^d x \left[ \frac{1}{2} z (\partial \phi_R)^2 + \frac{1}{2} m^2 \phi_R^2 + \frac{\lambda_4}{4!} \phi_R^4 + \frac{\sigma_4}{3!} \phi_R^3 \phi_L \right] \\
& + \int d^d x \left[ \frac{1}{2} z^* (\partial \phi_L)^2 + \frac{1}{2} m^{2*} \phi_L^2 + \frac{\lambda_4^*}{4!} \phi_L^4 + \frac{\sigma_4^*}{3!} \phi_L^3 \phi_R \right] \\
& + i \int d^d x \left[ z_\Delta (\partial \phi_R) \cdot (\partial \phi_L) + m_\Delta^2 \phi_R \phi_L + \frac{\lambda_\Delta}{2!2!} \phi_R^2 \phi_L^2 \right] \\
& - \int d^d x \left[ \frac{\lambda_3}{3!} \phi_R^3 - \frac{\lambda_3^*}{3!} \phi_L^3 + \frac{\sigma_3}{2!} \phi_R^2 \phi_L - \frac{\sigma_3^*}{2!} \phi_L^2 \phi_R \right]
\end{aligned} \tag{2.1}$$

### 2.1 Lindblad condition

Imposing CPT and demanding that the action (2.1) should be of the Lindblad form, we get four constraints among the coupling constants - one for field renormalisation, one for the mass, one for the cubic coupling and one for quartic coupling terms. We begin by tabulating all the power counting renormalisable Lindblad terms in the  $\phi^3 + \phi^4$  theory in Table. 1. Also tabulated are the conditions resulting from insisting that our action be of Lindblad form (we call these the

Lindblad couplings $\Gamma_{\alpha\beta}$	$L_\alpha^\dagger[\phi]$	$L_\beta[\phi]$	Imaginary coupling of $L_\alpha^\dagger L_\beta$	Lindblad condition
$z_\Delta$	$\partial_\mu \phi$	$\partial_\mu \phi$	$\text{Im } z$	$\text{Im } z = z_\Delta$
$m_\Delta^2$	$\phi$	$\phi$	$\text{Im } m^2$	$\text{Im } m^2 = m_\Delta^2$
$\frac{\lambda_\Delta}{2!2!}$	$\phi^2$	$\phi^2$	$\text{Im } \lambda_4$	$\text{Im } \lambda_4 = 3\lambda_\Delta - 4 \text{Im } \sigma_4$
$i\frac{\sigma_4}{3!}$	$\phi^3$	$\phi$	$\text{Im } \lambda_4$	
$-i\frac{\sigma_4^*}{3!}$	$\phi$	$\phi^3$	$\text{Im } \lambda_4$	
$i\frac{\sigma_3}{2!}$	$\phi^2$	$\phi$	$\text{Im } \lambda_3$	$\text{Im } \lambda_3 = -3 \text{Im } \sigma_3$
$-i\frac{\sigma_3^*}{2!}$	$\phi$	$\phi^2$	$\text{Im } \lambda_3$	

**Table 1:** Renormalisable Lindblad operators for  $\phi^3 + \phi^4$  theory

Lindblad conditions). We will now consider various parts of the action in turn and rewrite them in a way that the Lindblad conditions become manifest.

### Real terms of the action

The real part of the action is given by

$$\begin{aligned}
\text{Re}[S] = & - \int d^d x \left[ \frac{1}{2} \text{Re}[z] [(\partial\phi_R)^2 - (\partial\phi_L)^2] + \frac{1}{2} \text{Re}[m^2](\phi_R^2 - \phi_L^2) \right] \\
& - \int d^d x \left[ \frac{\text{Re } \lambda_4}{4!} (\phi_R^4 - \phi_L^4) + \frac{\text{Re } \sigma_4}{3!} \phi_R \phi_L (\phi_R^2 - \phi_L^2) \right] \\
& - \int d^d x \left[ \frac{\text{Re } \lambda_3}{3!} (\phi_R^3 - \phi_L^3) + \frac{\text{Re } \sigma_3}{2!} \phi_R \phi_L (\phi_R - \phi_L) \right]
\end{aligned} \tag{2.2}$$

We note that CPT constrains this action to vanish when  $\phi_R = \phi_L$ . As a result, there are no conditions on these real couplings from the Lindblad structure.

### Imaginary Quadratic terms of the action

The imaginary part of the quadratic terms is given by

$$\begin{aligned}
\text{Im}[S_2] = & - \int d^d x \left[ \frac{1}{2} \text{Im}[z] ((\partial\phi_R)^2 + (\partial\phi_L)^2) - z_\Delta (\partial\phi_R) \cdot (\partial\phi_L) \right] \\
& - \int d^d x \left[ \frac{1}{2} \text{Im}[m^2](\phi_R^2 + \phi_L^2) - m_\Delta^2 \phi_R \phi_L \right] \\
= & - \int d^d x \left[ \frac{1}{2} \text{Im}[z] (\partial\phi_R - \partial\phi_L)^2 + \frac{1}{2} \text{Im}[m^2](\phi_R - \phi_L)^2 \right] \\
& + \int d^d x \left[ (z_\Delta - \text{Im}[z]) (\partial\phi_R) \cdot (\partial\phi_L) + (m_\Delta^2 - \text{Im}[m^2]) \phi_R \phi_L \right]
\end{aligned} \tag{2.3}$$

The Lindblad condition is given by

$$z_\Delta = \text{Im}[z] , \quad m_\Delta^2 = \text{Im}[m^2] , \tag{2.4}$$

### Imaginary Cubic coupling

Now we compute the imaginary part of the cubic terms in the action

$$\begin{aligned}
-\text{Im}[S_3] &= \int d^d x \left[ \frac{\text{Im} \lambda_3}{3!} \phi_R^3 + \frac{\text{Im} \lambda_3}{3!} \phi_L^3 + \frac{\text{Im} \sigma_3}{2!} \phi_R^2 \phi_L + \frac{\text{Im} \sigma_3}{2!} \phi_L^2 \phi_R \right] \\
&= \int d^d x \left[ \frac{\text{Im} \lambda_3}{3!} (\phi_R - \phi_L)(\phi_R^2 - \phi_L^2) + \left( \frac{\text{Im} \lambda_3}{3!} + \frac{\text{Im} \sigma_3}{2!} \right) (\phi_R^2 \phi_L + \phi_L^2 \phi_R) \right] \quad (2.5)
\end{aligned}$$

The Lindblad condition is given by

$$\begin{aligned}
\frac{\text{Im} \lambda_3}{3!} + \frac{\text{Im} \sigma_3}{2!} &= 0 \\
\Rightarrow \text{Im} \lambda_3 + 3 \text{Im} \sigma_3 &= 0 \quad (2.6)
\end{aligned}$$

### Imaginary Quartic coupling

The imaginary part of action at the level quartic coupling is given by

$$\begin{aligned}
\text{Im}[S_4] &= - \int d^d x \left[ \frac{1}{4!} \text{Im}[\lambda_4] (\phi_R^4 + \phi_L^4) + \frac{1}{3!} \text{Im}[\sigma_4] (\phi_R^3 \phi_L + \phi_R \phi_L^3) - \frac{\lambda_\Delta}{2!2!} \phi_R^2 \phi_L^2 \right] \\
&= - \int d^d x \left[ \left( \frac{1}{4!} \text{Im}[\lambda_4] + \frac{1}{3!} \text{Im}[\sigma_4] \right) (\phi_R^2 - \phi_L^2)^2 + \frac{1}{3!} \text{Im}[\sigma_4] (\phi_R - \phi_L)(\phi_R^3 - \phi_L^3) \right] \quad (2.7) \\
&\quad + \int d^d x \left[ \frac{\lambda_\Delta}{2!2!} - 2 \text{Im} \left( \frac{\lambda_4}{4!} + \frac{\sigma_4}{3!} \right) \right] \phi_R^2 \phi_L^2
\end{aligned}$$

The Lindblad condition at for the quartic couplings is given by

$$\begin{aligned}
\frac{\lambda_\Delta}{2!2!} &= 2 \text{Im} \left( \frac{\lambda_4}{4!} + \frac{\sigma_4}{3!} \right) \\
\Rightarrow \text{Im} \lambda_4 + 4 \text{Im} \sigma_4 - 3 \lambda_\Delta &= 0 \quad (2.8)
\end{aligned}$$

## 2.2 Exact propagators

The ket field  $\phi_R$  and the bra field  $\phi_L$  in SK path-integral satisfy the following boundary condition (1.12)

$$\phi_R(t = \infty) = \phi_L(t = \infty) \quad (2.9)$$

Owing to this boundary condition and the mixing term between  $\phi_R$  and  $\phi_L$  fields, the kinetic matrix derived from the action (2.1) is given by

$$\mathcal{K} = \begin{pmatrix} i(z k^2 + m^2 - i\varepsilon) & z_\Delta k^2 + m_\Delta^2 - 2 \varepsilon \Theta(-k^0) \\ z_\Delta k^2 + m_\Delta^2 - 2 \varepsilon \Theta(k^0) & -i(z^* k^2 + (m^2)^* + i\varepsilon) \end{pmatrix} \quad (2.10)$$

where the  $\varepsilon$  prescription implements Schwinger-Keldysh boundary conditions. We define the kinetic matrix  $\mathcal{K}$  by

$$iS \ni -\frac{1}{2} \left( \phi_R(-k) \phi_L(-k) \right) \mathcal{K} \begin{pmatrix} \phi_R(k) \\ \phi_L(k) \end{pmatrix} \quad (2.11)$$

Its inverse (viz., the propagator) can be written as

$$\begin{aligned}
\mathcal{K}^{-1} &\equiv \begin{pmatrix} \langle \phi_R(-k) \phi_R(k) \rangle & \langle \phi_R(-k) \phi_L(k) \rangle \\ \langle \phi_L(-k) \phi_R(k) \rangle & \langle \phi_L(-k) \phi_L(k) \rangle \end{pmatrix} \\
&= \mathfrak{z}^{-1} \begin{pmatrix} \frac{-i}{\text{Re}[zk^2 + m^2] - i\varepsilon} & 2\pi\delta(\text{Re}[zk^2 + m^2])\Theta(-k^0) \\ 2\pi\delta(\text{Re}[zk^2 + m^2])\Theta(k^0) & \frac{i}{\text{Re}[zk^2 + m^2] + i\varepsilon} \end{pmatrix} \\
&\quad + \mathfrak{z}^{-1} \frac{(-i)}{\text{Re}[zk^2 + m^2] - i\varepsilon} \times \frac{i}{\text{Re}[zk^2 + m^2] + i\varepsilon} \times \begin{pmatrix} \text{Im}[zk^2 + m^2] & z_\Delta k^2 + m_\Delta^2 \\ z_\Delta k^2 + m_\Delta^2 & \text{Im}[zk^2 + m^2] \end{pmatrix}
\end{aligned} \tag{2.12}$$

where,

$$\mathfrak{z} \equiv 1 + \frac{(-i)}{\text{Re}[zk^2 + m^2] - i\varepsilon} \times \frac{i}{\text{Re}[zk^2 + m^2] + i\varepsilon} \times \left( (\text{Im}[zk^2 + m^2] - \varepsilon)^2 - (z_\Delta k^2 + m_\Delta^2 - \varepsilon)^2 \right) \tag{2.13}$$

Please note that when the Lindblad conditions (2.4) are satisfied, we have

$$\mathfrak{z} = 1 . \tag{2.14}$$

Further, it can be easily checked that in this limit, the sum of diagonal entries in the propagator matrix is equal to the sum of off-diagonal entries, i.e.,

$$(\mathcal{K}^{-1})_{RR} + (\mathcal{K}^{-1})_{LL} = (\mathcal{K}^{-1})_{RL} + (\mathcal{K}^{-1})_{LR} \tag{2.15}$$

The corresponding property in the unitary quantum field theory is the well-known relation between the various correlators in the Keldysh formalism [15]. This can equivalently be reformulated as the vanishing of two point function of two difference correlators :

$$(\mathcal{K}^{-1})_{R-L, R-L} = 0. \tag{2.16}$$

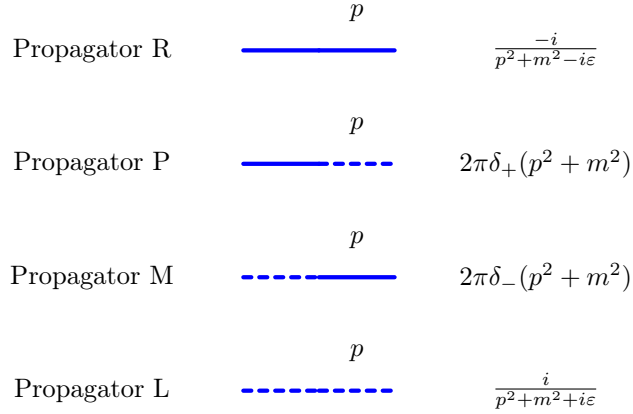
In this work, we will work in the limit where the non-unitary couplings  $\text{Im}[m^2]$  and  $m_\Delta^2$  are considered as perturbations to  $\text{Re}[m^2]$ , and similarly,  $\text{Im}[z^2]$  and  $z_\Delta^2$  are considered small compared to  $\text{Re}[z^2]$ . Further, since 1-loop correction to the propagators do not generate field renormalisation we can also set  $z = 1$ . In this limit, the propagators in equation (2.12) reduced to those given by figure 2.

### 2.3 Feynman rules

In this paper henceforth, we will set  $z = z_\Delta = 1$  (which is not renormalised at one-loop in  $d=4$  dimensions). We will treat all other parameters in our action except the real part of  $m^2$  (i.e.,  $\text{Re}(m^2)$ ) perturbatively. This includes  $\lambda_3, \sigma_3, \lambda_4, \sigma_4$  and  $\lambda_\Delta$ , as well as  $\text{Im} m^2$  and  $m_\Delta^2$ .

The propagators of  $\phi$  fields are given below. We have used solid blue and dotted blue lines for  $\phi_R$  (ket fields) and  $\phi_L$  (bra fields) fields respectively. Note that in the cut propagators P and M the energy is restricted to flow from the ket field to the bra field.

We will now set up the Veltman rules for the vertices to compute SK correlators in the open  $\phi^3 + \phi^4$  theory:



**Figure 2:** SK propagator for  $\phi$  fields

Vertex	Factor
$\phi_R^3$	$(-i\lambda_3)(2\pi)^d\delta(\sum p)$
$\phi_L^3$	$(i\lambda_3^*)(2\pi)^d\delta(\sum p)$
$\phi_R^2\phi_L$	$(-i\sigma_3)(2\pi)^d\delta(\sum p)$
$\phi_R\phi_L^2$	$(i\sigma_3^*)(2\pi)^d\delta(\sum p)$
$\phi_R^4$	$(-i\lambda_4)(2\pi)^d\delta(\sum p)$
$\phi_L^4$	$(i\lambda_4^*)(2\pi)^d\delta(\sum p)$
$\phi_R^3\phi_L$	$(-i\sigma_4)(2\pi)^d\delta(\sum p)$
$\phi_R\phi_L^3$	$(i\sigma_4^*)(2\pi)^d\delta(\sum p)$
$\phi_R^2\phi_L^2$	$(-\lambda_\Delta)(2\pi)^d\delta(\sum p)$

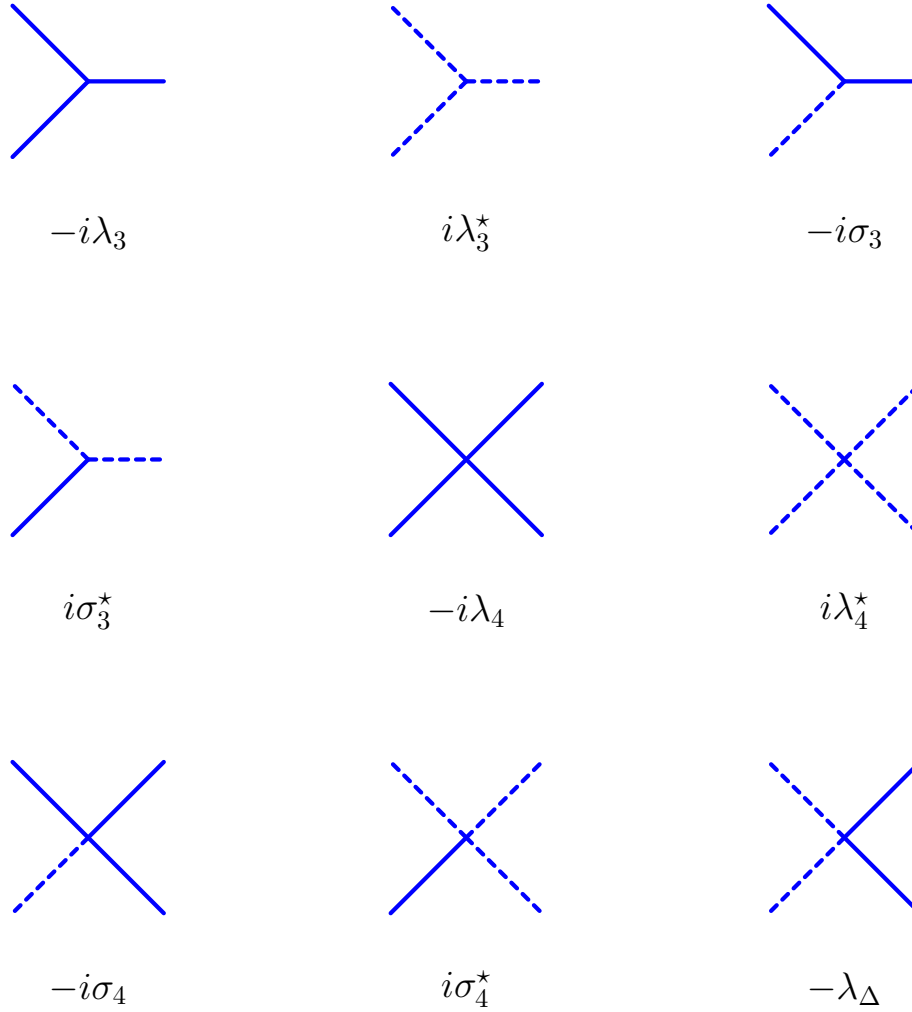
## 2.4 Lindblad condition from tree level correlators

In a unitary Schwinger-Keldysh theory, the correlator of difference operators vanishes to all order in perturbation theory. This is equivalent to Veltman's largest time equation (see for example [24]). One could ask whether this statement continues to hold true in the non-unitary theory. We have already remarked during our discussion of propagators around equation (2.12) that the quadratic Lindblad conditions are equivalent to the vanishing of difference operator two point functions. We can extend this to higher point functions simply. Consider the tree level correlator of three difference operators

$$\begin{aligned} & \langle (\phi_R(p_1) - \phi_L(p_1))(\phi_R(p_2) - \phi_L(p_2))(\phi_R(p_3) - \phi_L(p_3)) \rangle \\ & = -i(\lambda_3 - \lambda_3^*) - 4i(\sigma_3 - \sigma_3^*) = 2(\text{Im } \lambda_3 + 3 \text{Im } \sigma_3) \end{aligned} \quad (2.17)$$

the correlator of four difference operators is given by

$$\begin{aligned} & \langle (\phi_R(p_1) - \phi_L(p_1))(\phi_R(p_2) - \phi_L(p_2))(\phi_R(p_3) - \phi_L(p_3))(\phi_R(p_4) - \phi_L(p_4)) \rangle \\ & = -i(\lambda_4 - \lambda_4^*) - 4i(\sigma_4 - \sigma_4^*) - 6\lambda_\Delta = 2(\text{Im } \lambda_4 + 4 \text{Im } \sigma_4 - 3\lambda_\Delta) \end{aligned} \quad (2.18)$$



**Figure 3:** Diagrammatic Representation of all the Tree level processes

The correlators of the three and the four difference operators are precisely given by the Lindblad violating couplings. This implies that at tree level, the Lindblad conditions are the same as the vanishing of correlators of difference operators.

One can, in fact, show the following statement [22]: consider an open EFT, which is obtained by tracing out some subset of fields in an underlying unitary theory. Then, the unitarity of the underlying theory implies that the open EFT satisfies the Lindblad condition.

### 3 One loop beta function

In this section, we compute the beta function for all the mass terms and coupling constants that appear in the action of the open  $\phi^3 + \phi^4$  theory. The main aim in this section will be to demonstrate the following three claims :



1. Despite the novel UV divergences that occur in the open  $\phi^3 + \phi^4$  theory, one can use a simple extension of the standard counter-term method to deal with the divergences. Thus, the open  $\phi^3 + \phi^4$  theory is one-loop renormalisable.
2. Once these UV divergences are countered, the standard derivation of beta functions and RG running also goes through, except for the fact that one has to now also renormalise the non-unitary couplings.
3. We will also demonstrate that the running of a certain combinations of the couplings, the ones which given by the Lindblad conditions (equation (2.4), equation (2.6) and equation (2.8) respectively), under one-loop renormalisation are proportional to the Lindblad conditions.

We shall provide an all-order proof in the next section that the Lindblad conditions are never violated under perturbative corrections. Here we shall use the notations and results presented in appendix B.

### 3.1 One loop beta function for $m^2$

We will now begin a discussion of various loop diagrams. The simplest is perhaps the tadpole diagrams which can be cancelled by a counter-term linear in  $\phi_R$  and  $\phi_L$ . It is easily demonstrated that the necessary counter-terms do not violate the Lindblad condition (See appendix E).

Let us compute the one loop beta function for  $m^2$ . We shall consider all the one loop Feynman diagrams that contributes to the process  $\phi_R \rightarrow \phi_R$ . One can verify that there are mainly two types of diagrams - one class of diagrams due to the cubic couplings, as depicted in figure 4, and the other class of diagrams due to quartic couplings, depicted in figure 5.

The sum of the contribution from all the Feynman diagrams is given by

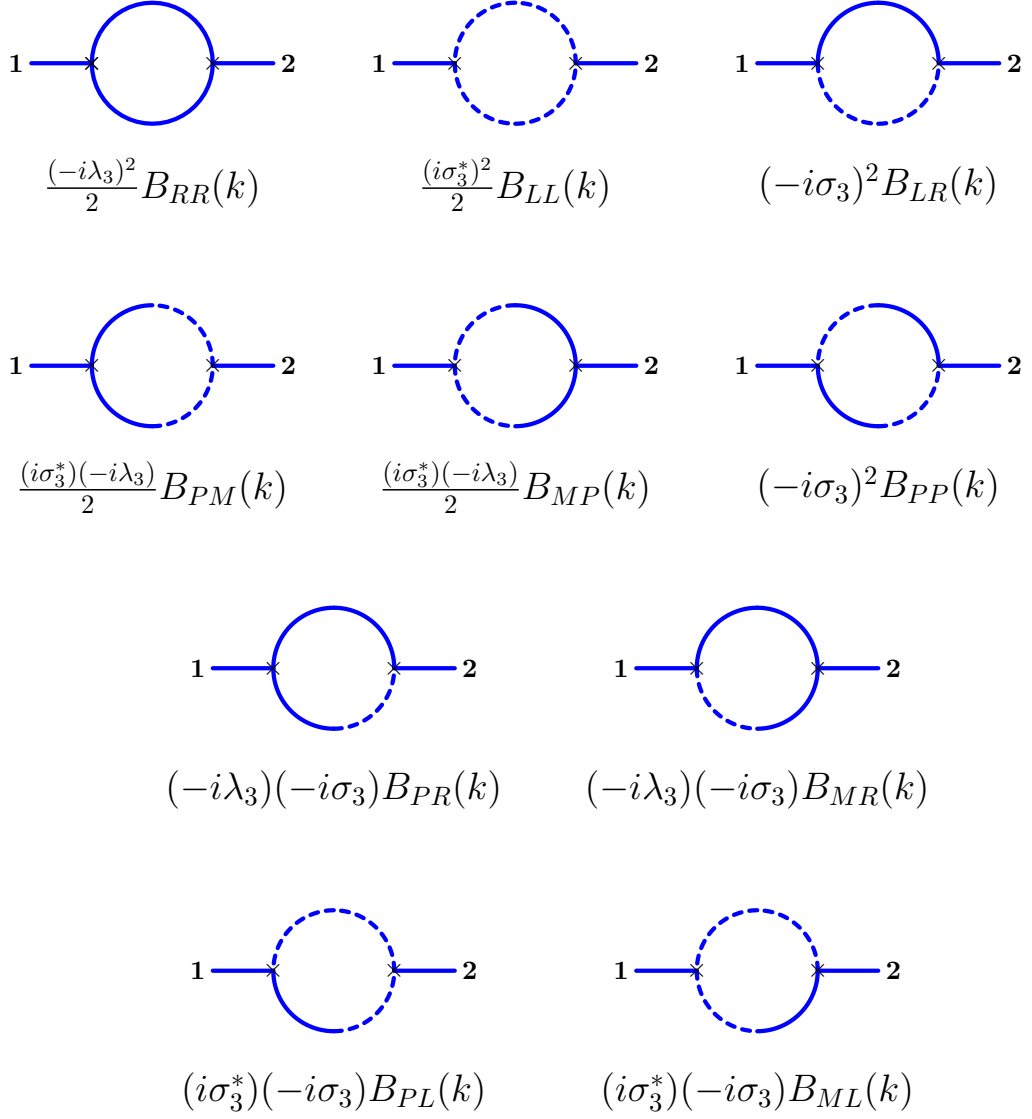
$$\begin{aligned}
& -im^2 \\
& + \frac{(-i\lambda_3)^2}{2} B_{RR}(k) + \frac{(i\sigma_3^*)^2}{2} B_{LL}(k) + (-i\sigma_3)^2 B_{LR}(k) \\
& + \frac{(i\sigma_3^*)(-i\lambda_3)}{2} B_{PM}(k) + \frac{(i\sigma_3^*)(-i\lambda_3)}{2} B_{MP}(k) + (-i\sigma_3)^2 B_{PP}(k) \\
& + (-i\lambda_3)(-i\sigma_3) B_{PR}(k) + (-i\lambda_3)(-i\sigma_3) B_{MR}(k) \\
& + (i\sigma_3^*)(-i\sigma_3) B_{PL}(k) + (i\sigma_3^*)(-i\sigma_3) B_{ML}(k) \\
& + \frac{(-i\lambda_4)}{2} A_R + \frac{(-\lambda_\Delta)}{2} A_L + (-i\sigma_4) A_M
\end{aligned} \tag{3.1}$$

Using the results in (B.79a)-(B.79d), we can see that the contribution is divergent and one needs to add one loop counter-terms  $\delta m^2$ , in the  $\overline{\text{MS}}$  scheme, to absorb the divergences.

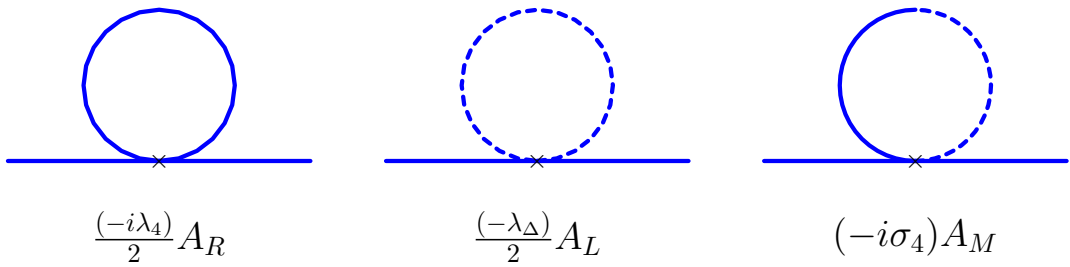
$$\begin{aligned}
\delta m^2 \Big|_{\overline{\text{MS}}} &= -\frac{1}{(4\pi)^2} \left[ (\lambda_3)^2 - (\sigma_3^*)^2 + 2 \{ \lambda_3 \sigma_3 + |\sigma_3|^2 \} \right] \left[ \frac{1}{d-4} + \frac{1}{2} (\gamma_E - \ln 4\pi) \right] \\
&\quad - \frac{1}{(4\pi)^2} [\lambda_4 - i\lambda_\Delta + 2\sigma_4] \left[ \frac{1}{d-4} + \frac{1}{2} (\gamma_E - \ln 4\pi) \right] (\text{Re } m^2)
\end{aligned} \tag{3.2}$$

Using the standard methods of quantum field theory, one can then compute the one loop beta function as

$$\beta_{m^2} = \frac{1}{(4\pi)^2} \left[ (\lambda_3)^2 - (\sigma_3^*)^2 + 2 \{ \lambda_3 \sigma_3 + |\sigma_3|^2 \} + (\lambda_4 - i\lambda_\Delta + 2\sigma_4) (\text{Re } m^2) \right] \tag{3.3}$$



**Figure 4:** One Loop corrections to  $m^2$  due to cubic couplings

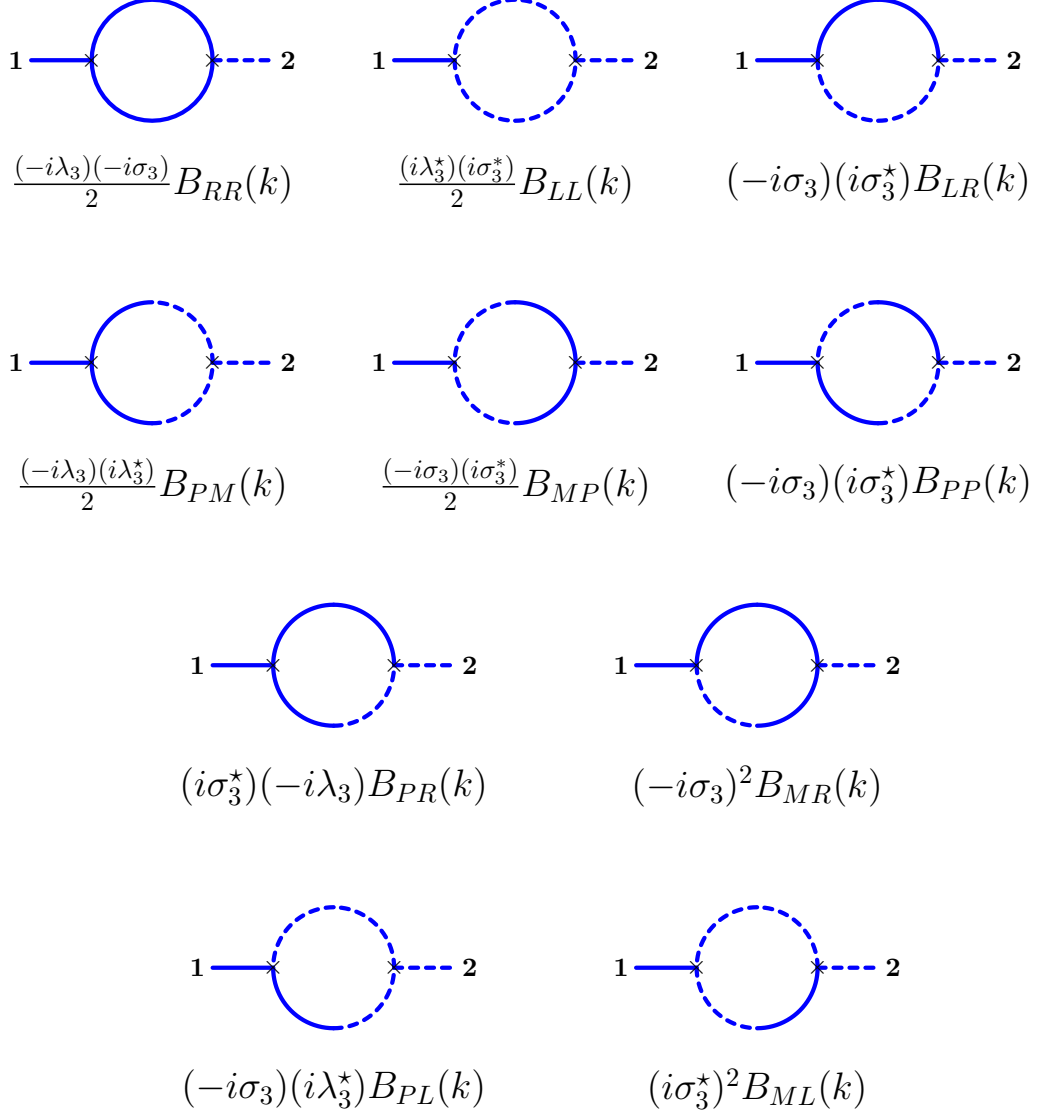


**Figure 5:** One loop correction to  $m^2$  due to quartic couplings

$$1 \text{ --- } \bullet \text{ --- } 2$$

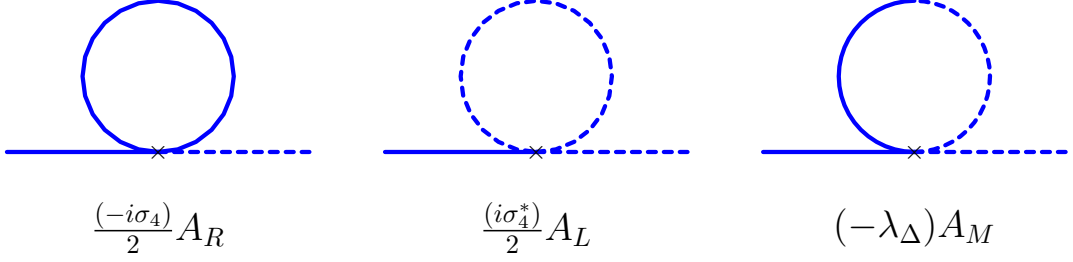
$$-i\delta m^2$$

**Figure 6:** Diagrammatic representation of the one loop counter-term for  $m^2$



**Figure 7:** One Loop corrections to  $m_\Delta^2$  due to cubic couplings

If set  $\sigma_3 = \sigma_4 = \lambda_\Delta = 0$ , then we get back the standard results of  $\phi^3 + \phi^4$  theory in  $d = 4$  space-time dimensions.



**Figure 8:** One loop correction to  $m_\Delta^2$  due to quartic couplings

### 3.2 One loop beta function for $m_\Delta^2$

Now, we will compute the one loop beta function for  $m_\Delta^2$ . As in the case of  $m^2$ , there will again be two classes of diagrams. The diagrams due to cubic and quartic couplings are as shown in figure 7 and in figure 8 respectively. The sum over all the contributions is given by

$$\begin{aligned}
& -m_\Delta^2 \\
& + \frac{(-i\lambda_3)(-i\sigma_3)}{2} B_{RR}(k) + \frac{(i\lambda_3^*)(i\sigma_3^*)}{2} B_{LL}(k) + (-i\sigma_3)(i\sigma_3^*) B_{LR}(k) \\
& + \frac{(-i\lambda_3)(i\lambda_3^*)}{2} B_{PM}(k) + \frac{(-i\sigma_3)(i\sigma_3^*)}{2} B_{MP}(k) + (-i\sigma_3)(i\sigma_3^*) B_{PP}(k) \\
& + (i\sigma_3^*)(-i\lambda_3) B_{PR}(k) + (-i\sigma_3)^2 B_{MR}(k) + (-i\sigma_3)(i\lambda_3^*) B_{PL}(k) + (i\sigma_3^*)^2 B_{ML}(k) \\
& + \frac{(-i\sigma_4)}{2} A_R + \frac{(i\sigma_4^*)}{2} A_L + (-\lambda_\Delta) A_M
\end{aligned} \tag{3.4}$$

Some of these one loop contributions are divergent and one needs to add one loop counter-terms. The  $m_\Delta^2$  counter-term in  $\overline{\text{MS}}$  scheme is given by

$$\begin{aligned}
\delta m_\Delta^2 \Big|_{\overline{\text{MS}}} &= -\frac{1}{(4\pi)^2} \left[ -4(\text{Re } \lambda_3 + \text{Re } \sigma_3) \text{Im } \sigma_3 + (2\lambda_\Delta - 2\text{Im } \sigma_4)(\text{Re } m^2) \right] \\
& \left[ \frac{1}{d-4} + \frac{1}{2}(\gamma_E - \ln 4\pi) \right]
\end{aligned} \tag{3.5}$$

and the beta function for  $m_\Delta^2$  is given by

$$\beta_{m_\Delta^2} = \frac{1}{(4\pi)^2} \left[ -4(\text{Re } \lambda_3 + \text{Re } \sigma_3) \text{Im } \sigma_3 + (2\lambda_\Delta - 2\text{Im } \sigma_4)(\text{Re } m^2) \right] \tag{3.6}$$

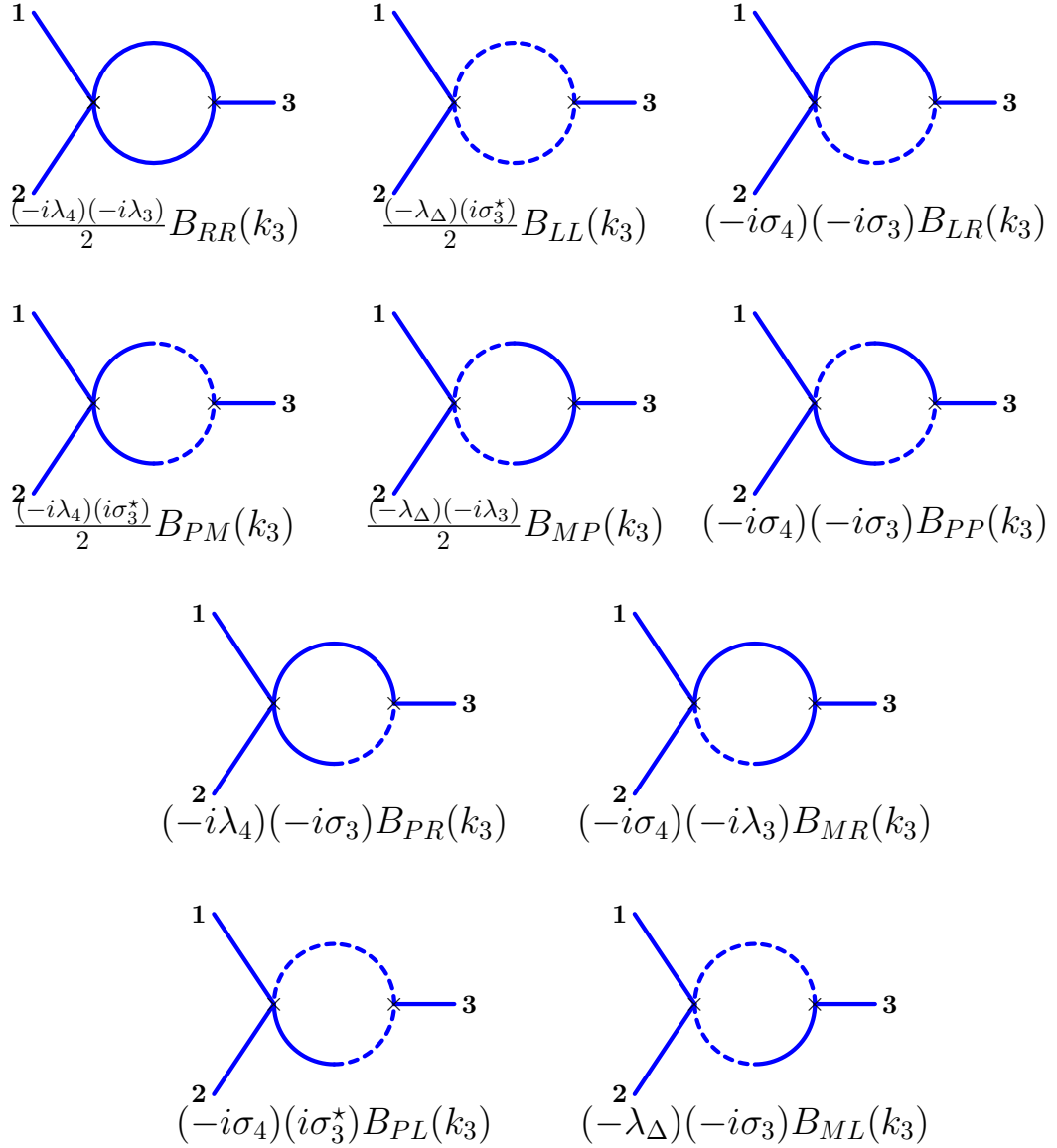
### 3.3 Checking Lindblad condition for mass renormalization

From equation (3.3), we find that the beta function for  $\text{Im } m^2$  is given by

$$\begin{aligned}
\frac{d(\text{Im } m^2)}{d \ln \mu} &= \frac{1}{(4\pi)^2} \left[ 2(\text{Re } \lambda_3 + \text{Re } \sigma_3)(\text{Im } \lambda_3 + \text{Im } \sigma_3) \right. \\
& \left. + (\text{Im } \lambda_4 + 2\text{Im } \sigma_4 - \lambda_\Delta)(\text{Re } m^2) \right]
\end{aligned} \tag{3.7}$$

Now, using equation (3.7) and equation (3.6), one gets the beta function for  $(\text{Im } m^2 - m_\Delta^2)$

$$\beta_{(\text{Im } m^2 - m_\Delta^2)} = \frac{2}{(4\pi)^2} \left[ (\text{Im } \lambda_3 + 3\text{Im } \sigma_3)(\text{Re } \lambda_3 + \text{Re } \sigma_3) + (\text{Im } \lambda_4 + 4\text{Im } \sigma_4 - 3\lambda_\Delta)(\text{Re } m^2) \right] \tag{3.8}$$



**Figure 9:** Diagrammatic representation of the Ten 1-Loop Integrals  $\phi_R\phi_R \rightarrow \phi_R$

equation (3.8) shows that the one loop beta function for Lindblad violating mass terms vanish in the absence of Lindblad violating cubic (equation (2.6)) and quartic coupling (equation (2.8)) at the tree level.

### 3.4 One loop beta function for $\lambda_3$

Now we will compute the one loop beta function for various cubic couplings. The Passarino-Veltman  $C$  and  $D$  integrals will have no contribution to the one loop  $\beta$  function for the cubic (and quartic) couplings, since they are UV finite<sup>3</sup>. Hence, we shall not consider those Feynman

<sup>3</sup>Note that the standard  $C$  and  $D$  integrals are well-known to be UV finite in the Euclidean theory. Since the SK versions of these integrals are different analytic continuations of these Euclidean integrals, they continue to

diagrams in our analysis. We begin with the beta function computation of  $\lambda_3$ . The diagrams for one of the channels are depicted in figure 9. The other two channels are obtained by interchanging  $1 \longleftrightarrow 3$  and  $2 \longleftrightarrow 3$ . The sum over the all the Feynman diagrams is given by

$$\begin{aligned}
& -i\lambda_3 \\
& + \frac{(-i\lambda_4)(-i\lambda_3)}{2} B_{RR}(k_3) + \frac{(-\lambda_\Delta)(i\sigma_3^*)}{2} B_{LL}(k_3) + (-i\sigma_4)(-i\sigma_3) B_{LR}(k_3) \\
& + \frac{(-i\lambda_4)(i\sigma_3^*)}{2} B_{PM}(k_3) + \frac{(-\lambda_\Delta)(-i\lambda_3)}{2} B_{MP}(k_3) + (-i\sigma_4)(-i\sigma_3) B_{PP}(k_3) \\
& + (-i\lambda_4)(-i\sigma_3) B_{PR}(k_3) + (-i\sigma_4)(-i\lambda_3) B_{MR}(k_3) \\
& + (-i\sigma_4)(i\sigma_3^*) B_{PL}(k_3) + (-\lambda_\Delta)(-i\sigma_3) B_{ML}(k_3) \\
& + \text{Two more channels}
\end{aligned} \tag{3.9}$$

Using the results in (B.79a)-(B.79d), we see that the one loop contributions are divergent and we need to add one loop counter-terms  $\delta\lambda_3$  to cancel the divergences.

$$\begin{aligned}
\delta\lambda_3 \Big|_{\overline{\text{MS}}} = & -\frac{3}{(4\pi)^2} \left[ \lambda_4\lambda_3 - 2\lambda_\Delta \text{Im} \sigma_3 + \lambda_4\sigma_3 + \sigma_4\lambda_3 + \sigma_4\sigma_3^* \right] \\
& \left[ \frac{1}{d-4} + \frac{1}{2}(\gamma_E - \ln 4\pi) \right]
\end{aligned} \tag{3.10}$$

Following the standard methods of quantum field theory, we compute the one loop beta function to be

$$\beta_{\lambda_3} = \frac{3}{(4\pi)^2} \left[ \lambda_4\lambda_3 - 2\lambda_\Delta \text{Im} \sigma_3 + \lambda_4\sigma_3 + \sigma_4\lambda_3 + \sigma_4\sigma_3^* \right] \tag{3.11}$$

### 3.5 One loop beta function for $\sigma_3$

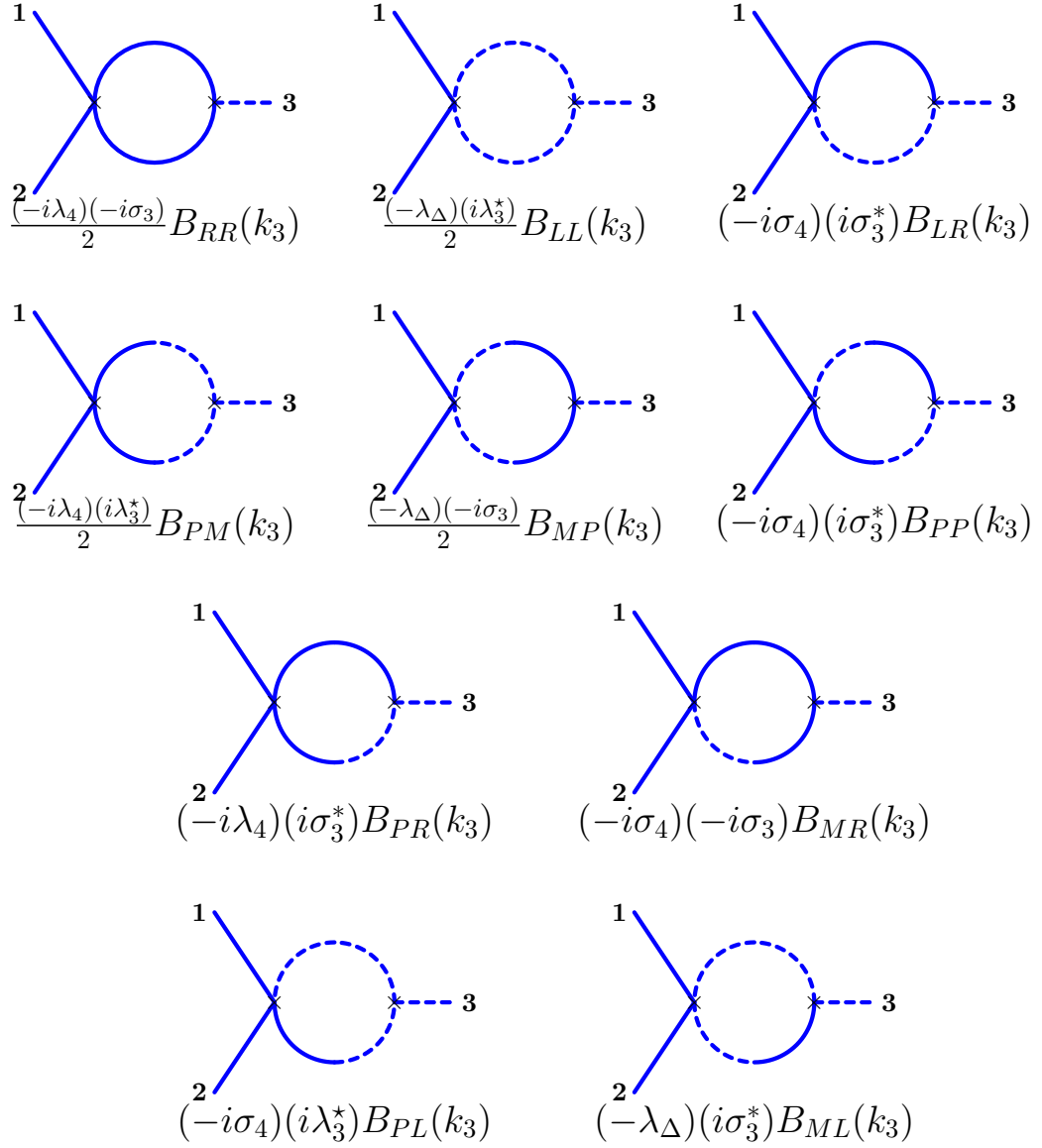
As described in the previous subsection, we will only consider PV  $B$  type diagrams for two of the channels are depicted in figure 10 and 11. The remaining channel is obtained by interchanging  $1 \longleftrightarrow 2$  in the diagrams in figure 11. The sum over all the contributions is given by

$$-i\sigma_3 + i\mathcal{M}_1(k_3) + i\mathcal{M}_2(k_2) + i\mathcal{M}_2(k_1) \tag{3.12}$$

Here  $i\sigma_3$  is the tree level contribution. The term  $i\mathcal{M}_1(k_3)$  denotes the sum over Feynman diagrams in figure 10 whereas  $i\mathcal{M}_2(k_2)$  denotes the sum over Feynman diagrams in figure 11. The contribution  $i\mathcal{M}_2(k_1)$  is obtained by interchanging  $1 \leftrightarrow 2$  in figure 11. The expression for  $i\mathcal{M}_1(k_3)$  is given by

$$\begin{aligned}
i\mathcal{M}_1(k_3) = & \frac{(-i\lambda_4)(-i\sigma_3)}{2} B_{RR}(k_3) + \frac{(-\lambda_\Delta)(i\lambda_3^*)}{2} B_{LL}(k_3) + (-i\sigma_4)(i\sigma_3^*) B_{LR}(k_3) \\
& + \frac{(-i\lambda_4)(i\lambda_3^*)}{2} B_{PM}(k_3) + \frac{(-\lambda_\Delta)(-i\sigma_3)}{2} B_{MP}(k_3) + (-i\sigma_4)(i\sigma_3^*) B_{PP}(k_3) \\
& + (-i\lambda_4)(i\sigma_3^*) B_{PR}(k_3) + (-i\sigma_4)(-i\sigma_3) B_{MR}(k_3) \\
& + (-i\sigma_4)(i\lambda_3^*) B_{PL}(k_3) + (-\lambda_\Delta)(i\sigma_3^*) B_{ML}(k_3)
\end{aligned} \tag{3.13}$$

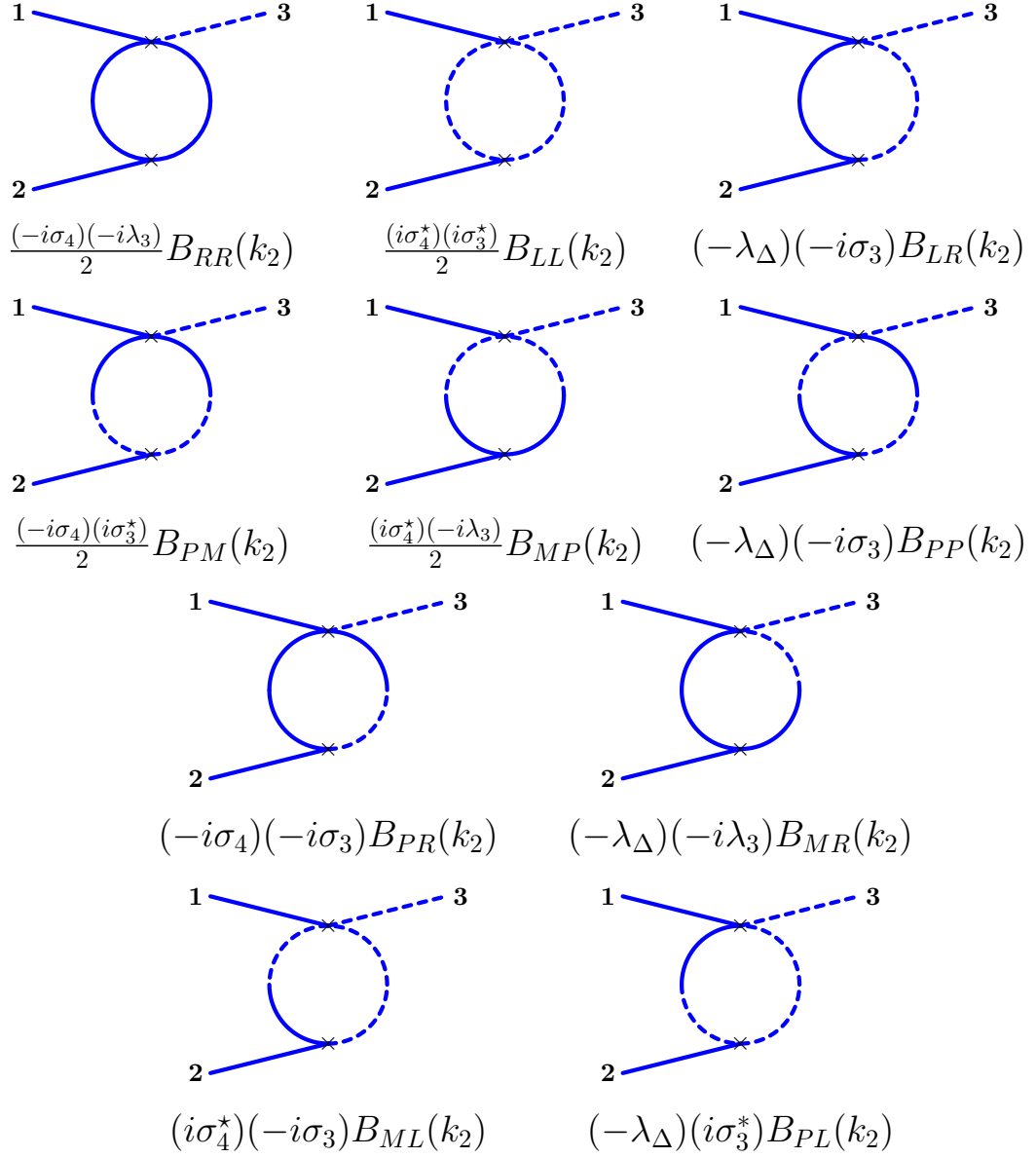
be UV finite. We will leave the detailed computation including these finite contributions to future work.



**Figure 10:** Diagrammatic representation of the Ten 1-Loop Integrals  $\phi_R \phi_R \rightarrow \phi_L$

The divergent contributions from  $i\mathcal{M}_1(k_3)$  is cancelled by the following counter-term

$$\delta\sigma_3 \Big|_{\overline{\text{MS}}}^{(1)} = -\frac{1}{(4\pi)^2} \left[ 2i\lambda_4 \text{Im} \sigma_3 - i\lambda_\Delta (\sigma_3^* + \lambda_3^*) + \sigma_4 \lambda_3^* + \sigma_4 \sigma_3 \right] \left[ \frac{1}{d-4} + \frac{1}{2} (\gamma_E - \ln 4\pi) \right] \quad (3.14)$$



**Figure 11:** Diagrammatic representation of the Ten 1-Loop Integrals  $\phi_R \phi_R \rightarrow \phi_L$

The expression for  $i\mathcal{M}_2(k_2)$  is given by

$$\begin{aligned}
i\mathcal{M}_2(k_2) = & \frac{(-i\sigma_4)(-i\lambda_3)}{2} B_{RR}(k_2) + \frac{(i\sigma_4^*)(i\sigma_3^*)}{2} B_{LL}(k_2) + (-\lambda_\Delta)(-i\sigma_3) B_{LR}(k_2) \\
& + \frac{(-i\sigma_4)(i\sigma_3^*)}{2} B_{PM}(k_2) + \frac{(i\sigma_4^*)(-i\lambda_3)}{2} B_{MP}(k_2) + (-\lambda_\Delta)(-i\sigma_3) B_{PP}(k_2) \\
& + (-i\sigma_4)(-i\sigma_3) B_{PR}(k_2) + (-\lambda_\Delta)(-i\lambda_3) B_{MR}(k_2) + (i\sigma_4^*)(-i\sigma_3) B_{PL}(k_2) \\
& + (-\lambda_\Delta)(i\sigma_3^*) B_{ML}(k_2)
\end{aligned} \tag{3.15}$$

The divergent contribution from  $i\mathcal{M}_2(k_2)$  (and from  $i\mathcal{M}_2(k_1)$ ) are cancelled by the following



counter-term

$$\delta\sigma_3\Big|_{\overline{\text{MS}}}^{(2)} = -\frac{2}{(4\pi)^2} \left[ \sigma_4\lambda_3 + 2i\text{Im}[\sigma_4\sigma_3] - i\lambda_\Delta(\lambda_3 + \sigma_3^*) + \sigma_4^*\sigma_3 \right] \left[ \frac{1}{d-4} + \frac{1}{2}(\gamma_E - \ln 4\pi) \right] \quad (3.16)$$

Hence the total one loop beta function for  $\sigma_3$  is given by

$$\beta_{\sigma_3} \equiv \frac{d\sigma_3}{d\ln\mu} = \frac{1}{(4\pi)^2} \left[ 2i\lambda_4\text{Im}\sigma_3 - i\lambda_\Delta(\sigma_3^* + \lambda_3^*) + \sigma_4\lambda_3^* + \sigma_4\sigma_3 + 2\sigma_4\lambda_3 + 4i\text{Im}[\sigma_4\sigma_3] - 2i\lambda_\Delta(\lambda_3 + \sigma_3^*) + 2\sigma_4^*\sigma_3 \right] \quad (3.17)$$

### 3.6 Checking Lindblad condition at the level of cubic couplings

From equation (3.11), we obtain the beta function for  $\text{Im}\lambda_3$  as

$$\frac{d(\text{Im}\lambda_3)}{d\ln\mu} = \frac{3}{(4\pi)^2} \left[ \text{Re}\lambda_4(\text{Im}\lambda_3 + \text{Im}\sigma_3) + \text{Re}\sigma_4(\text{Im}\lambda_3 - \text{Im}\sigma_3) + (\text{Re}\lambda_3 + \text{Re}\sigma_3)(\text{Im}\lambda_4 + \text{Im}\sigma_4) \right] \quad (3.18)$$

and the beta function of  $\text{Im}\sigma_3$  can be computed from the imaginary part of equation (3.17). We obtain

$$\frac{d(\text{Im}\sigma_3)}{d\ln\mu} = \frac{1}{(4\pi)^2} \left[ 2\text{Re}\lambda_4\text{Im}\sigma_3 + \text{Re}\sigma_4(7\text{Im}\sigma_3 + \text{Im}\lambda_3) + 3(\text{Re}\lambda_3 + \text{Re}\sigma_3)(\text{Im}\sigma_4 - \lambda_\Delta) \right] \quad (3.19)$$

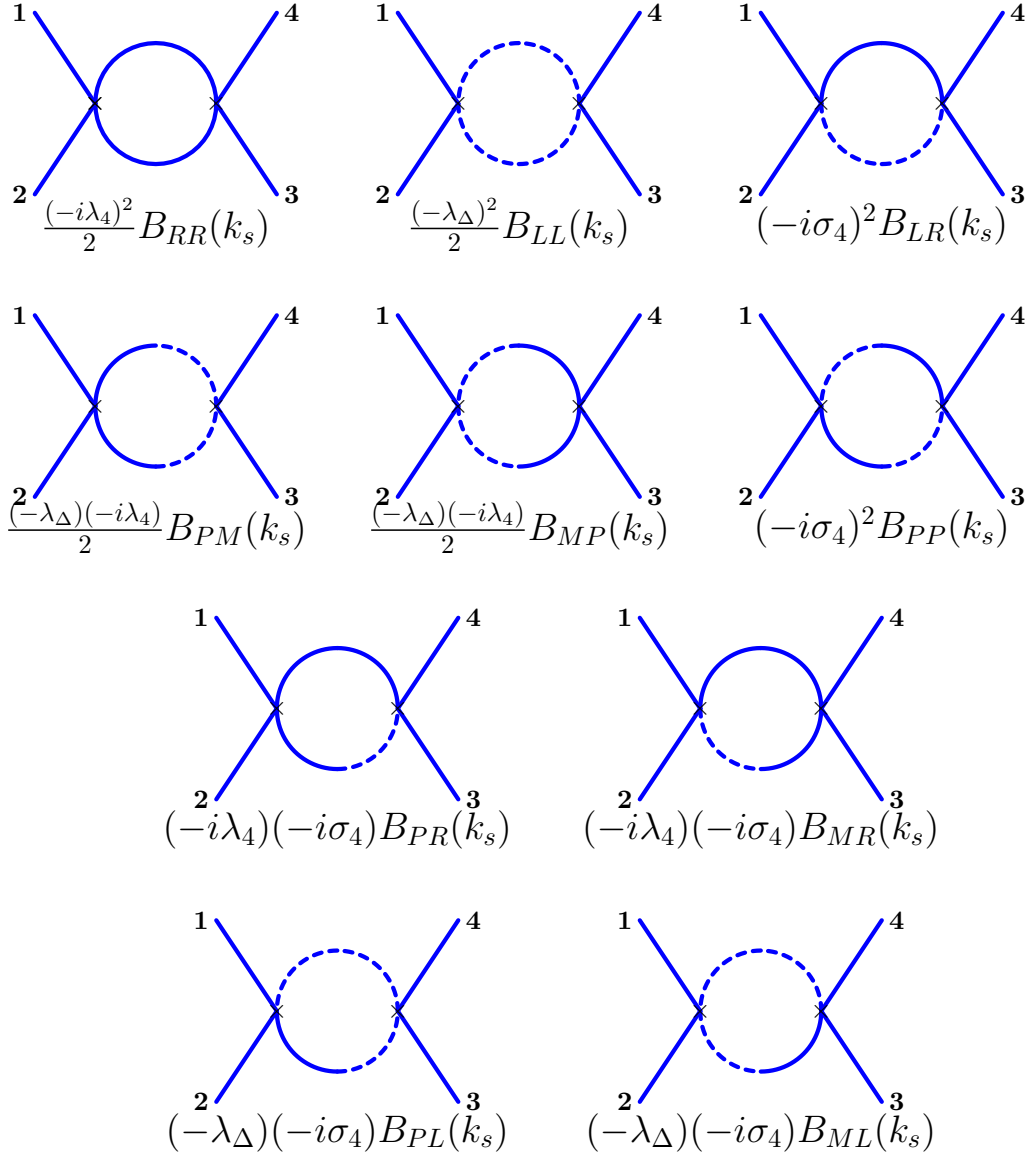
Adding these two equations we get

$$\frac{d}{d\ln\mu} [\text{Im}\lambda_3 + 3\text{Im}\sigma_3] = \frac{3}{(4\pi)^2} \left[ (\text{Re}\lambda_4 + 2\text{Re}\sigma_4)(\text{Im}\lambda_3 + 3\text{Im}\sigma_3) + (\text{Re}\lambda_3 + \text{Re}\sigma_3)(\text{Im}\lambda_4 + 4\text{Im}\sigma_4 - 3\lambda_\Delta) \right] \quad (3.20)$$

Again, one can see that the one loop beta function for the Lindblad violating cubic coupling is zero when there is no Lindblad violating coupling in the tree level Lagrangian.

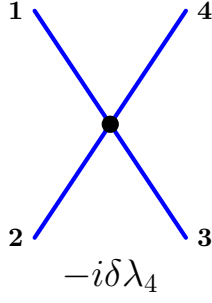
### 3.7 One loop beta function for $\lambda_4$

Now we proceed to compute the one loop beta function for the quartic couplings. We will only consider the bubble diagrams since the triangle and box diagrams are finite. Let us consider all



**Figure 12:** Diagrammatic representation of the Ten 1-Loop Integrals  $\phi_R\phi_R \rightarrow \phi_R\phi_R$  (Here  $k_s = k_1 + k_2$ )

the one loop Feynman diagrams that contribute to the process  $\phi_R + \phi_R \rightarrow \phi_R + \phi_R$ . All the



**Figure 13:** Diagrammatic representation of the one loop counter-term for  $\lambda_4$

diagrams are depicted in figure 12. The sum over all the Feynman diagrams is given by

$$\begin{aligned}
& -i\lambda_4 \\
& + \frac{(-i\lambda_4)^2}{2} B_{RR}(k_s) + \frac{(-\lambda_\Delta)^2}{2} B_{LL}(k_s) + (-i\sigma_4)^2 B_{LR}(k_s) \\
& + \frac{(-\lambda_\Delta)(-i\lambda_4)}{2} B_{PM}(k_s) + \frac{(-\lambda_\Delta)(-i\lambda_4)}{2} B_{MP}(k_s) + (-i\sigma_4)^2 B_{PP}(k_s) \\
& + (-i\lambda_4)(-i\sigma_4) B_{PR}(k_s) + (-i\lambda_4)(-i\sigma_4) B_{MR}(k_s) \\
& + (-\lambda_\Delta)(-i\sigma_4) B_{PL}(k_s) + (-\lambda_\Delta)(-i\sigma_4) B_{ML}(k_s) \\
& + (k_s \longleftrightarrow k_t) + (k_s \longleftrightarrow k_u)
\end{aligned} \tag{3.21}$$

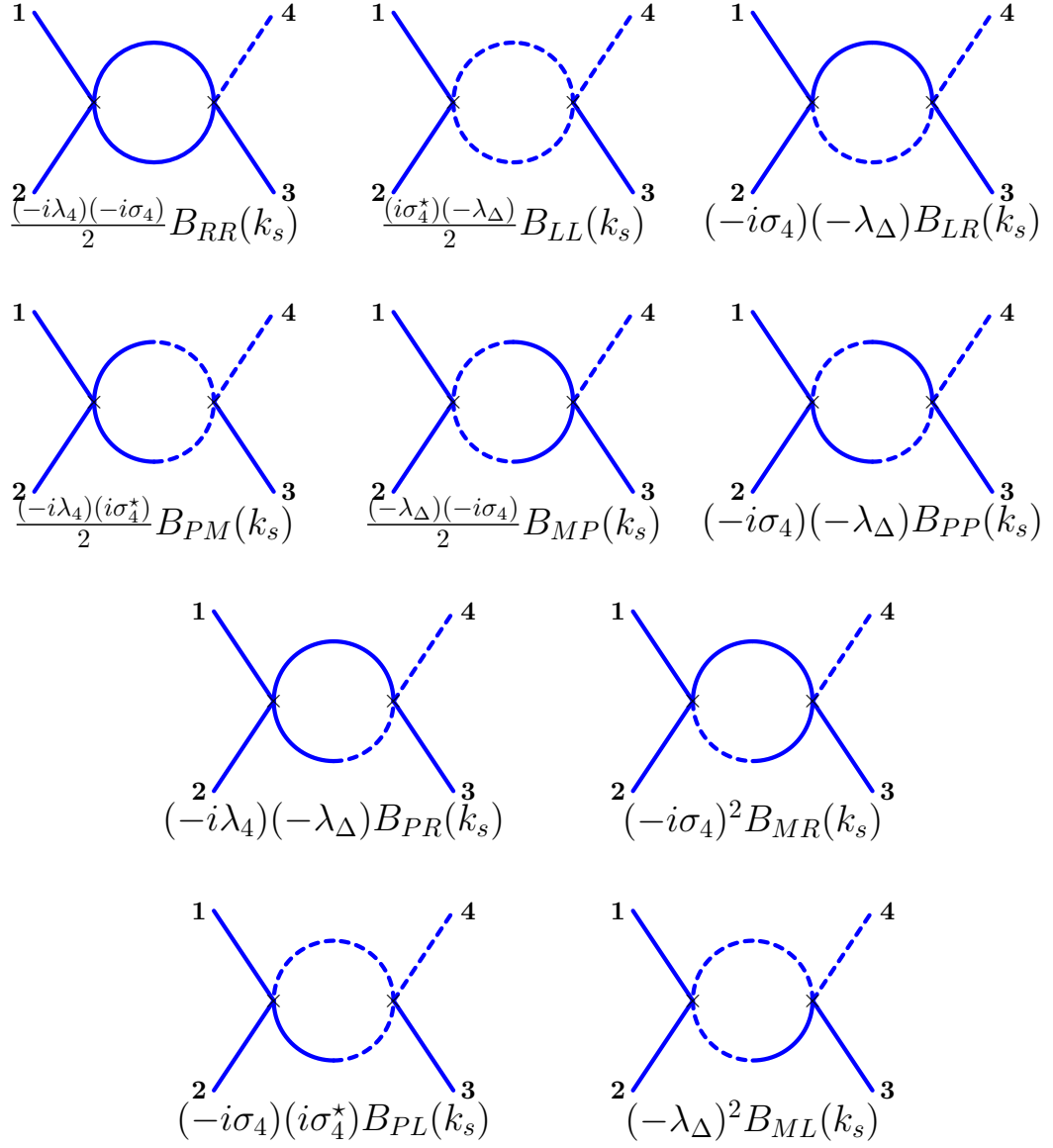
Using the results in (B.79a)-(B.79d), it's easy to see that the contribution is divergent and we need to add a one loop counter-term  $\delta\lambda_4$  to cancel the divergences;

$$\delta\lambda_4 \Big|_{\overline{\text{MS}}} = -\frac{3}{(4\pi)^2} \left[ \lambda_4^2 + 2\sigma_4(\lambda_4 + i\lambda_\Delta) + \lambda_\Delta^2 \right] \left[ \frac{1}{d-4} + \frac{1}{2}(\gamma_E - \ln 4\pi) \right] \tag{3.22}$$

Using the standard methods of quantum field theory, we can compute the one loop beta function to be

$$\beta_{\lambda_4} = \frac{3}{(4\pi)^2} \left[ \lambda_4^2 + 2\sigma_4(\lambda_4 + i\lambda_\Delta) + \lambda_\Delta^2 \right] = \frac{3}{(4\pi)^2} (\lambda_4 + 2\sigma_4 - i\lambda_\Delta)(\lambda_4 + i\lambda_\Delta) \tag{3.23}$$

By setting  $\sigma_4 = \lambda_\Delta = 0$  we recover the standard result of unitary  $\phi^4$  theory.



**Figure 14:** Diagrammatic representation of the Ten 1-Loop Integrals  $\phi_R\phi_R \rightarrow \phi_R\phi_L$

### 3.8 One loop beta function for $\sigma_4$

Again, only the Passarino-Veltman  $B$  type diagrams contribute to the one loop beta function for  $\sigma_4$ . All the  $B$  type diagrams are depicted in figure 14. The sum over all of them is given by

$$\begin{aligned}
& -i\sigma_4 \\
& + \frac{(-i\lambda_4)(-i\sigma_4)}{2} B_{RR}(k_s) + \frac{(i\sigma_4^*)(-\lambda_\Delta)}{2} B_{LL}(k_s) + (-i\sigma_4)(-\lambda_\Delta) B_{LR}(k_s) \\
& + \frac{(-\lambda_4)(i\sigma_4^*)}{2} B_{PM}(k_s) + \frac{(-\lambda_\Delta)(-i\sigma_4)}{2} B_{MP}(k_s) + (-i\sigma_4)(-\lambda_\Delta) B_{PP}(k_s) \\
& + (-i\lambda_4)(-\lambda_\Delta) B_{PR}(k_s) + (-i\sigma_4)^2 B_{MR}(k_s) \\
& + (-i\sigma_4)(i\sigma_4^*) B_{PL}(k_s) + (-\lambda_\Delta)^2 B_{ML}(k_s) \\
& + (k_s \longleftrightarrow k_t) + (k_s \longleftrightarrow k_u)
\end{aligned} \tag{3.24}$$

The one loop counter-term for  $\sigma_4$  is given by

$$\delta\sigma_4 \Big|_{\overline{\text{MS}}} = -\frac{3}{(4\pi)^2} \left[ \sigma_4^2 + (\lambda_4 + \sigma_4^*)(\sigma_4 - i\lambda_\Delta) + \lambda_\Delta^2 \right] \left[ \frac{1}{d-4} + \frac{1}{2}(\gamma_E - \ln 4\pi) \right] \tag{3.25}$$

and the one loop beta function is found to be

$$\beta_{\sigma_4} = \frac{3}{(4\pi)^2} \left[ \sigma_4^2 + (\lambda_4 + \sigma_4^*)(\sigma_4 - i\lambda_\Delta) + \lambda_\Delta^2 \right] \tag{3.26}$$

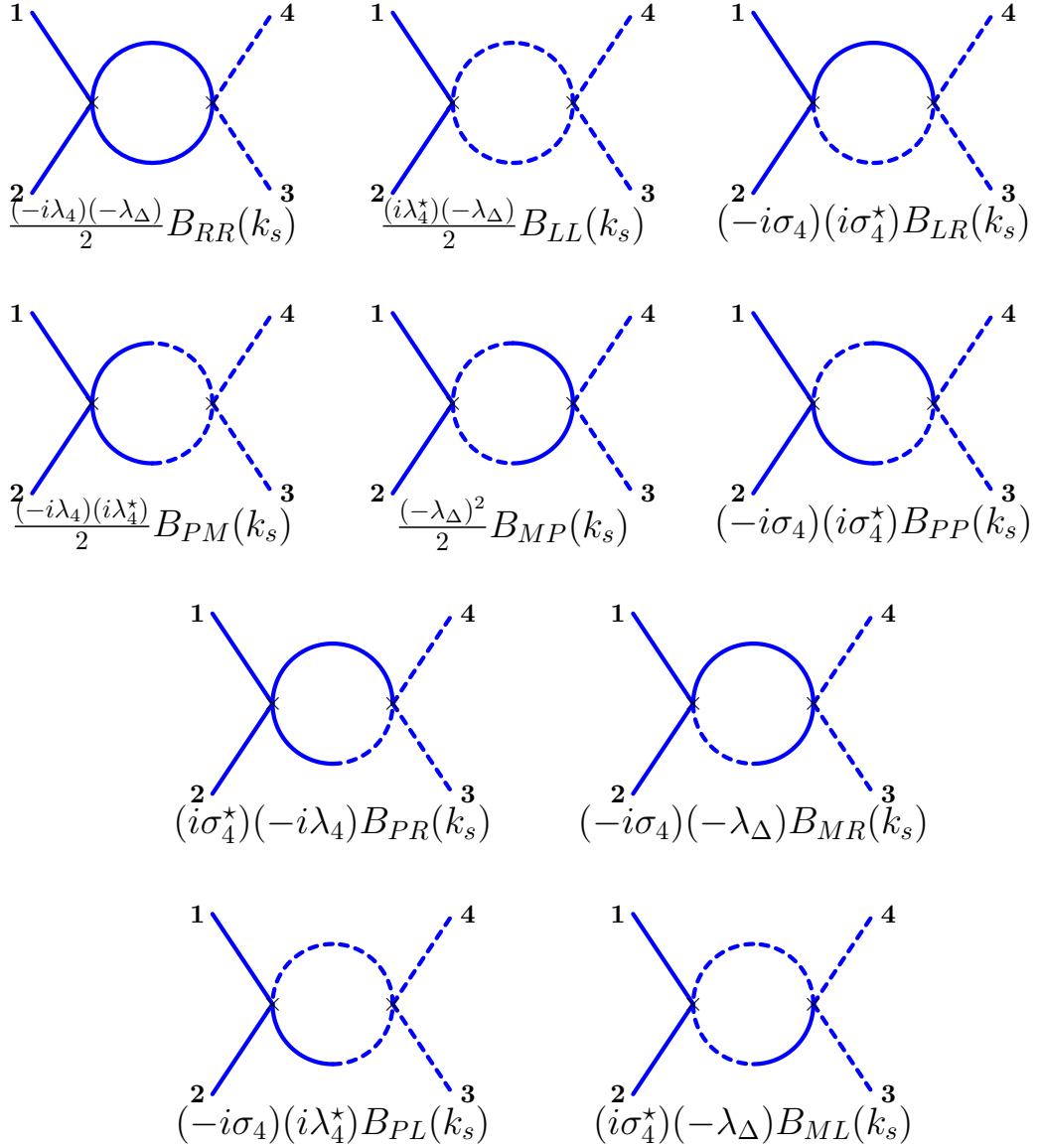
### 3.9 One loop beta function for $\lambda_\Delta$

The Passarino-Veltman  $B$  type contributions for  $s$ -channel and  $t$ -channel is being shown in figure 15 and figure 16 respectively.  $u$ -channels diagrams are obtained by interchanging  $1 \leftrightarrow 2$  in figure 16. The sum over all the contributions is given as

$$\begin{aligned}
& -\lambda_\Delta \\
& + \frac{(-i\lambda_4)(-\lambda_\Delta)}{2} B_{RR}(k_s) + \frac{(i\lambda_4^*)(-\lambda_\Delta)}{2} B_{LL}(k_s) + (-i\sigma_4)(i\sigma_4^*) B_{LR}(k_s) \\
& + \frac{(-i\lambda_4)(i\lambda_4^*)}{2} B_{PM}(k_s) + \frac{(-\lambda_\Delta)^2}{2} B_{MP}(k_s) + (-i\sigma_4)(i\sigma_4^*) B_{PP}(k_s) \\
& + (i\sigma_4^*)(-i\lambda_4) B_{PR}(k_s) + (-i\sigma_4)(-\lambda_\Delta) B_{MR}(k_s) \\
& + (-i\sigma_4)(i\lambda_4^*) B_{PL}(k_s) + (i\sigma_4^*)(-\lambda_\Delta) B_{ML}(k_s) \\
& + \frac{(-i\sigma_4)(-i\sigma_4)}{2} B_{RR}(k_t) + \frac{(i\sigma_4^*)(i\sigma_4^*)}{2} B_{LL}(k_t) + (-\lambda_\Delta)^2 B_{LR}(k_t) \\
& + \frac{(-i\sigma_4)(i\sigma_4^*)}{2} B_{PM}(k_t) + \frac{(i\sigma_4^*)(-i\sigma_4)}{2} B_{MP}(k_t) + (-\lambda_\Delta)^2 B_{PP}(k_t) \\
& + (-i\sigma_4)(-\lambda_\Delta) B_{PR}(k_t) + (-i\sigma_4)(-\lambda_\Delta) B_{MR}(k_t) \\
& + (i\sigma_4^*)(-\lambda_\Delta) B_{PL}(k_t) + (i\sigma_4^*)(-\lambda_\Delta) B_{ML}(k_t) \\
& + (k_t \longleftrightarrow k_u)
\end{aligned} \tag{3.27}$$

The one-loop divergence can be removed by adding the following counter-term

$$\begin{aligned}
\delta\lambda_\Delta \Big|_{\overline{\text{MS}}} = & -\frac{1}{(4\pi)^2 i} \left[ (\lambda_4 + 2\sigma_4^*)(\sigma_4^* + i\lambda_\Delta) + 3i\sigma_4\lambda_\Delta - c.c. \right] \\
& \left[ \frac{1}{d-4} + \frac{1}{2}(\gamma_E - \ln 4\pi) \right]
\end{aligned} \tag{3.28}$$



**Figure 15:** Diagrammatic representation of the Ten 1-Loop Integrals  $\phi_R\phi_R \rightarrow \phi_L\phi_L$  (Here  $k_t = k_1 + k_2$ )

and one loop beta function for  $\lambda_\Delta$  is given by

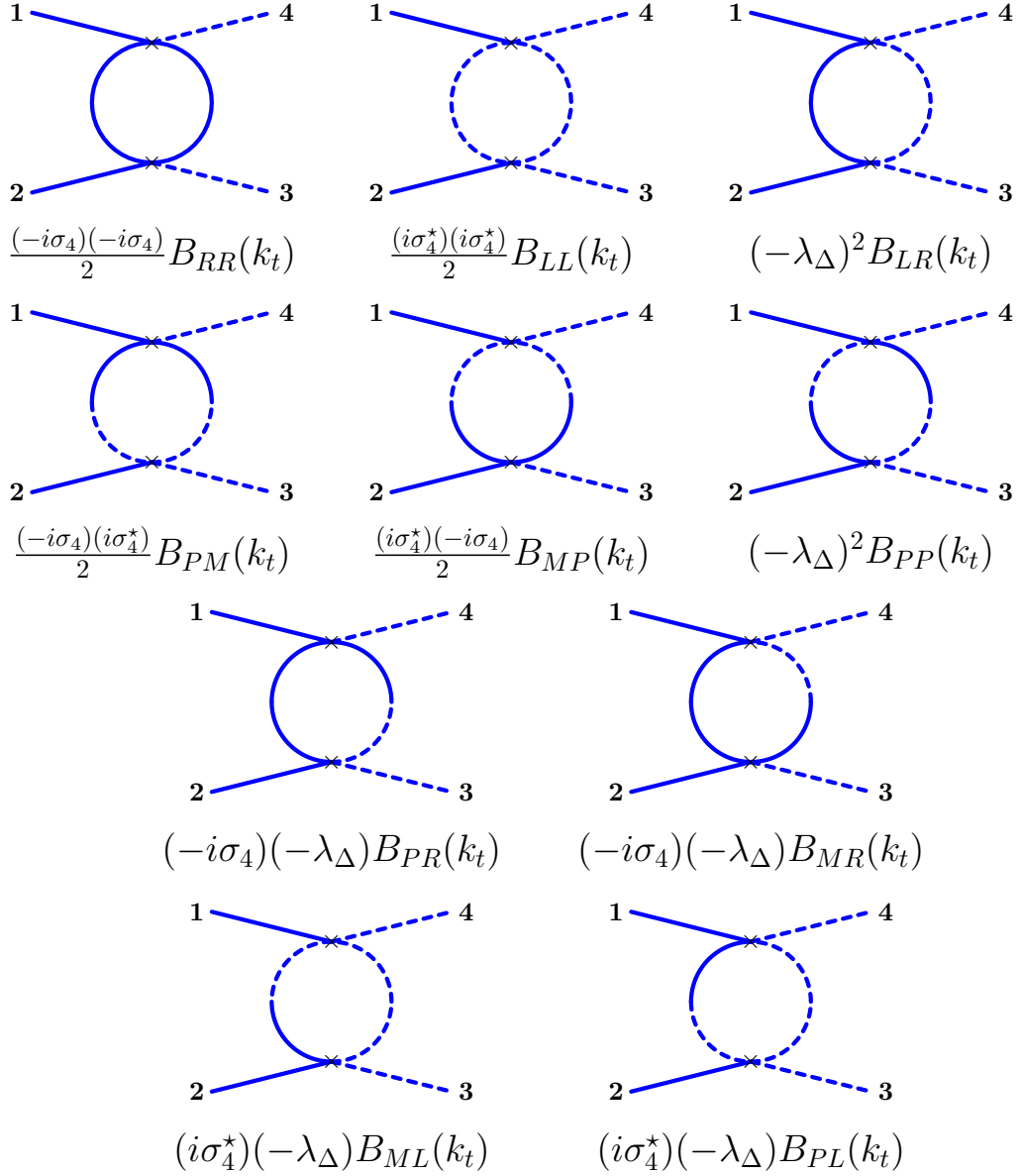
$$\begin{aligned}
\beta_{\lambda_\Delta} &= \frac{1}{(4\pi)^2 i} \left[ \lambda_4(\sigma_4^* + i\lambda_\Delta) - 2\sigma_4^2 + 5i\sigma_4\lambda_\Delta - \lambda_4^*(\sigma_4 - i\lambda_\Delta) + 2(\sigma_4^*)^2 + 5i\sigma_4^*\lambda_\Delta \right] \\
&= \frac{1}{(4\pi)^2 i} \left[ (\lambda_4 + 2\sigma_4^*)(\sigma_4^* + i\lambda_\Delta) + 3i\sigma_4\lambda_\Delta - c.c. \right]
\end{aligned} \tag{3.29}$$

### 3.10 Checking Lindblad condition for quartic couplings

From equation (3.23), equation (3.26) and equation (3.29), we can compute the one loop beta function for the Lindblad combination. We have

$$\beta_{(\text{Im } \lambda_4 + 4 \text{ Im } \sigma_4 - 3\lambda_\Delta)} = \frac{6}{(4\pi)^2} (\text{Im } \lambda_4 + 4 \text{ Im } \sigma_4 - 3\lambda_\Delta) (\text{Re } \lambda_4 + 2\text{Re } \sigma_4) \quad (3.30)$$

This equation, along with (3.7) and (3.8), implies that if one starts with a Lindblad theory then one loop renormalization preserves the Lindblad condition.



**Figure 16:** Diagrammatic representation of the Ten 1-Loop Integrals  $\phi_R\phi_R \rightarrow \phi_L\phi_L$  (Here  $k_t = k_1 + k_4$ )

### 3.11 Summary of the results

We started with the most general Lagrangian of a mixed system described by a scalar field with cubic and quartic coupling in (1.1). Using this action, we have demonstrated that the standard counter-term technique of unitary QFTs can be extended to deal with the one-loop UV divergences of the open EFT. We have then computed the beta functions of this open EFT, summarized in equation (1.3), (1.4) and (1.5) of the introduction. One can then use these beta functions to determine the running of the Lindblad violating combinations ( $\text{Im } m^2 - m_\Delta^2$ ),



$(\text{Im } \lambda_3 + 3\text{Im } \sigma_3)$  and  $(\text{Im } \lambda_4 + 4\text{Im } \sigma_4 - 3\lambda_\Delta)$  giving Eq. (1.6). The equation Eq.(1.6) shows that the beta function of the Lindblad violating couplings are proportional to the Lindblad violating couplings. In other words, if we set the Lindblad violating coupling to zero at tree level then the Lindblad violating coupling will not be generated under one loop renormalization.

## 4 Computation in the average-difference basis

In section 3, we had computed the one loop beta functions for various couplings of an open  $\phi^3 + \phi^4$  theory. In particular, by looking at the Lindblad violating couplings, we found that the Lindblad condition is preserved under one loop renormalization. In this section, we will rewrite the perturbation theory in a different basis where this fact is manifest. We would also like to prove that the preservation of Lindblad conditions hold to arbitrary perturbative order. The proof that we present here is very much inspired by a corresponding argument in the context of cutting rules in a unitary theory and uses a version of Feynman tree theorem.

The basis we shift to is often termed the Keldysh basis. It is made of the average and difference of bra and ket fields. This basis has an advantage that the difference operator decouplings are more manifest in this basis while it obscures the cutting rule interpretation of various diagrams involved. While the unitary vertices are mixed up with the Feynman-Vernon couplings in this basis, the computations do greatly simplify owing to lesser number of divergent diagrams and vanishing of difference-difference propagator. Our discussion here would necessarily be brief, since the details are straightforward and similar to the computation in the previous section. For a more detailed presentation, we refer the reader to appendix D

### 4.1 Action in the average-difference basis

We define  $\phi_d$  and  $\phi_a$  such that

$$\phi_d = \phi_R - \phi_L \quad \phi_a = \frac{1}{2}(\phi_R + \phi_L) \quad (4.1)$$

where the subscripts  $d$  and  $a$  denote ‘difference’ and ‘average’ respectively.

The Lagrangian in this basis is given by

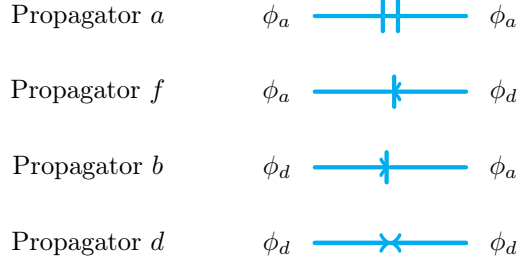
$$\begin{aligned} i\mathcal{L} = & + \frac{1}{2 \times 2!} (\text{Im } z + z_\Delta) (\partial\phi_d)^2 + (-i)(\text{Re } z)(\partial\phi_a) \cdot (\partial\phi_d) \\ & + \frac{1}{2 \times 2!} (\text{Im } m^2 + m_\Delta^2) \phi_d^2 + (-i)(\text{Re } m^2) \phi_a \phi_d \\ & + (-i)(\text{Re } \lambda_3 + \text{Re } \sigma_3) \frac{\phi_a^2 \phi_d}{2!} + \frac{1}{2} (\text{Im } \lambda_3 - \text{Im } \sigma_3) \frac{\phi_a \phi_d^2}{2!} + \frac{(-i)}{4} (\text{Re } \lambda_3 - 3 \text{Re } \sigma_3) \frac{\phi_d^3}{3!} \\ & + (-i)(\text{Re } \lambda_4 + 2 \text{Re } \sigma_4) \frac{\phi_a^3 \phi_d}{3!} + \frac{1}{2} (\text{Im } \lambda_4 + \lambda_\Delta) \frac{\phi_a^2 \phi_d^2}{2!2!} + \frac{(-i)}{4} (\text{Re } \lambda_4 - 2 \text{Re } \sigma_4) \frac{\phi_a \phi_d^3}{3!} \quad (4.2) \\ & + \frac{1}{8} (\text{Im } \lambda_4 - 4 \text{Im } \sigma_4 - 3\lambda_\Delta) \frac{\phi_d^4}{4!} \\ & + \frac{1}{2!} 2(\text{Im } z - z_\Delta) (\partial\phi_a)^2 + \frac{1}{2!} 2(\text{Im } m^2 - m_\Delta^2) \phi_a^2 \\ & + 2(\text{Im } \lambda_3 + 3 \text{Im } \sigma_3) \frac{\phi_a^3}{3!} + 2(\text{Im } \lambda_4 + 4 \text{Im } \sigma_4 - 3\lambda_\Delta) \frac{\phi_a^4}{4!} \end{aligned}$$

The Feynman rules in this basis are given in figure 33. Note that the terms in the last two lines of the Lagrangian involves only the average fields  $\phi_a$ . The coefficients of the purely average couplings are exactly the Lindblad violating couplings. This is expected for the following reason : since  $\phi_d$  vanishes when  $\phi_R = \phi_L$ , the terms that can contribute to the imaginary part of the action, in that limit, are the pure  $\phi_a$  vertices. Since all Lindblad terms vanish in this limit, it follows that pure  $\phi_a$  vertices should be Lindblad violating. In addition, we observe that in the open  $\phi^3 + \phi^4$  theory, all Lindblad violating couplings are of pure average type. This clear separation of the Lindblad violating couplings is the most salient aspect of this basis, making it easy to trace their renormalisation.

The propagators in this basis are given by [15, 23, 24]

$$\begin{aligned}
\text{a} : \langle \mathcal{T}_{SK} \phi_a \phi_a \rangle &= \frac{1}{2} \langle \mathcal{T}_{SK} \phi_R \phi_R \rangle + \frac{1}{2} \langle \mathcal{T}_{SK} \phi_L \phi_L \rangle \\
\text{f} : \langle \mathcal{T}_{SK} \phi_a \phi_d \rangle &= \langle \mathcal{T}_{SK} \phi_R \phi_R \rangle - \langle \mathcal{T}_{SK} \phi_R \phi_L \rangle \\
\text{b} : \langle \mathcal{T}_{SK} \phi_d \phi_a \rangle &= \langle \mathcal{T}_{SK} \phi_R \phi_R \rangle - \langle \mathcal{T}_{SK} \phi_L \phi_R \rangle \\
\text{d} : \langle \mathcal{T}_{SK} \phi_d \phi_d \rangle &= 0
\end{aligned} \tag{4.3}$$

Please note that we will use a different color for propagators in the average-difference basis. Also, we shall be using results presented in appendix C. In this basis, only the tadpole  $A_a$  diverges



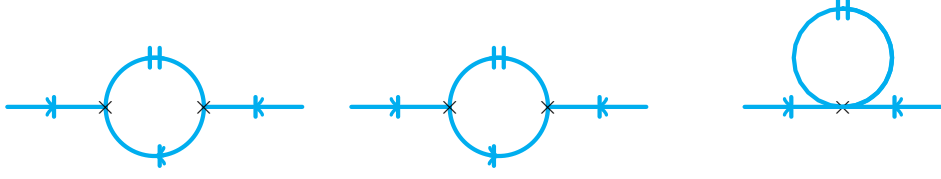
**Figure 17:** Propagators in the average-difference basis

(C.1) and its divergence is same as the divergence of usual PV  $A$  diagram. All other  $A$  integrals,  $A_f, A_b$  and  $A_d$ , vanish. Similarly, only the bubbles  $B_{af}, B_{ab}$  diverge and their divergence is half the divergence of the usual PV  $B$  diagram (C.3).

## 4.2 One loop computations

As mentioned before, the computation greatly simplifies in this basis. All the computations in average-difference basis can be found in appendix D. Here we shall demonstrate only a few examples. For instance, let us compute the beta function of one of the Lindblad violating terms,  $(\text{Im } m^2 - m_\Delta^2)$ . In figure 18, we have considered all the divergent diagrams (i.e., the diagrams involving  $A_a, B_{af}$  and  $B_{ab}$ ) that contribute to the process  $\phi_d \rightarrow \phi_d$ . The total contribution to the process is given by

$$\begin{aligned}
2(\text{Im } m^2 - m_\Delta^2) + 2(\text{Im } \lambda_3 + 3 \text{Im } \sigma_3) \times (-i)(\text{Re } \lambda_3 + \text{Re } \sigma_3)(B_{af} + B_{ab}) \\
+ 2(\text{Im } \lambda_4 + 4 \text{Im } \sigma_4 - 3\lambda_\Delta)(\text{Re } m^2)A_a
\end{aligned} \tag{4.4}$$



**Figure 18:** Renormalization of the Lindblad violating mass term in the average-difference basis

Hence, the one loop beta function for the Lindblad violating mass term is given by

$$\frac{d}{d\ln\mu}(\text{Im } m^2 - m_\Delta^2) = \frac{1}{(4\pi)^2} \left[ 2(\text{Im } \lambda_3 + 3 \text{Im } \sigma_3)(\text{Re } \lambda_3 + \text{Re } \sigma_3) + (\text{Re } m^2)(\text{Im } \lambda_4 + 4 \text{Im } \sigma_4 - 3\lambda_\Delta) \right] \quad (4.5)$$

We had obtained the same result (equation (3.8)) in the other basis. Notice that the beta function of the Lindblad violating term can easily be computed just by computing one process in this basis.

Similarly, one can calculate the beta function of the Lindblad violating term  $(\text{Im } \lambda_3 + 3 \text{Im } \sigma_3)$ . Divergent diagrams for one particular channel is depicted in figure 19. There are two more channels. The total contribution is given as



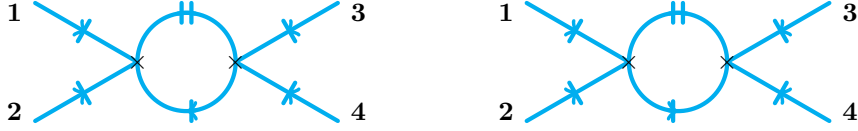
**Figure 19:** Renormalization of the Lindblad violating cubic coupling in the average-difference basis

$$\begin{aligned} & 2(\text{Im } \lambda_3 + 3 \text{Im } \sigma_3) \\ & + 2(\text{Im } \lambda_3 + 3 \text{Im } \sigma_3) \times (-i)(\text{Re } \lambda_4 + 2 \text{Re } \sigma_4)[B_{af}(k_1) + B_{af}(k_2) + B_{af}(k_3)] \\ & + 2(\text{Im } \lambda_4 + 4 \text{Im } \sigma_4 - 3\lambda_\Delta) \times (-i)(\text{Re } \lambda_3 + \text{Re } \sigma_3)[B_{ab}(k_1) + B_{ab}(k_2) + B_{ab}(k_3)] \end{aligned} \quad (4.6)$$

Following the standard procedures, we can very easily compute the one loop beta function and it is given by

$$\begin{aligned} \frac{d}{d\ln\mu}(\text{Im } \lambda_3 + 3 \text{Im } \sigma_3) &= \frac{3}{(4\pi)^2}(\text{Im } \lambda_3 + 3 \text{Im } \sigma_3)(\text{Re } \lambda_4 + 2 \text{Re } \sigma_4) \\ &+ \frac{3}{(4\pi)^2}(\text{Im } \lambda_4 + 4 \text{Im } \sigma_4 - 3\lambda_\Delta)(\text{Re } \lambda_3 + \text{Re } \sigma_3) \end{aligned} \quad (4.7)$$

Now, let us we compute the beta function of Lindblad violating term  $(\text{Im } \lambda_4 + 4 \text{Im } \sigma_4 - 3\lambda_\Delta)$  by computing the process  $\phi_d\phi_d \rightarrow \phi_d\phi_d$  via  $\phi_a^4$  vertex, which is depicted in figure 20. The total contribution is given by



**Figure 20:** Renormalization of the Lindblad violating quartic coupling in the average-difference basis

$$\begin{aligned}
& 2(\text{Im } \lambda_4 + 4 \text{ Im } \sigma_4 - 3\lambda_\Delta) \\
& + (2 \text{ diagrams})(3 \text{ channels}) \times 2(\text{Im } \lambda_4 + 4 \text{ Im } \sigma_4 - 3\lambda_\Delta) \\
& \times (-i)(\text{Re } \lambda_4 + 2 \text{ Re } \sigma_4) \times \frac{i}{2(4\pi)^2} \left( \frac{2}{d-4} + \ln \frac{1}{4\pi e^{-\gamma_E}} \right)
\end{aligned} \tag{4.8}$$

Hence, the one loop beta function is

$$\frac{d}{d \ln \mu} (\text{Im } \lambda_4 + 4 \text{ Im } \sigma_4 - 3\lambda_\Delta) = \frac{6}{(4\pi)^2} (\text{Im } \lambda_4 + 4 \text{ Im } \sigma_4 - 3\lambda_\Delta) (\text{Re } \lambda_4 + 2 \text{ Re } \sigma_4) \tag{4.9}$$

The usefulness of average-difference basis is quite evident from these three calculations. The complete computation in average-difference basis can be found in appendix D.

### 4.3 Lindblad condition is never violated by perturbative corrections

In this section, we will give an all order perturbative argument for why Lindblad conditions are not violated to arbitrary order in perturbation theory. Consider the action in the average-difference basis given in (4.2). From this expression we note that all the Lindblad violating couplings of open  $\phi^3 + \phi^4$  theory appear as the coupling constants for the pure average vertices. Our argument below can be easily extended to any open QFT which has the property that all Lindblad violating vertices are pure average vertices. Note that the converse is always true in an open EFT : any pure average vertex is necessarily Lindblad violating (since it contributes to the action even in the  $\phi_R = \phi_L$  limit).

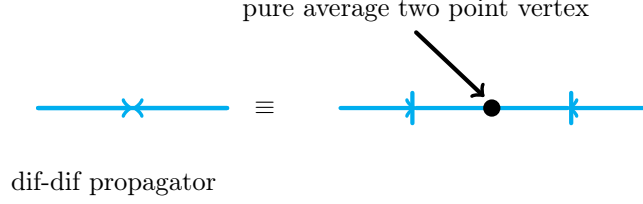
Now we want to show that if we start from the open  $\phi^3 + \phi^4$  theory, then the Lindblad condition(s) are never violated under perturbative corrections using the fact that they are all of pure average type. In other words, by assuming that there is no pure average vertex at tree level, and that there is no difference-difference propagator, we would like to show that such a vertex/propagator can never be generated under loop corrections. We will prove it in three steps.

We will begin with an

- **Assumption:** At tree level, one has no pure-average vertex and no pure-difference propagator. All Lindblad violating couplings are assumed to be pure average vertices and hence are taken to vanish at tree level.
- **Statement 1 :** Say we assume that there is no pure-average 1PI 2 point vertex generated at  $g$  loop. Then, it implies that there is no pure-difference 1 PI propagator generated at  $g$

loop.

**Proof** : According to our starting assumption, there is no tree level pure-difference propagator. Such a propagator can then only be generated by a Feynman diagram of type depicted in figure 21.



**Figure 21:** Pure difference propagator from loop correction(s)

So, any contribution to pure-difference 1 PI propagator is of the form

$$(\text{difference to average tree level propagator}) \times (\text{pure-average 1PI 2 point vertex}) \times (\text{average to diff tree level propagator}).$$

Thus, if there are no pure-average 1PI vertices, there are no pure-difference 1PI propagator.(QED)

- **Statement 2** : If there is no pure-average 1PI vertex at  $g$  loops, there is no such vertex at  $g + 1$  loops. This statement via induction, then implies that pure-average 1PI vertices are never generated at any loop order. By our previous statement, this implies then that pure-difference 1 PI propagators are also never generated at any loop order. In order to prove this, we first prove

- **Statement 2a:** Consider a Feynman diagram contributing to a pure-average 1PI vertex. There must be at least one vertex (internal or external) such that the following is true : there exists a closed path completely made of  $b$ -type propagators which begins and ends in that vertex (it may or may not pass through external vertices).

**Proof** : Since we are considering a diagram contributing to a pure-average 1PI vertex, all the external propagators at every external vertex are of  $a$ -type. By our assumption, there is no pure-average 1PI vertex. Thus, there should be at least one  $d$ -type line leaving at a given external vertex. Since there is no pure-difference propagator, this  $d$ -type line necessarily converts itself into an  $a$ -type line : thus the propagator is of average-difference  $b$ -type with the arrow leaving the external vertex. This propagator thus ends as an  $a$ -type line either in the vertex that one began with, or another external vertex or an internal vertex.

In the first case, we have obtained the desired result : there exists a closed path completely made of  $b$ -type propagators which begins and ends in that vertex.

In the second case, we note that the external vertex has an external  $a$ -type leg, and

the  $b$ -type propagator which went from the starting vertex also ends with an  $a$ -type leg on the second vertex. Since there are no pure-average vertices, there should necessarily be a  $d$ -type leg which is going out of the second vertex. The  $d$ -type leg can again only be a part of an  $b$ -type propagator since there is no pure-difference propagator. A similar argument also applies to the third case of an internal vertex. We can now follow the  $b$ -type propagators and repeat the argument again. This process would terminate (since we are looking at a finite graph) and we would return to some vertex on the path for second time, closing the loop. (QED)

- **Statement 2b:** Any Feynman diagram with a closed path completely made of  $b$ -type propagators is zero.

**Proof:** In position space,  $b$ -type propagators are just retarded propagators. The  $b$ -type propagator, using equation (4.3), in position space is given by,

$$\begin{aligned}
& \int \frac{d^4 p}{(2\pi)^4} \left( \frac{-i}{p^2 + m^2 - i\epsilon} - 2\pi\delta_-(p^2 + m^2) \right) e^{ip(x-y)} \\
&= \int \frac{d^4 p}{(2\pi)^4} \frac{-i}{p^2 + m^2 - i\epsilon} e^{ip(x-y)} - \int \frac{d^4 p}{(2\pi)^3} \Theta(-p_0) \delta(p^2 + m^2) e^{ip(x-y)} \\
&= \int \frac{d^3 p}{(2\pi)^3} e^{i\vec{p}\cdot(\vec{x}-\vec{y})} \left( \Theta(x_0 - y_0) \frac{e^{-i\omega_p(x_0-y_0)}}{2\omega_p} + \Theta(y_0 - x_0) \frac{e^{i\omega_p(x_0-y_0)}}{2\omega_p} \right) \\
&\quad - \int \frac{d^3 p}{(2\pi)^3} e^{i\vec{p}\cdot(\vec{x}-\vec{y})} \frac{e^{i\omega_p(x_0-y_0)}}{2\omega_p} (\Theta(x_0 - y_0) + \Theta(y_0 - x_0)) \\
&= \Theta(x_0 - y_0) \int \frac{d^3 p}{(2\pi)^3} e^{i\vec{p}\cdot(\vec{x}-\vec{y})} \left( \frac{e^{-i\omega_p(x_0-y_0)}}{2\omega_p} - \frac{e^{i\omega_p(x_0-y_0)}}{2\omega_p} \right) \\
&= G_R(x - y)
\end{aligned} \tag{4.10}$$

where,  $\omega_p = (\vec{p}^2 + m^2)^{\frac{1}{2}}$  and  $G_R(x - y)$  denotes the retarded propagator.

We will now use the result that a closed loop of retarded propagators is identically zero. This statement is a part of the Feynman tree theorem [30]. A closed loop of retarded propagators can be written as

$$\int \frac{d^d p}{(2\pi)^d} \prod_i G_R^i(p + k_i) = 0 \tag{4.11}$$

where,  $k_i$  denotes the external momenta. Since all the poles in a retarded propagator are below the real  $p_0$  axis. So, one can close the contour from above, picking no residues and, as a result, the integral vanishes. (QED)

- Statement 2a and 2b imply that if there is no pure average vertex operator or a pure difference propagator at  $g$  loop then there will be no such vertex/propagator at  $g + 1$  loop. From this we conclude, via induction, that if there is no Lindblad violating coupling at tree level, such a coupling is never generated by perturbative corrections.(QED)

This then concludes our argument in the average-difference basis that the Lindblad violating couplings are never generated in loops. The readers familiar with cutting rule arguments ala Veltman in unitary theories would recognise the style of the above argument. The proof that difference operators decouple at arbitrary loops in a unitary theory, or equivalently the proof that Keldysh causal structure is preserved under loop corrections for a unitary theory bear a close resemblance to the proof above. The surprise here is that the argument goes through even without assuming unitarity. We also note the perturbative nature of the above argument, since it invokes the fact that the graphs at any given loop order are finite. It would be interesting to try and give a non-perturbative proof of the statement of this section.

With this formal proof in hand, in next section, we will now turn to a preliminary study of the RG running in our open EFT. The interesting question is to map out behaviour novel to open EFTs which cannot be found in unitary QFTs.

## 5 Running of the coupling constants and physical meaning

In this section, we will perform an analysis of the running of couplings from our 1-loop beta functions. Given the many couplings involved in the the RG equations in (1.3),(1.4) and (1.5), we will begin with a judicious rewriting of our equations. Once the Lindblad conditions are imposed, we obtain the following count for the couplings :

1. 5 quartic couplings + 1 lindblad condition (1.7)  $\implies$  4 independent quartic couplings
2. 4 cubic couplings+ 1 lindblad condition (1.7)  $\implies$  3 independent cubic couplings
3. 3 mass terms + 1 lindblad condition (1.7)  $\implies$  2 independent mass terms

Our RG equations for these 9 independent variables can then be recast into the following

convenient form :

$$\begin{aligned}
\beta_{\text{Re } \lambda_4 + 2\text{Re } \sigma_4} &= \frac{3}{(4\pi)^2} (\text{Re } \lambda_4 + 2\text{Re } \sigma_4)^2 \\
\beta_{\text{Im } \lambda_4 + \text{Im } \sigma_4} &= \frac{5}{(4\pi)^2} (\text{Im } \lambda_4 + \text{Im } \sigma_4) (\text{Re } \lambda_4 + 2\text{Re } \sigma_4) \\
\beta_{\text{Re } \lambda_4} &= \frac{1}{3(4\pi)^2} \left( 9\text{Re } \lambda_4 (\text{Re } \lambda_4 + 2\text{Re } \sigma_4) - 8(\text{Im } \lambda_4 + \text{Im } \sigma_4)^2 \right) \\
\beta_{\text{Im } \lambda_4 - 4\text{Im } \sigma_4} &= \frac{10}{(4\pi)^2} \text{Re } \lambda_4 (\text{Im } \lambda_4 + \text{Im } \sigma_4) \\
\beta_{\text{Re } \lambda_3 + \text{Re } \sigma_3} &= \frac{3}{(4\pi)^2} (\text{Re } \lambda_3 + \text{Re } \sigma_3) (\text{Re } \lambda_4 + 2\text{Re } \sigma_4) \\
\beta_{\text{Im } \lambda_3} &= -3\beta_{\text{Im } \sigma_3} = \frac{1}{(4\pi)^2} (3(\text{Im } \lambda_4 + \text{Im } \sigma_4) (\text{Re } \lambda_3 + \text{Re } \sigma_3) + 2\text{Im } \lambda_3 (\text{Re } \lambda_4 + 2\text{Re } \sigma_4)) \\
\beta_{\text{Re } \lambda_3 - \text{Re } \sigma_3} &= \frac{1}{3(4\pi)^2} (9\text{Re } \lambda_4 (\text{Re } \lambda_3 + \text{Re } \sigma_3) - 8\text{Im } \lambda_3 (\text{Im } \lambda_4 + \text{Im } \sigma_4)) \\
\beta_{\text{Re } m^2} &= \frac{1}{(4\pi)^2} \left( (\text{Re } \lambda_3 + \text{Re } \sigma_3)^2 + \text{Re } m^2 (\text{Re } \lambda_4 + 2\text{Re } \sigma_4) \right) \\
\beta_{\text{Im } m^2} &= \beta_{m_\Delta^2} = \frac{2}{3(4\pi)^2} (2\text{Im } \lambda_3 (\text{Re } \lambda_3 + \text{Re } \sigma_3) + \text{Re } m^2 (\text{Im } \lambda_4 + \text{Im } \sigma_4))
\end{aligned} \tag{5.1}$$

Note the simple structure of the 9 coupled differential equations given above. We have ordered them such that the  $j$ th equation depends only on the variables appearing in the first  $j - 1$  equations. As a result, a step by step method of solution becomes viable : one can start by solving the first equation for a given initial condition and then use the solution of the first equation as an input to solve the second equation and so on, for all the subsequent equations.

The first, the second and the fifth equation imply the existence of the fixed point, given by

$$\text{Re } \lambda_4 = -2\text{Re } \sigma_4, \quad \text{Im } \lambda_4 = -\text{Im } \sigma_4 \tag{5.2}$$

$$\text{Re } \lambda_3 = -\text{Re } \sigma_3. \tag{5.3}$$

To analyse the nature of this fixed point, we turn to the first equation which drives them all. It can be written as

$$\beta_{|\text{Re } \lambda_4 + 2\text{Re } \sigma_4|} = \text{sign}(\text{Re } \lambda_4 + 2\text{Re } \sigma_4) \frac{3}{(4\pi)^2} |\text{Re } \lambda_4 + 2\text{Re } \sigma_4|^2 \tag{5.4}$$

This implies that depending on the sign of the initial value,  $\text{Re } \lambda_4 + 2\text{Re } \sigma_4$  either increases or decreases as we go to higher energy scales. As we will see, this sign controls whether the theory is UV free or IR free. We recognise in the RG equation for  $\text{Re } \lambda_4 + 2\text{Re } \sigma_4$  the usual  $\phi^4$  coupling RG equation with  $\text{Re } \lambda_4 + 2\text{Re } \sigma_4$  serving as an effective  $\phi^4$  coupling. The asymptotically free regime and the negative beta function corresponds to this effective  $\phi^4$  coupling turning negative and is hence akin to the theory studied by Symanzik [31].<sup>4</sup>

We will begin by performing a linearised analysis around the fixed point mentioned above and follow it up with a more detailed numerical analysis.

---

<sup>4</sup>We would like to thank Nima Arkani-Hamed for a discussion of this issue and bringing the relevant literature to our attention.



## 5.1 Linearized analysis around the fixed point

In this section, we study linearized beta functions around the fixed points and find the eigenvalues and eigenvectors of the beta function matrix. Consider small deviations around the fixed points

$$\begin{aligned} \text{Re } \lambda_4 + 2 \text{Re } \sigma_4 &= \epsilon_1 \\ \text{Im } \lambda_4 + \text{Im } \sigma_4 &= \epsilon_2 \\ \text{Re } \lambda_3 + \text{Re } \sigma_3 &= \epsilon_3 \end{aligned} \tag{5.5}$$

where, we have assumed

$$|\epsilon_i| \ll 1 \quad \forall i = 1, 2, 3 \tag{5.6}$$

The linearized beta functions for  $\text{Re } \lambda_4 + 2\text{Re } \sigma_4$ ,  $\text{Im } \lambda_4 + \text{Im } \sigma_4$  and  $\text{Re } \lambda_3 + \text{Re } \sigma_3$  are zero. This suggests that  $\epsilon_1$ ,  $\epsilon_2$  and  $\epsilon_3$  remain constant (i.e., they are marginal couplings at the fixed point).

The rest of the linearized beta functions about the fixed point can be written as

$$\frac{d}{dt} \mathcal{G}(t) = \mathcal{B} \mathcal{G}(t) \tag{5.7}$$

in terms of the RG time  $t \equiv \frac{\ln \mu}{(4\pi)^2}$ . Here we have defined the coupling constant matrix  $\mathcal{G}$  as

$$\mathcal{G} \equiv \begin{pmatrix} \text{Re } \lambda_4 \\ \text{Im } \lambda_4 - 4\text{Im } \sigma_4 \\ \text{Im } \lambda_3 \\ \text{Re } \lambda_3 - \text{Re } \sigma_3 \\ \text{Re } m^2 \\ \text{Im } m^2 \end{pmatrix} \tag{5.8}$$

and the beta function matrix  $\mathcal{B}$  is given by

$$\mathcal{B} \equiv \begin{pmatrix} 3\epsilon_1 & 0 & 0 & 0 & 0 & 0 \\ 10\epsilon_2 & 0 & 0 & 0 & 0 & 0 \\ 0 & 0 & 2\epsilon_1 & 0 & 0 & 0 \\ 3\epsilon_3 & 0 & -\frac{8\epsilon_2}{3} & 0 & 0 & 0 \\ 0 & 0 & 0 & 0 & \epsilon_1 & 0 \\ 0 & 0 & \frac{4\epsilon_3}{3} & 0 & \frac{2\epsilon_2}{3} & 0 \end{pmatrix} \tag{5.9}$$

The six eigenvalues of the matrix  $\mathcal{B}$  are  $-0, 0, 0, \epsilon_1, 2\epsilon_1, 3\epsilon_1$ . The corresponding eigenvectors are given by:

$$\begin{pmatrix} 0 \\ 1 \\ 0 \\ 0 \\ 0 \\ 0 \end{pmatrix}, \begin{pmatrix} 0 \\ 0 \\ 0 \\ 1 \\ 0 \\ 0 \end{pmatrix}, \begin{pmatrix} 0 \\ 0 \\ 0 \\ 0 \\ 0 \\ 1 \end{pmatrix}, \begin{pmatrix} 0 \\ 0 \\ 0 \\ 0 \\ 3\epsilon_1 \\ 2\epsilon_2 \end{pmatrix}, \begin{pmatrix} 0 \\ 0 \\ 3\epsilon_1 \\ -4\epsilon_2 \\ 0 \\ 2\epsilon_3 \end{pmatrix}, \begin{pmatrix} 3\epsilon_1 \\ 10\epsilon_2 \\ 0 \\ 3\epsilon_3 \\ 0 \\ 0 \end{pmatrix} \tag{5.10}$$

Eigenvalues of the matrix  $\mathcal{B}$  suggest that three out of the six coupling combinations are marginal at the fixed point. The asymptotic behavior of the rest of the variables depend only on the sign of  $\epsilon_1$  or  $\text{Re } \lambda_4 + 2\text{Re } \sigma_4$ . A positive  $\epsilon_1$  would mean that the couplings become relevant in UV, whereas a negative  $\epsilon_1$  would mean that the couplings are relevant in IR. This conforms to the intuition we presented in the beginning of this section : the coupling  $\text{Re } \lambda_4 + 2\text{Re } \sigma_4$  runs like the quartic coupling of an ordinary  $\phi^4$  theory : the theory is IR free for positive value of this combination whereas it is UV free (asymptotically free) for negative value of this combination. This coupling then drives all other couplings to be either IR free or asymptotically free.

Let us now extend our analysis beyond the linearised regime around the fixed points, given by

$$\text{Re } \lambda_4 = -2\text{Re } \sigma_4, \quad \text{Im } \lambda_4 = -\text{Im } \sigma_4 \quad (5.11)$$

$$\text{Re } \lambda_3 = -\text{Re } \sigma_3. \quad (5.12)$$

We will begin by re-examining eqn.(5.1) to gain more qualitative insight on the nature of running in this theory:

1. We will begin with the statement that, depending on the sign of the initial value,  $\text{Re } \lambda_4 + 2\text{Re } \sigma_4$  either increases or decreases as we go to higher energy scales . Thus, we can have two distinct scenarios
  - (a)  $\text{Re } \lambda_4 + 2\text{Re } \sigma_4 > 0$
  - (b)  $\text{Re } \lambda_4 + 2\text{Re } \sigma_4 < 0$ .
2. The second equation depends upon the sign of  $(\text{Re } \lambda_4 + 2\text{Re } \sigma_4)$  as well as on the sign of the initial value of  $\text{Im } \lambda_4 + \text{Im } \sigma_4$ . For instance, keeping a positive  $\text{Re } \lambda_4 + 2\text{Re } \sigma_4$  and a negative initial value of  $\text{Im } \lambda_4 + \text{Im } \sigma_4$  would result in a decreasing behavior as shown in figure 23 and figure 25. Thus, we have two further sub-cases, depending upon the sign of  $\text{Im } \lambda_4 + \text{Im } \sigma_4$ .
3. The third and fourth equation implies that the evolution of  $\text{Re } \lambda_4$  and  $\text{Im } \lambda_4 - 4\text{Im } \sigma_4$  depends only on the values of  $\text{Re } \lambda_4 + 2\text{Re } \sigma_4$  and  $\text{Im } \lambda_4 + \text{Im } \sigma_4$ , given the assumption that the imaginary couplings are small compared to the real ones.
4. The fifth equation is similar to the second equation. Hence, there will again be two sub-cases.
5. It's easy to verify that, with the help of similar reasonings, the remaining equations will not provide us with further sub-cases.

We found that the key conclusion remains unchanged for  $\text{Re } \lambda_3 + \text{Re } \sigma_3 \geq 0$ . So we will always be considering the case  $\text{Re } \lambda_3 + \text{Re } \sigma_3 \geq 0$  together. Thus, we conclude that we can broadly have 8 cases in total and they basically correspond to the two sides of either of these three fixed points: each fixed point will provide two cases and we have  $2^3$  cases altogether.

With this insight, we will proceed to a more detailed numerical analysis.

## 5.2 Numerical analysis of RG equations

In this subsection, we continue our analysis of the various possible cases in the RG evolution equations. It is useful to have a rough criteria to check the validity of our analysis and as to when the analysis can be interpreted physically. We will perform this analysis only for the Lindblad theory, where the coupling constants obey the Lindblad conditions. We shall always work in a regime where the imaginary couplings are smaller compared to the real ones (since this is the regime where our beta functions were derived). Moreover, we will demand the following bounds

$$\lambda_\Delta < 0, \quad m_\Delta^2 < 0 \quad (5.13)$$

which seem to be reasonable from the point of microscopic unitarity[22]. We will deem the couplings which do not satisfy this bound as unphysical in the following. The initial conditions are chosen keeping these physical bounds in consideration and we shall analyse the dynamics corresponding to all the possible behaviors.

### 5.2.1 I: $\text{Re } \lambda_4 + 2\text{Re } \sigma_4 > 0$ , $\text{Im } \lambda_4 + \text{Im } \sigma_4 > 0$ and $\text{Re } \lambda_3 + \text{Re } \sigma_3 \geq 0$

The first equation in (5.1) tells us that the sign of  $\text{Re } \lambda_4 + 2\text{Re } \sigma_4$  will remain positive in this regime. In particular,  $\text{Re } \lambda_4 + 2\text{Re } \sigma_4$  evolves in the same way as  $\lambda_{\text{Unitary}}$ <sup>5</sup>. Now, from the second equation, one can see that  $\text{Im } \lambda_4 + \text{Im } \sigma_4$  will keep increasing if it starts at a positive initial value, but at a slower rate compared to  $\text{Re } \lambda_4 + 2\text{Re } \sigma_4$ . Similarly, from the third and fourth equation, one can see that, keeping in mind the assumptions, both  $\text{Re } \lambda_4$  and  $\text{Im } \lambda_4 - 4\text{Im } \sigma_4$  will increase in the way as shown in figure 22. Note here that  $\text{Im } \lambda_4 - 4\text{Im } \sigma_4$  rises faster than  $\text{Im } \lambda_4 + \text{Im } \sigma_4$  and thus, it results in a continuously increasing  $\text{Im } \lambda_4$  and a decreasing  $\text{Im } \sigma_4$  as shown in the second diagram in figure 22. Also, the increase of  $\text{Im } \lambda_4$  is faster than the decrease of  $\text{Im } \sigma_4$  and thus, under the RG flow,  $\lambda_\Delta$  becomes positive, which is unphysical. Evolution of the remaining cubic couplings and mass terms variables will not affect the evolution  $\text{Im } \lambda_4$  and  $\text{Im } \sigma_4$ . So, both the sub-cases due to different signs of  $\text{Re } \lambda_3 + \text{Re } \sigma_3$  would have a positive  $\lambda_\Delta$  and thus, these two cases can be deemed as unphysical.

### 5.2.2 II: $\text{Re } \lambda_4 + 2\text{Re } \sigma_4 > 0$ , $\text{Im } \lambda_4 + \text{Im } \sigma_4 < 0$ and $\text{Re } \lambda_3 + \text{Re } \sigma_3 \geq 0$

The evolution of each variable for this case is depicted in figure 23. We observe that the couplings do not violate the physical conditions throughout. One can see that the couplings become stronger in the UV and attain a Landau pole.

### 5.2.3 III: $\text{Re } \lambda_4 + 2\text{Re } \sigma_4 < 0$ , $\text{Im } \lambda_4 + \text{Im } \sigma_4 > 0$ and $\text{Re } \lambda_3 + \text{Re } \sigma_3 \geq 0$

This is a case where the couplings are relevant in IR and remain within the physical bounds throughout as can be observed in figure 24. In this case,  $\text{Re } \lambda_4 + 2\text{Re } \sigma_4$  becomes asymptotically free as can be seen from the first equation in (5.1). The second and fifth equation, meanwhile, tells us that  $\text{Im } \lambda_4 + \text{Im } \sigma_4$  and  $\text{Re } \lambda_3 + \text{Re } \sigma_3$  would go to zero as we go to higher energies. This would also mean that  $\text{Im } \lambda_4 - 4\text{Im } \sigma_4$  becomes constant as  $\text{Im } \lambda_4 + \text{Im } \sigma_4$  goes to zero.  $\text{Im } \lambda_4$  and  $\text{Im } \sigma_4$  become constant at higher energies and  $\lambda_\Delta$  attains a fixed point. With similar reasonings, one can predict the behavior of other couplings.

---

<sup>5</sup> $\lambda_{\text{Unitary}}$  denotes the coupling constant of an unitary  $\phi^4$  theory

$\text{Re } \lambda_4 + 2\text{Re } \sigma_4$	$\text{Im } \lambda_4 + \text{Im } \sigma_4$	$\text{Re } \lambda_3 + \text{Re } \sigma_3$	Conclusion
$> 0$	$> 0$	$\geq 0$	Unphysical
$> 0$	$< 0$	$\geq 0$	Landau pole
$< 0$	$> 0$	$\geq 0$	Relevant in IR
$< 0$	$< 0$	$\geq 0$	Unphysical

**Table 2:** Running of coupling constants

#### 5.2.4 IV: $\text{Re } \lambda_4 + 2\text{Re } \sigma_4 < 0$ , $\text{Im } \lambda_4 + \text{Im } \sigma_4 < 0$ and $\text{Re } \lambda_3 + \text{Re } \sigma_3 \geq 0$

One can observe from figure 25 that this case can be deemed as unphysical as  $\lambda_\Delta$  attains a positive value. It basically comes about due to the sign of  $\text{Im } \lambda_4 + \text{Im } \sigma_4$  as can be seen from the second equation in (5.1).

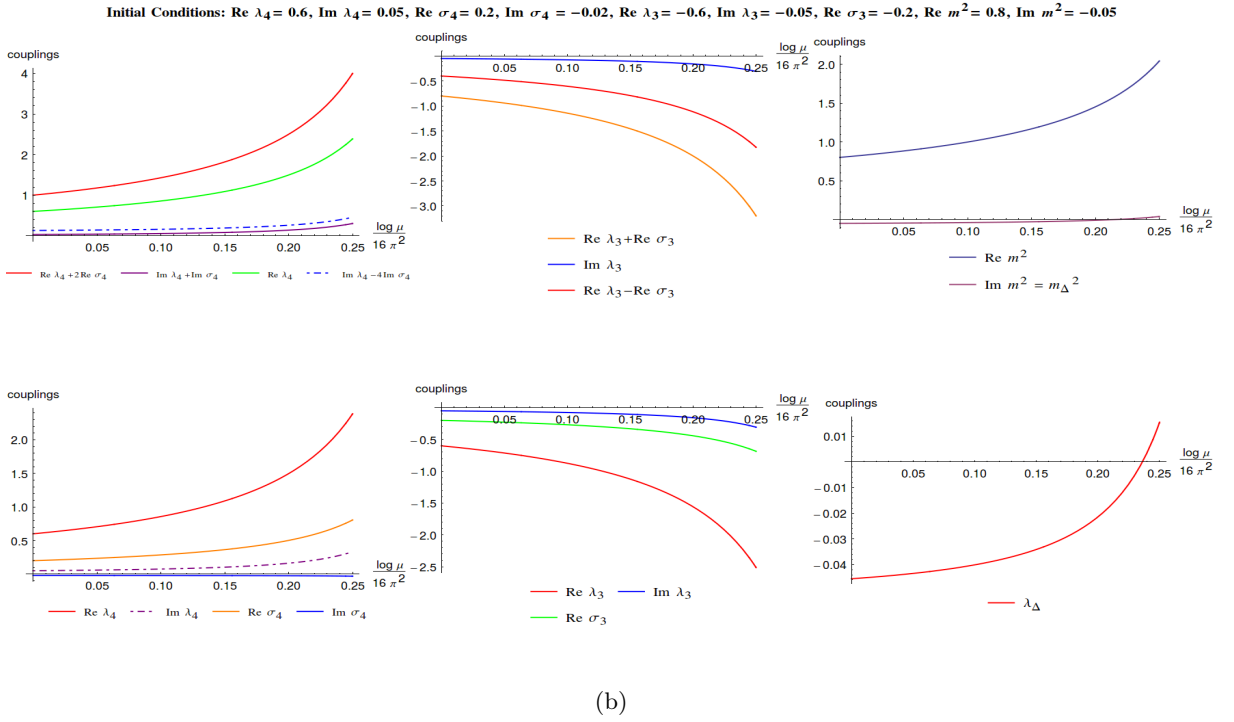
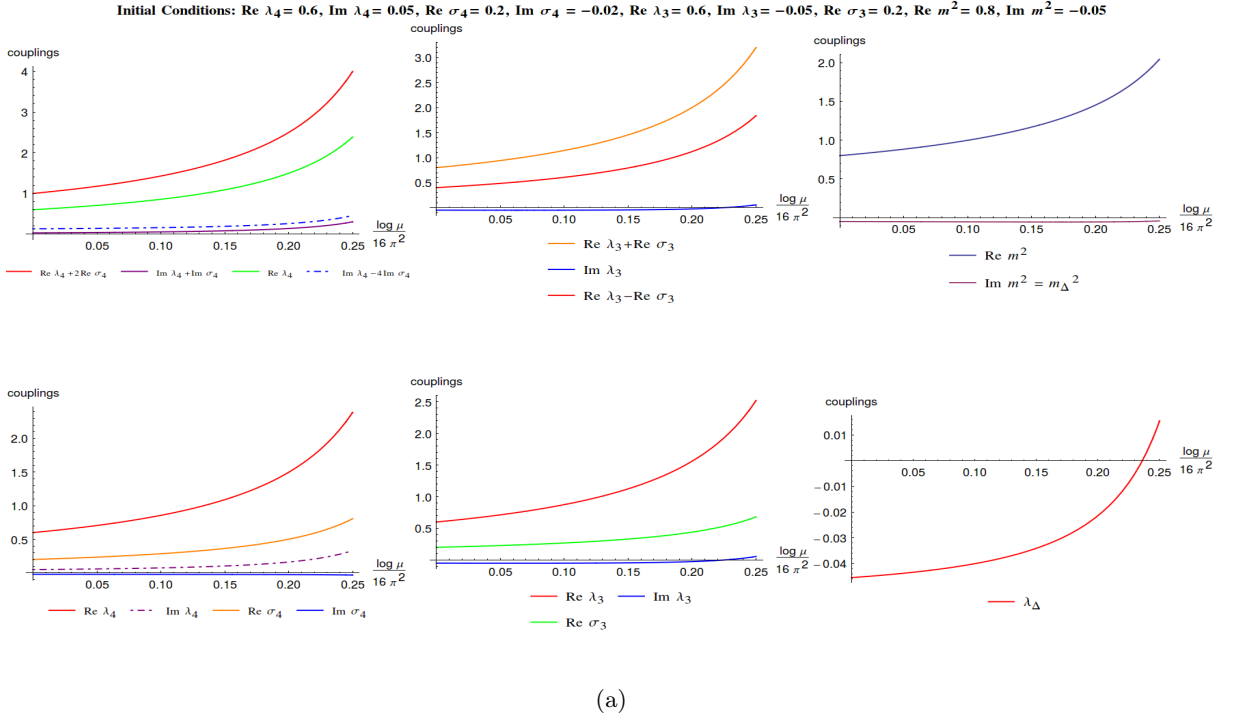
## 6 Conclusion and Future directions

In this work, we considered a simple  $\phi^3 + \phi^4$  toy model of an open quantum field theory in which the renormalisation and the running of couplings could be studied. By enumerating all power-counting renormalisable terms, we demonstrate that the theory is 1-loop renormalisable whereby all UV divergences can be absorbed into appropriate counter-terms. This is in analogy with the standard result for a unitary QFT. The novelty lies in the non-unitary Feynman-Vernon couplings and the corresponding UV divergences which result in a  $\beta$  function for such non-unitary couplings. One of the main results of our paper is that these beta functions surprisingly protect a particular fine-tuning of couplings which is associated with demanding that the non-unitary evolution be that of Lindblad form. We end with an all loop argument on why this protection should extend to any order on perturbation theory.

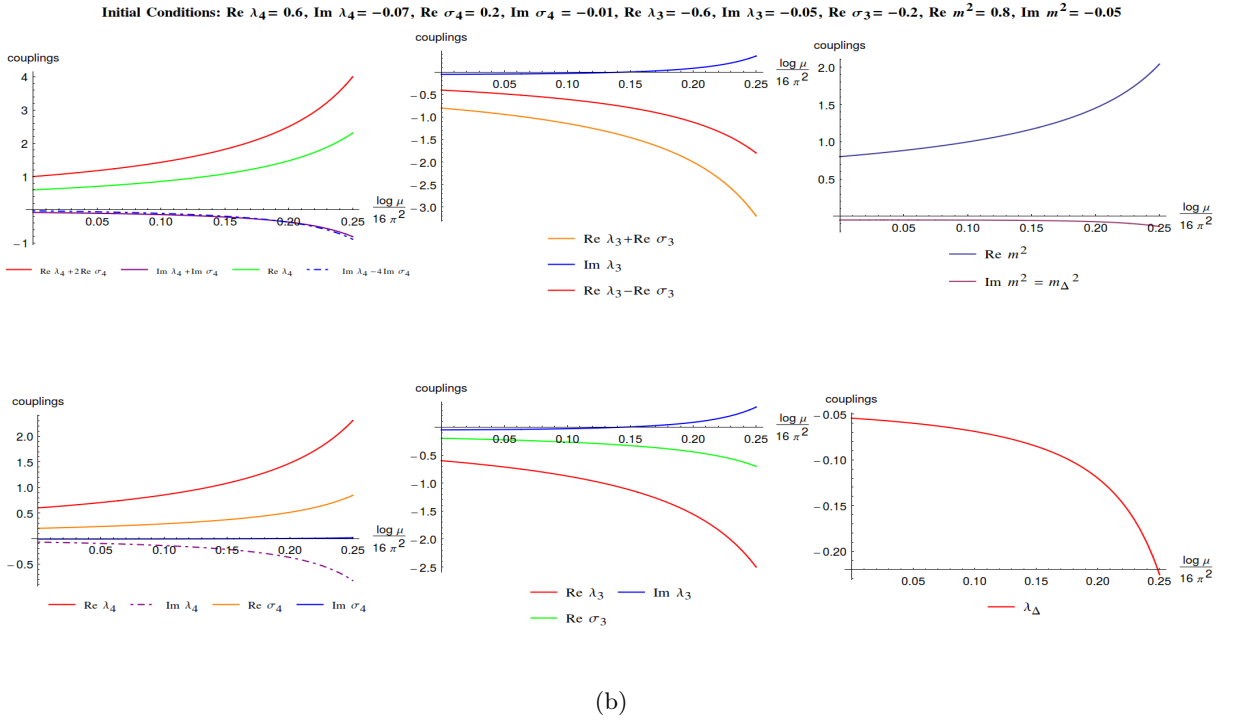
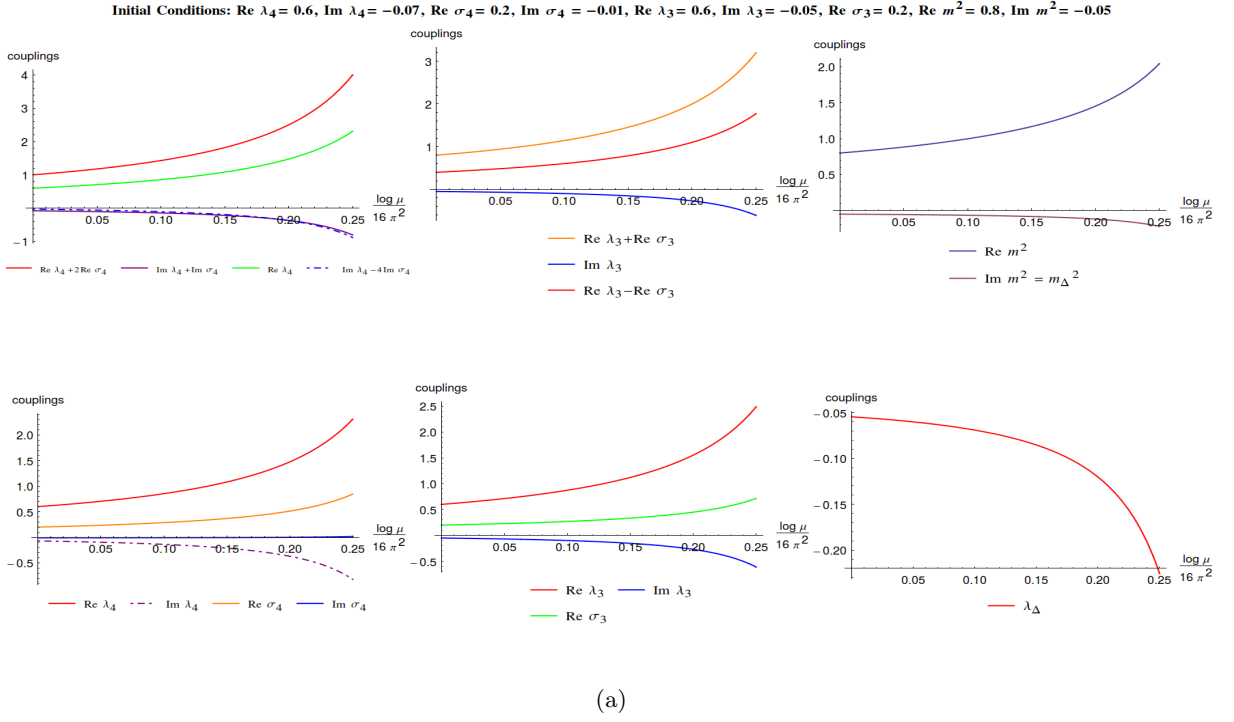
The work described in this article has various natural extensions - to large  $N$  models, to theories with fermions and theories with gauge fields. Given our experience with supersymmetric field theories, open versions of supersymmetric theories may well provide an exactly solvable model of an open QFT where one can study non-perturbative physics as well as dualities. We hope to return to these issues in the immediate future.

With this work, we hope to have convinced the reader of the charms of hitherto unexplored world of open quantum field theories. In many aspects, they closely mimic the familiar paradigm of unitary quantum field theories but yet deviate from them in interesting ways. Very basic conceptual issues like renormalisation or anomalies or non-perturbative physics (as that of instantons) are yet ill-understood.

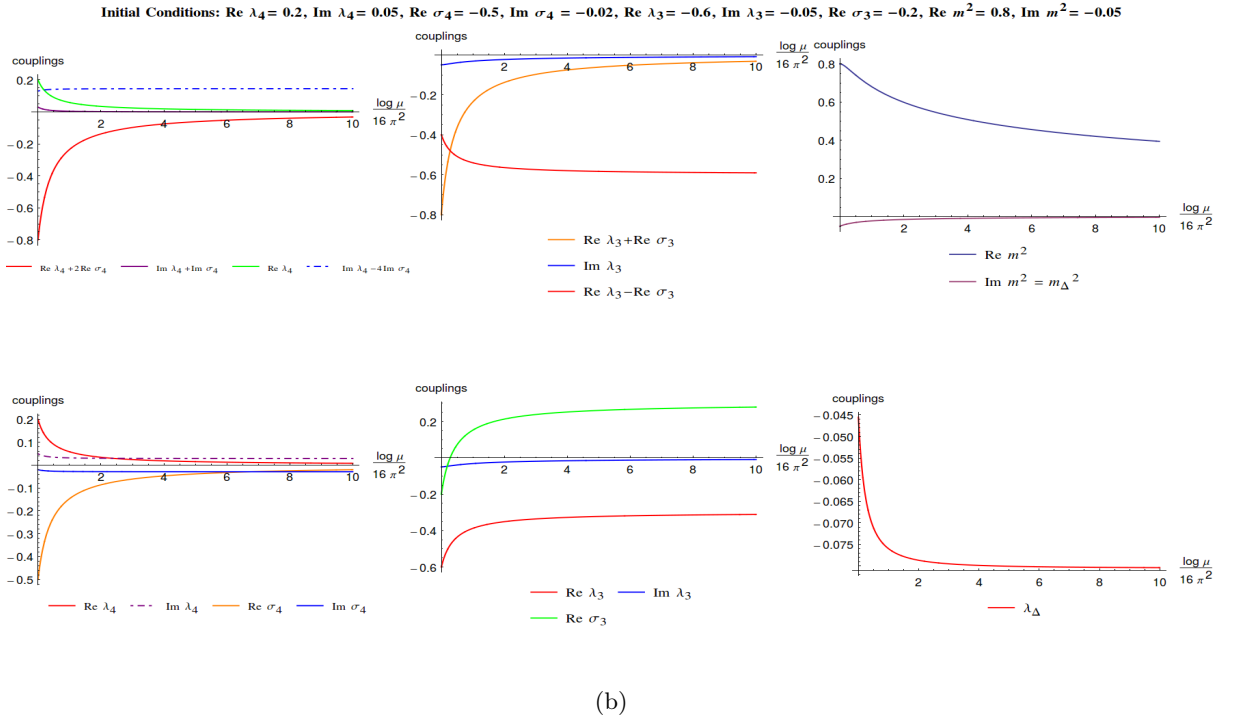
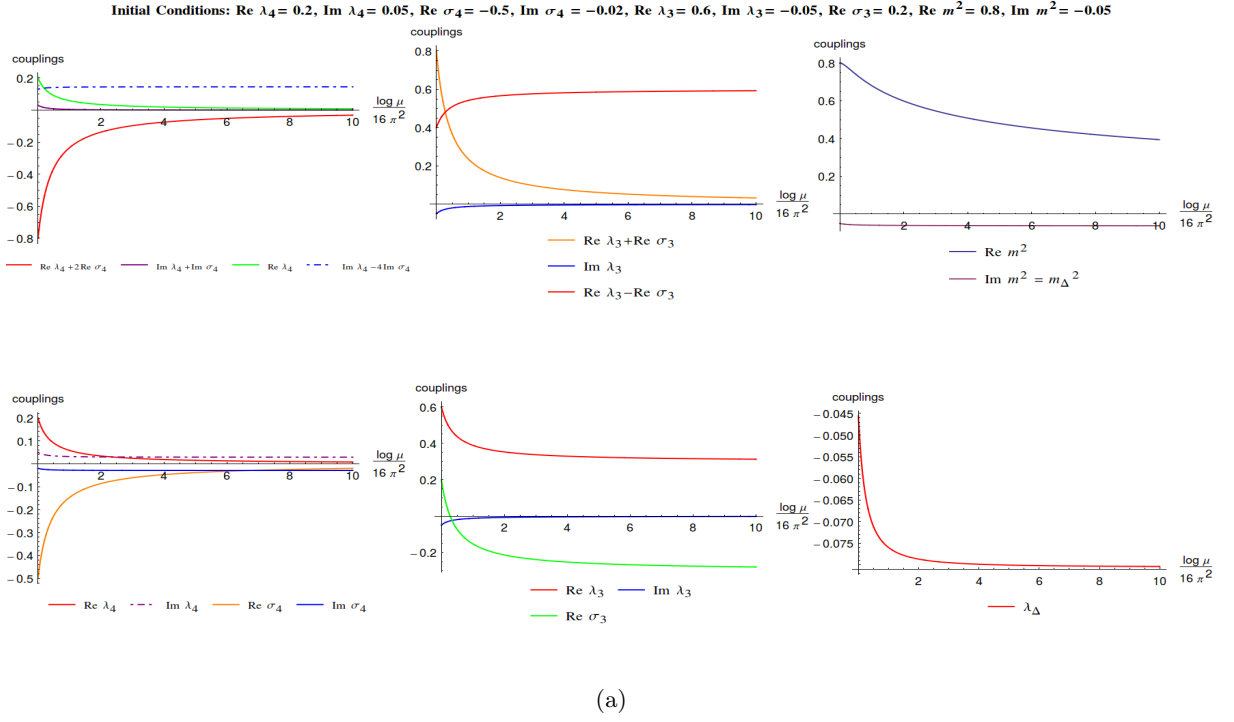
**Acknowledgements** We would like to thank David Poulin and John Preskill for their unpublished notes [32] and John Preskill for discussions. We thank Chi-Ming Chang, Michael Geracie, Felix Haehl, William R. Kelly, Manas Kulkarni, Shiraz Minwalla, David M. Ramirez, Mukund Rangamani and Krishnendu Ray for useful discussions. We thank Amin A. Nizami for pointing out various typos in the first version of this draft. CJ and RL gratefully acknowledge support from



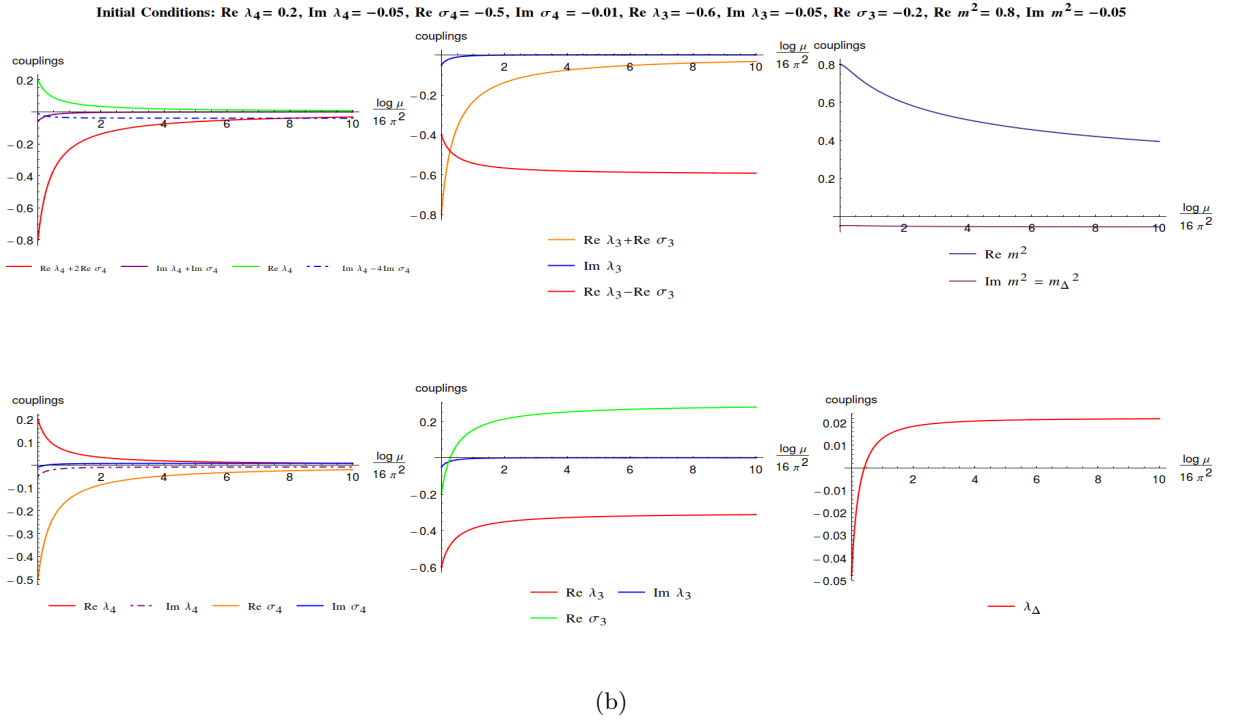
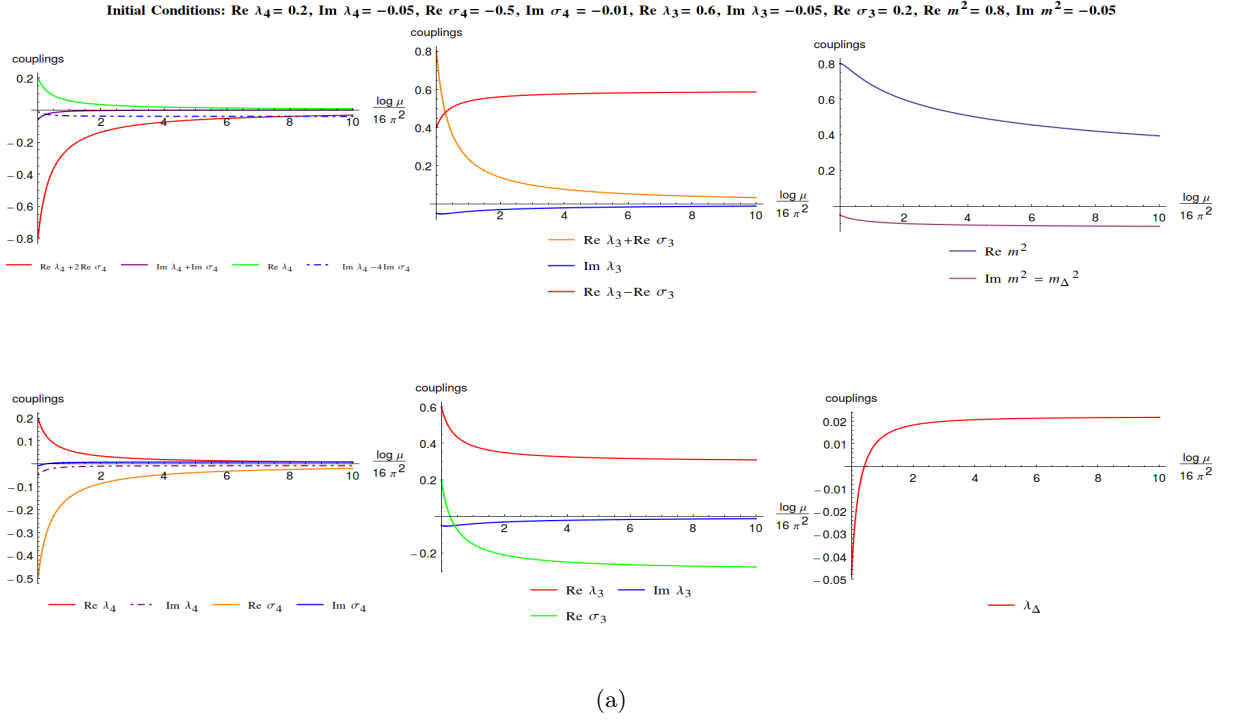
**Figure 22:** Figures showing the evolution of all the couplings for the case  $\text{Re } \lambda_4 + 2\text{Re } \sigma_4 > 0, \text{Im } \lambda_4 + \text{Im } \sigma_4 > 0$  and the two subcases -  $\text{Re } \lambda_3 + \text{Re } \sigma_3 > 0$ (figure a) and  $\text{Re } \lambda_3 + \text{Re } \sigma_3 < 0$  (figure b)



**Figure 23:** Figures showing the evolution of all the couplings for the case  $\text{Re } \lambda_4 + 2\text{Re } \sigma_4 > 0, \text{Im } \lambda_4 + \text{Im } \sigma_4 < 0$  and the two subcases -  $\text{Re } \lambda_3 + \text{Re } \sigma_3 > 0$ (figure a) and  $\text{Re } \lambda_3 + \text{Re } \sigma_3 < 0$ (figure b)



**Figure 24:** Figures showing the evolution of all the couplings for the case  $\text{Re } \lambda_4 + 2\text{Re } \sigma_4 < 0, \text{Im } \lambda_4 + \text{Im } \sigma_4 > 0$  and the two sub-cases -  $\text{Re } \lambda_3 + \text{Re } \sigma_3 > 0$  (figure a) and  $\text{Re } \lambda_3 + \text{Re } \sigma_3 < 0$  (figure b)



**Figure 25:** Figures showing the evolution of all the couplings for the case  $\text{Re } \lambda_4 + 2\text{Re } \sigma_4 < 0$ ,  $\text{Im } \lambda_4 + \text{Im } \sigma_4 < 0$  and the two sub-cases -  $\text{Re } \lambda_3 + \text{Re } \sigma_3 > 0$ (figure (a)) and  $\text{Re } \lambda_3 + \text{Re } \sigma_3 < 0$ (figure b)



International Centre for Theoretical Sciences, Tata Institute of Fundamental Research (ICTS-TIFR), Bengaluru. A.R. would like to thank ICTS-TIFR, Bengaluru for hospitality during the initial stages of this work. A. would like to thank support from Kishore Vaigyanik Protsahana Yojana (KVPY) funded by the Department of Science and Technology, Government of India. A. would also like to thank Indian Institute of Science (IISc) and ICTS-TIFR for the hospitality provided during this work. RL would also like to acknowledge his debt to all those who have generously supported and encouraged the pursuit of science in India.

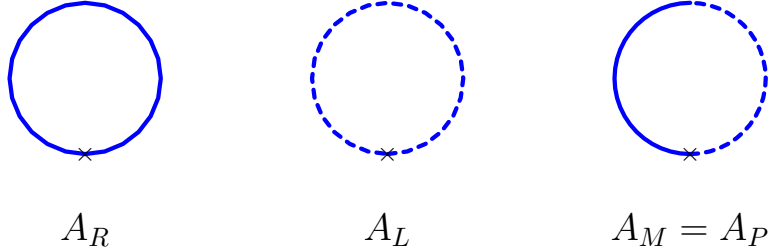
## A Notations and Conventions

### A.1 Most commonly used acronyms

- SK - Schwinger-Keldysh
- FV - Feynman-Vernon
- PV - Passarino-Veltman
- The loop integrals are named as the following. We start from the left(bottom) vertex and move in the counter-clockwise direction for s-channel(t, u channel) diagrams(s).

### A.2 Conventions for Feynman integrals

Since more general diagrams can appear in this context we will introduce a suitable notation. Following the standard notation [33, 34], we will use  $A$  for tadpole diagrams and  $B$  for bubble diagrams. In addition, we will use  $R, L, P, M$  as subscripts to denote the corresponding propagators as present in the diagrams. 2.



**Figure 26:** PV One loop  $A$  type integrals in SK theory

We are using slightly different normalization from [34] for Passarino-Veltman integrals. The relation between our integrals and the integrals in [34] is given below

$$A_0^{PV} = -(4\pi)^2 A_R \quad (\text{A.1})$$

$$B_0^{PV} = i(4\pi)^2 B_{RR} \quad (\text{A.2})$$

$$C_0^{PV} = (4\pi)^2 C_{RRR} \quad (\text{A.3})$$

$$D_0^{PV} = -i(4\pi)^2 D_{RRRR} \quad (\text{A.4})$$

We also note that Passarino-Veltman definitions use mostly negative metric  $\eta_{\mu\nu} = \text{diag}(1, 1, 1, 1)$ , while in this work we use mostly positive metric  $\eta_{\mu\nu} = \text{diag}(1, 1, 1, 1)$ . This fact has to be taken into account while comparing our expressions in terms of momentum-square against the standard expressions in discussions of PV integrals.

In SK theory there are four  $A$  type integrals. They are given by

$$\begin{aligned}
A_R(k) &\equiv \mu^{4-d} \int \frac{d^d p}{(2\pi)^{d_i}} \frac{1}{p^2 + m^2 - i\varepsilon} \\
A_L(k) &\equiv \mu^{4-d} \int \frac{d^d p}{(2\pi)^{d_i}} \frac{(-1)}{p^2 + m^2 + i\varepsilon} \\
A_P(k) &\equiv \mu^{4-d} \int \frac{d^d p}{(2\pi)^{d_i}} 2\pi i \delta_+(p^2 + m^2) \\
A_M(k) &\equiv \mu^{4-d} \int \frac{d^d p}{(2\pi)^{d_i}} 2\pi i \delta_-(p^2 + m^2)
\end{aligned} \tag{A.5}$$

Here

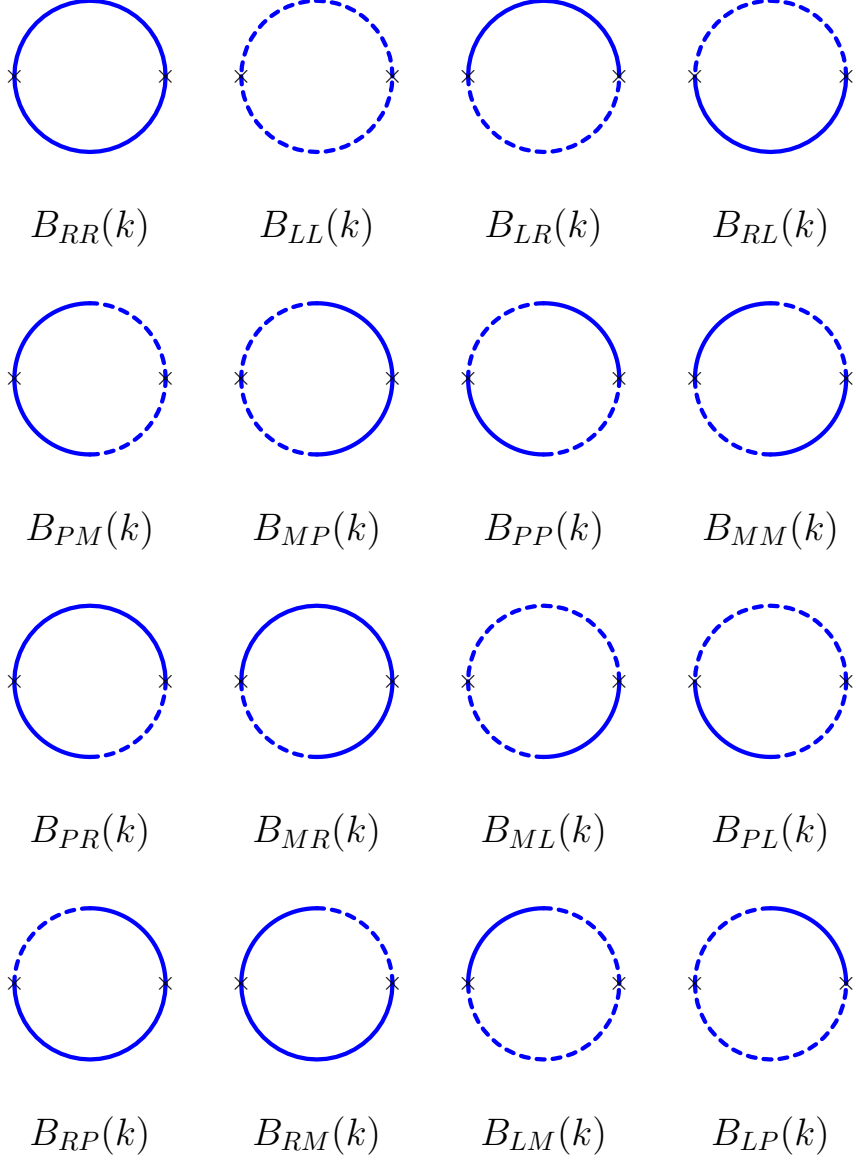
$$\delta_+(p^2 + m^2) \equiv \Theta(p^0) \delta(p^2 + m^2) \tag{A.6}$$

$$\delta_-(p^2 + m^2) \equiv \Theta(-p^0) \delta(p^2 + m^2) \tag{A.7}$$

In SK theory of one-scalar, there are ten  $B$  type integrals (compared to one  $B$  type integral in ordinary QFT of a single scalar). For the sake of generality, we will evaluate the most general scalar B-type integrals with unequal masses,  $m$  and  $\bar{m}$ , that can occur in an open EFT perturbation theory. These are 16 in number and they are defined as:

$$\begin{aligned}
B_{RR}(k) &\equiv \mu^{4-d} \int \frac{d^d p}{(2\pi)^{d_i}} \frac{d^d q}{(2\pi)^{d_i}} \frac{1}{p^2 + m^2 - i\varepsilon} \times \frac{1}{q^2 + \bar{m}^2 - i\varepsilon} \times (2\pi)^d \delta^d(p - q - k) \\
B_{LL}(k) &\equiv \mu^{4-d} \int \frac{d^d p}{(2\pi)^{d_i}} \frac{d^d q}{(2\pi)^{d_i}} \frac{(-1)}{p^2 + m^2 + i\varepsilon} \times \frac{(-1)}{q^2 + \bar{m}^2 + i\varepsilon} \times (2\pi)^d \delta^d(p - q - k) \\
B_{RL}(k) &\equiv \mu^{4-d} \int \frac{d^d p}{(2\pi)^{d_i}} \frac{d^d q}{(2\pi)^{d_i}} \frac{1}{p^2 + m^2 - i\varepsilon} \times \frac{(-1)}{q^2 + \bar{m}^2 + i\varepsilon} \times (2\pi)^d \delta^d(p - q - k) \\
B_{LR}(k) &\equiv \mu^{4-d} \int \frac{d^d p}{(2\pi)^{d_i}} \frac{d^d q}{(2\pi)^{d_i}} \frac{(-1)}{p^2 + m^2 + i\varepsilon} \times \frac{1}{q^2 + \bar{m}^2 - i\varepsilon} \times (2\pi)^d \delta^d(p - q - k)
\end{aligned} \tag{A.8}$$

$$\begin{aligned}
B_{PM}(k) &\equiv \mu^{4-d} \int \frac{d^d p}{(2\pi)^{d_i}} \frac{d^d q}{(2\pi)^{d_i}} 2\pi i \delta_+(p^2 + m^2) \times 2\pi i \delta_-(q^2 + \bar{m}^2) \times (2\pi)^d \delta^d(p - q - k) \\
B_{MP}(k) &\equiv \mu^{4-d} \int \frac{d^d p}{(2\pi)^{d_i}} \frac{d^d q}{(2\pi)^{d_i}} 2\pi i \delta_-(p^2 + m^2) \times 2\pi i \delta_+(q^2 + \bar{m}^2) \times (2\pi)^d \delta^d(p - q - k) \\
B_{PP}(k) &\equiv \mu^{4-d} \int \frac{d^d p}{(2\pi)^{d_i}} \frac{d^d q}{(2\pi)^{d_i}} 2\pi i \delta_+(p^2 + m^2) \times 2\pi i \delta_+(q^2 + \bar{m}^2) \times (2\pi)^d \delta^d(p - q - k) \\
B_{MM}(k) &\equiv \mu^{4-d} \int \frac{d^d p}{(2\pi)^{d_i}} \frac{d^d q}{(2\pi)^{d_i}} 2\pi i \delta_-(p^2 + m^2) \times 2\pi i \delta_-(q^2 + \bar{m}^2) \times (2\pi)^d \delta^d(p - q - k)
\end{aligned} \tag{A.9}$$



**Figure 27:** PV one loop  $B$  type integrals in SK theory. The momentum and mass corresponding to the lower propagator is denoted by  $p^\mu$  and  $m$  respectively, whereas the momentum and mass corresponding to the upper propagator are  $q^\mu$  and  $\bar{m}$  respectively. The momenta  $p$  and  $q$  are taken to flow anti-clockwise in the loop.

$$\begin{aligned}
B_{PR}(k) &\equiv \mu^{4-d} \int \frac{d^d p}{(2\pi)^{d_i}} \frac{d^d q}{(2\pi)^{d_i}} 2\pi i \delta_+(p^2 + m^2) \frac{1}{q^2 + \bar{m}^2 - i\varepsilon} \times (2\pi)^d \delta^d(p - q - k) \\
B_{MR}(k) &\equiv \mu^{4-d} \int \frac{d^d p}{(2\pi)^{d_i}} \frac{d^d q}{(2\pi)^{d_i}} 2\pi i \delta_-(p^2 + m^2) \frac{1}{q^2 + \bar{m}^2 - i\varepsilon} \times (2\pi)^d \delta^d(p - q - k) \\
B_{PL}(k) &\equiv \mu^{4-d} \int \frac{d^d p}{(2\pi)^{d_i}} \frac{d^d q}{(2\pi)^{d_i}} 2\pi i \delta_+(p^2 + m^2) \frac{(-1)}{q^2 + \bar{m}^2 + i\varepsilon} \times (2\pi)^d \delta^d(p - q - k) \\
B_{ML}(k) &\equiv \mu^{4-d} \int \frac{d^d p}{(2\pi)^{d_i}} \frac{d^d q}{(2\pi)^{d_i}} 2\pi i \delta_-(p^2 + m^2) \frac{(-1)}{q^2 + \bar{m}^2 + i\varepsilon} \times (2\pi)^d \delta^d(p - q - k)
\end{aligned} \tag{A.10}$$

$$\begin{aligned}
B_{RP}(k) &\equiv \mu^{4-d} \int \frac{d^d p}{(2\pi)^{d_i}} \frac{d^d q}{(2\pi)^{d_i}} \frac{1}{p^2 + m^2 - i\varepsilon} 2\pi i \delta_+(q^2 + \bar{m}^2) \times (2\pi)^d \delta^d(p - q - k) \\
B_{RM}(k) &\equiv \mu^{4-d} \int \frac{d^d p}{(2\pi)^{d_i}} \frac{d^d q}{(2\pi)^{d_i}} \frac{1}{p^2 + m^2 - i\varepsilon} 2\pi i \delta_-(q^2 + \bar{m}^2) \times (2\pi)^d \delta^d(p - q - k) \\
B_{LP}(k) &\equiv \mu^{4-d} \int \frac{d^d p}{(2\pi)^{d_i}} \frac{d^d q}{(2\pi)^{d_i}} \frac{(-1)}{p^2 + m^2 + i\varepsilon} 2\pi i \delta_+(q^2 + \bar{m}^2) \times (2\pi)^d \delta^d(p - q - k) \\
B_{LM}(k) &\equiv \mu^{4-d} \int \frac{d^d p}{(2\pi)^{d_i}} \frac{d^d q}{(2\pi)^{d_i}} \frac{(-1)}{p^2 + m^2 + i\varepsilon} 2\pi i \delta_-(q^2 + \bar{m}^2) \times (2\pi)^d \delta^d(p - q - k)
\end{aligned} \tag{A.11}$$

In the following appendix, we will evaluate these integrals and their divergences.

## B Evaluating Passarino-Veltman Loop Integrals for open $\phi^3 + \phi^4$ theory

In this section, we describe in some detail the loop integrals that appear in the perturbation theory of open  $\phi^3 + \phi^4$  theory. While some of the integrals are familiar from usual QFT textbooks and a few other integrals occur in discussions of cutting rules, as far as the authors are aware, the majority of the integrals described in this section are not analyzed elsewhere. Hence, these integrals are described in some detail with a special focus on the new kind of features that occur when we try to do integrals in the real time (most of the integrals in this section do not admit Wick rotation because of their unusual  $i\varepsilon$  prescriptions) .

### B.1 Passarino-Veltman $A$ type integrals

There are four  $A$  type PV integrals :  $A_R, A_L, A_P, A_M$ . They satisfy the following relations

$$A_R = A_L^* \quad A_P = A_P^* \tag{B.1}$$

$$A_R + A_L = A_P + A_M \equiv 2A_P \tag{B.2}$$

First we compute the integral  $A_R$

$$\begin{aligned}
A_R &= \mu^{4-d} \int \frac{d^d p}{(2\pi)^d} \frac{-i}{p^2 + m^2 - i\varepsilon} = \int \frac{d^d p}{(2\pi)^{d_i}} \frac{1}{\omega_p^2 - (p^0)^2 - i\varepsilon} \\
&= \mu^{4-d} \int \frac{d^{d-1} p}{(2\pi)^{d-1}} \frac{1}{2\omega_p} = \mu^{4-d} \frac{\text{Vol}(\mathbb{S}^{d-2})}{2(2\pi)^{d-1}} \int_m \left( \sqrt{\omega_p^2 - m^2} \right)^{d-3} d\omega_p \\
&= \Gamma\left[\frac{1}{2}(2-d)\right] \frac{m^2}{(4\pi)^2} \left( \frac{m^2}{4\pi\mu^2} \right)^{\frac{d-4}{2}} \\
&= \frac{m^2}{(4\pi)^2} \frac{2}{d-4} + \frac{m^2}{(4\pi)^2} \left\{ \ln \frac{m^2}{4\pi\mu^2 e^{-\gamma_E}} - 1 \right\} + O(d-4)
\end{aligned} \tag{B.3}$$

Using this result and the relations (B.1)-(B.2), we can determine  $A_L$  and  $A_P$ .  $A_L, A_P$  and  $A_M$  are given by

$$A_R = A_L = A_P = A_M = \frac{m^2}{(4\pi)^2} \left( \frac{2}{d-4} + \ln \frac{m^2}{4\pi\mu^2 e^{-\gamma_E}} - 1 \right) \tag{B.4}$$

## B.2 Integrals $B_{PM}(k)$ and $B_{MP}(k)$

We will now consider the following two integrals

$$\begin{aligned}
B_{PM}(k) &\equiv \mu^{4-d} \int \frac{d^d p}{(2\pi)^{d_i}} \frac{d^d q}{(2\pi)^{d_i}} 2\pi i \delta_+(p^2 + m^2) \times 2\pi i \delta_-(q^2 + \bar{m}^2) \times (2\pi)^d \delta^d(p - q - k) \\
B_{MP}(k) &\equiv \mu^{4-d} \int \frac{d^d p}{(2\pi)^{d_i}} \frac{d^d q}{(2\pi)^{d_i}} 2\pi i \delta_-(p^2 + m^2) \times 2\pi i \delta_+(q^2 + \bar{m}^2) \times (2\pi)^d \delta^d(p - q - k)
\end{aligned}
\tag{B.5}$$

These integrals are well-known in discussions of cutting rules and we mainly discuss them here for completeness. They represent the amplitudes for the two body decay of a particle with mass  $\sqrt{-k^2}$  to decay into two particles of mass  $m$  and  $\bar{m}$ . It follows that the integral  $B_{PM}(k)$  vanishes unless  $k^\mu$  is future time-like, whereas  $B_{MP}(k)$  is zero unless  $k^\mu$  is past time-like. Since  $B_{MP}(k) = B_{PM}(-k)$ , it suffices to argue this for  $B_{PM}(k)$ . The mathematical reasoning is as follows : if  $k^\mu$  were to be space-like, we can go to a frame where  $k^0 = 0$  and the energy delta function then gives  $\delta(\omega_p + \bar{\omega}_q) = 0$ , thus reducing the amplitude to zero. If  $k^\mu$  is time-like and we move to its rest frame by setting  $k^\mu = \{M, \vec{0}\}$  where  $M = \text{sgn}(k^0)\sqrt{-k^2}$ . The energy delta function for  $B_{PM}(k)$  then gives  $\delta(\omega_p + \bar{\omega}_q - M) = 0$ , thus forcing  $M > 0$ , i.e.,  $k^\mu$  should be future time-like.

By performing  $p^0$  and  $q^0$  integrals in the rest frame of  $k^\mu$ , we can reduce both integrals to the two body phase space integral. Let us begin by defining the basic kinematics of a particle of mass  $M = \sqrt{-k^2}$  decaying into two particles of mass  $m$  and  $\bar{m}$ . Let  $p_*$  be the momentum with which these two particles fly away in the rest frame of  $M$ . Energy-momentum conservation then fixes

$$\begin{aligned}
p_* &= \frac{1}{2M} \left[ M^2 - (m + \bar{m})^2 \right]^{1/2} \left[ M^2 - (m - \bar{m})^2 \right]^{1/2} \\
&= \frac{M}{2} \left[ 1 - 2 \left( \frac{m^2 + \bar{m}^2}{M^2} \right) + \left( \frac{m^2 - \bar{m}^2}{M^2} \right)^2 \right]^{1/2} \\
\omega_p^* &\equiv \sqrt{p_*^2 + m^2} = \frac{1}{2M} (M^2 + m^2 - \bar{m}^2) \\
\bar{\omega}_p^* &\equiv \sqrt{p_*^2 + \bar{m}^2} = \frac{1}{2M} (M^2 + \bar{m}^2 - m^2)
\end{aligned}
\tag{B.6}$$

These expressions make sense only when the argument of the square root is positive, i.e., when  $M \geq m + \bar{m}$  which is the condition for the two body decay to be kinematically possible. In this regime,  $\omega_p^*$  and  $\bar{\omega}_p^*$  are both positive as we would expect. Another useful identity is

$$\frac{1}{(2\omega_p)(2\bar{\omega}_p)} \delta(\omega_p + \bar{\omega}_p - M) = \frac{1}{4Mp_*} \delta(|p| - p_*)
\tag{B.7}$$

Let us now compute this integral in terms of these kinematic variables. We have

$$\begin{aligned}
B_{PM}(k) &= \mu^{4-d} \int \frac{d^{d-1}p}{(2\pi)^{d-1}(2\omega_p)} \frac{d^{d-1}q}{(2\pi)^{d-1}(2\bar{\omega}_q)} \times (2\pi)^d \delta^{d-1}(\vec{p}-\vec{q}) \delta(\omega_p + \omega_q - M) \\
&= \mu^{4-d} \int \frac{d^{d-1}p}{(2\pi)^{d-1}(2\omega_p)(2\bar{\omega}_p)} 2\pi \delta(\omega_p + \bar{\omega}_p - M) \\
&= \mu^{4-d} \frac{\text{Vol}(\mathbb{S}^{d-2})}{(2\pi)^{d-2}} \int_0^\infty \frac{p^{d-2} d^d p}{(2\omega_p)(2\bar{\omega}_p)} \delta(\omega_p + \bar{\omega}_p - M) = \mu^{4-d} \frac{\text{Vol}(\mathbb{S}^{d-2}) p_\star^{d-3}}{4M(2\pi)^{d-2}} \\
&= \frac{\text{Vol}(\mathbb{S}^{d-2})}{32\pi^2} \left( \frac{M}{4\pi\mu} \right)^{d-4} \left( \frac{2p_\star}{M} \right)^{d-3}
\end{aligned} \tag{B.8}$$

which is the two-body phase space as advertised.

Restoring the kinematic constraints, we get

$$\begin{aligned}
B_{PM}(k) &= \frac{\text{Vol}(\mathbb{S}^{d-2})}{32\pi^2} \left( \frac{-k^2}{(4\pi\mu)^2} \right)^{\frac{d-4}{2}} \left[ 1 + 2 \left( \frac{m^2 + \bar{m}^2}{k^2} \right) + \left( \frac{m^2 - \bar{m}^2}{k^2} \right)^2 \right]^{\frac{d-3}{2}} \\
&\quad \times \Theta(-k^2 - (m + \bar{m})^2) \Theta(k^0)
\end{aligned} \tag{B.9}$$

The integral can then be expanded near  $d = 4$  to get

$$B_{PM}(k) = \frac{\Theta(-k^2 - (m + \bar{m})^2) \Theta(k^0)}{8\pi} \left[ 1 + 2 \left( \frac{m^2 + \bar{m}^2}{k^2} \right) + \left( \frac{m^2 - \bar{m}^2}{k^2} \right)^2 \right]^{\frac{1}{2}} \tag{B.10}$$

Replacing  $k^\mu$  by  $-k^\mu$  we get

$$B_{MP}(k) = \frac{\Theta(-k^2 - (m + \bar{m})^2) \Theta(-k^0)}{8\pi} \left[ 1 + 2 \left( \frac{m^2 + \bar{m}^2}{k^2} \right) + \left( \frac{m^2 - \bar{m}^2}{k^2} \right)^2 \right]^{\frac{1}{2}}. \tag{B.11}$$

These two expressions can be added to get

$$B_{PM}(k) + B_{MP}(k) = \frac{\Theta(-k^2 - (m + \bar{m})^2)}{8\pi} \left[ 1 + 2 \left( \frac{m^2 + \bar{m}^2}{k^2} \right) + \left( \frac{m^2 - \bar{m}^2}{k^2} \right)^2 \right]^{\frac{1}{2}} \tag{B.12}$$

When  $m = \bar{m}$ , we can write

$$\boxed{B_{PM}(k) = \frac{\Theta(k^0)\Theta(-k^2 - 4m^2)}{8\pi} \sqrt{1 + \frac{4m^2}{k^2}}} \tag{B.13}$$

and

$$\boxed{B_{MP}(k) = \frac{\Theta(-k^0)\Theta(-k^2 - 4m^2)}{8\pi} \sqrt{1 + \frac{4m^2}{k^2}}} \tag{B.14}$$

### B.3 Integrals $B_{PP}(k)$ and $B_{MM}(k)$

We now turn to the ‘cross-cut’ integrals  $B_{PP}(k)$  and  $B_{MM}(k)$  which do not occur in the usual discussions of cutting rules in a unitary theory. They are loop integrals peculiar to open QFTs with their own characteristic kinematic behavior.

### B.3.1 Time-like $k^\mu$

We will begin by examining  $B_{PP}(k)$  for time-like  $k^\mu$ . In the rest frame of  $k^\mu$  i.e.,  $k^\mu = (M, \vec{0})$ , we can do similar manipulations as in the previous subsection to get

$$\begin{aligned}
B_{PP}(k) &\equiv \mu^{4-d} \int \frac{d^d p}{(2\pi)^{d_i}} \frac{d^d q}{(2\pi)^{d_i}} 2\pi i \delta_+(p^2 + m^2) 2\pi i \delta_+(q^2 + \bar{m}^2) (2\pi)^d \delta^d(p - q - k) \\
&= \mu^{4-d} \int \frac{d^{d-1} p}{(2\pi)^{d-1} 2\omega_p} \frac{d^{d-1} q}{(2\pi)^{d-1} 2\bar{\omega}_q} \delta(\omega_p - \bar{\omega}_q - M) (2\pi)^d \delta^{d-1}(\vec{p} - \vec{q}) \\
&= \mu^{4-d} \int \frac{d^{d-1} p}{(2\pi)^{d-2}} \frac{1}{2\omega_p} \frac{1}{2\bar{\omega}_p} \delta(\omega_p - \bar{\omega}_p - M) \\
&= \frac{\mu^{4-d} \text{Vol}(\mathbb{S}^{d-2})}{(2\pi)^{d-2}} \int_0^\infty \frac{p^{d-2} dp}{(2\omega_p)(2\bar{\omega}_p)} \delta(\omega_p - \bar{\omega}_p - M) = \frac{\text{Vol}(\mathbb{S}^{d-2})}{32\pi^2} \left(\frac{|M|}{4\pi\mu}\right)^{d-4} \left(\frac{2p_\star}{|M|}\right)^{d-3}
\end{aligned} \tag{B.15}$$

where we have used

$$\frac{1}{(2\omega_p)(2\bar{\omega}_p)} \delta(\omega_p - \bar{\omega}_p - M) = \frac{1}{4|M|p_\star} \delta(|p| - p_\star) \tag{B.16}$$

with  $p_\star$  being the appropriate momentum which solves the kinematics (see below).

For  $M > 0$ , i.e.,  $k^\mu$  being future time-like, we recognize the integral as the one describing the phase space for a deep in-elastic scattering process :  $\bar{m}$  with momentum  $p$  strikes against the target  $M$  at rest converting it into the particle  $m$  traveling with momentum  $p$ . The kinematics is solved by

$$\begin{aligned}
p_\star &= \frac{1}{2M} \left[ (m + \bar{m})^2 - M^2 \right]^{1/2} \left[ (m - \bar{m})^2 - M^2 \right]^{1/2} \\
&= \frac{M}{2} \left[ 1 - 2 \left( \frac{m^2 + \bar{m}^2}{M^2} \right) + \left( \frac{m^2 - \bar{m}^2}{M^2} \right)^2 \right]^{1/2} \\
\omega_p^\star &\equiv \sqrt{p_\star^2 + m^2} = \frac{1}{2M} (m^2 + M^2 - \bar{m}^2) \\
\bar{\omega}_p^\star &\equiv \sqrt{p_\star^2 + \bar{m}^2} = \frac{1}{2M} (m^2 - M^2 - \bar{m}^2)
\end{aligned} \tag{B.17}$$

which is sensible for  $M < m - \bar{m}$ . Thus, in this kinematic regime we get

$$\begin{aligned}
B_{PP}(k) &\ni \frac{\text{Vol}(\mathbb{S}^{d-2})}{32\pi^2} \left( \frac{-k^2}{(4\pi\mu)^2} \right)^{\frac{d-4}{2}} \left[ 1 + 2 \left( \frac{m^2 + \bar{m}^2}{k^2} \right) + \left( \frac{m^2 - \bar{m}^2}{k^2} \right)^2 \right]^{\frac{d-3}{2}} \\
&\quad \times \Theta((m - \bar{m})^2 + k^2) \Theta(k^0)
\end{aligned} \tag{B.18}$$

For  $M < 0$ , i.e.,  $k^\mu$  being past time-like, we recognize the integral as the one describing the phase space for the two body decay of  $\bar{m}$  into a particle of mass  $|M|$  and  $m$ . The kinematics is

solved by

$$\begin{aligned}
p_\star &= \frac{1}{2|M|} \left[ (m + \bar{m})^2 - M^2 \right]^{1/2} \left[ (m - \bar{m})^2 - M^2 \right]^{1/2} \\
&= \frac{|M|}{2} \left[ 1 - 2 \left( \frac{m^2 + \bar{m}^2}{M^2} \right) + \left( \frac{m^2 - \bar{m}^2}{M^2} \right)^2 \right]^{1/2} \\
\omega_p^\star &\equiv \sqrt{p_\star^2 + m^2} = \frac{1}{2|M|} (\bar{m}^2 - m^2 - M^2) \\
\bar{\omega}_p^\star &\equiv \sqrt{p_\star^2 + \bar{m}^2} = \frac{1}{2|M|} (\bar{m}^2 - m^2 + M^2)
\end{aligned} \tag{B.19}$$

which is sensible for  $\bar{m} > |M| + m$ . Thus, in this kinematic regime we get

$$\begin{aligned}
B_{PP}(k) &\ni \frac{\text{Vol}(\mathbb{S}^{d-2})}{32\pi^2} \left( \frac{-k^2}{(4\pi\mu)^2} \right)^{\frac{d-4}{2}} \left[ 1 + 2 \left( \frac{m^2 + \bar{m}^2}{k^2} \right) + \left( \frac{m^2 - \bar{m}^2}{k^2} \right)^2 \right]^{\frac{d-3}{2}} \\
&\quad \times \Theta((\bar{m} - m)^2 + k^2) \Theta(-k^0)
\end{aligned} \tag{B.20}$$

Thus, we conclude that for time-like  $k^\mu$ ,

$$\begin{aligned}
B_{PP}(k) &\ni \frac{\text{Vol}(\mathbb{S}^{d-2})}{32\pi^2} \left( \frac{-k^2}{(4\pi\mu)^2} \right)^{\frac{d-4}{2}} \left[ 1 + 2 \left( \frac{m^2 + \bar{m}^2}{k^2} \right) + \left( \frac{m^2 - \bar{m}^2}{k^2} \right)^2 \right]^{\frac{d-3}{2}} \\
&\quad \times \Theta((\bar{m} - m)^2 + k^2) \Theta(-k^2)
\end{aligned} \tag{B.21}$$

Note that  $B_{PP}(k) = B_{PP}(-k)$  could have been directly deduced from the integral form.

### B.3.2 Space-like $k^\mu$

We will next study  $B_{PP}(k)$  when  $k^\mu$  is space-like. We set  $k^\mu = \{0, Q = \sqrt{k^2}, \vec{0}_{d-2}\}$  where we take  $Q > 0$  without loss of generality. We have

$$\begin{aligned}
B_{PP}(k) &\equiv \mu^{4-d} \int \frac{d^d p}{(2\pi)^{d_i}} \frac{d^d q}{(2\pi)^{d_i}} 2\pi i \delta_+(p^2 + m^2) 2\pi i \delta_+(q^2 + \bar{m}^2) (2\pi)^d \delta^d(p - q - k) \\
&= \mu^{4-d} \int \frac{d^{d-1} p}{(2\pi)^{d-1}(2\omega_p)} \frac{d^{d-1} q}{(2\pi)^{d-1}(2\bar{\omega}_q)} \times (2\pi)^d \delta^{d-2}(\vec{p}_\perp - \vec{q}_\perp) \delta(p_\parallel - q_\parallel - Q) \delta(\omega_p - \bar{\omega}_q) \\
&= \mu^{4-d} \int \frac{d^{d-1} p}{(2\pi)^{d-1}(2\omega_p)(2\bar{\omega}_{p\perp})} 2\pi \delta(\omega_p - \bar{\omega}_{p\perp}) = \frac{\mu^{4-d}}{(2Q)} \int \frac{d^{d-2} p_\perp}{(2\pi)^{d-2}(2\omega_{p\perp})}
\end{aligned} \tag{B.22}$$

where, in the penultimate step we have defined  $\bar{\omega}_{p\perp} \equiv p_\perp^2 + (Q - p_\parallel)^2 + \bar{m}^2$ . In the last step, we have used

$$\frac{1}{(2\omega_p)(2\bar{\omega}_{p\perp})} \delta(\omega_p - \bar{\omega}_{p\perp}) = \frac{1}{4Q\omega_{p\perp}} \delta(p_\parallel - p_\parallel^\star) \tag{B.23}$$

with the definitions

$$\begin{aligned}
p_\parallel^\star &\equiv \frac{1}{2Q} (\bar{m}^2 - m^2 + Q^2) \\
(\omega_{p\perp})^2 &\equiv p_\perp^2 + (p_\parallel^\star)^2 + m^2 = p_\perp^2 + \frac{1}{4Q^2} \left[ (m + \bar{m})^2 + Q^2 \right] \left[ (m - \bar{m})^2 + Q^2 \right].
\end{aligned} \tag{B.24}$$



The rest of the integral is  $(d - 2)$  dimensional transverse phase space with the transverse mass given by

$$\begin{aligned} m_{\perp} &\equiv \frac{1}{2Q} \left[ (m + \bar{m})^2 + Q^2 \right]^{1/2} \left[ (m - \bar{m})^2 + Q^2 \right]^{1/2} \\ &= \frac{Q}{2} \left[ 1 + 2 \left( \frac{m^2 + \bar{m}^2}{Q^2} \right) + \left( \frac{m^2 - \bar{m}^2}{Q^2} \right)^2 \right]^{1/2} \end{aligned} \quad (\text{B.25})$$

We thus get

$$\begin{aligned} B_{PP}(k) &= \mu^{4-d} \frac{\text{Vol}(\mathbb{S}^{d-3})}{4Q(2\pi)^{d-2}} \int_{m_{\perp}}^{\infty} \left( \sqrt{\omega_{p_{\perp}}^2 - m_{\perp}^2} \right)^{d-4} d\omega_{p_{\perp}} \\ &= \mu^{4-d} \frac{\text{Vol}(\mathbb{S}^{d-2})}{(2\pi)^{d-1}} \frac{m_{\perp}^{d-3}}{4Q} \Gamma\left(\frac{3}{2} - \frac{d}{2}\right) \Gamma\left(\frac{d}{2} - \frac{1}{2}\right) \\ &= \frac{\text{Vol}(\mathbb{S}^{d-2})}{32\pi^2} \left( \frac{Q}{4\pi\mu} \right)^{d-4} \left( \frac{2m_{\perp}}{Q} \right)^{d-3} \frac{1}{2\pi} \Gamma\left(\frac{3}{2} - \frac{d}{2}\right) \Gamma\left(\frac{d}{2} - \frac{1}{2}\right) \end{aligned} \quad (\text{B.26})$$

Restoring the kinematical constraints, we get

$$\begin{aligned} B_{PP}(k) &\ni \frac{\text{Vol}(\mathbb{S}^{d-2})}{32\pi^2} \left( \frac{k^2}{(4\pi\mu)^2} \right)^{\frac{d-4}{2}} \left[ 1 + 2 \left( \frac{m^2 + \bar{m}^2}{k^2} \right) + \left( \frac{m^2 - \bar{m}^2}{k^2} \right)^2 \right]^{\frac{d-3}{2}} \\ &\quad \times \Theta(k) \frac{1}{2\pi} \Gamma\left(\frac{3}{2} - \frac{d}{2}\right) \Gamma\left(\frac{d}{2} - \frac{1}{2}\right) \end{aligned} \quad (\text{B.27})$$

Putting together the various kinematical regimes, we obtain

$$\begin{aligned} B_{PP}(k) &= \frac{\text{Vol}(\mathbb{S}^{d-2})}{32\pi^2} \left[ 1 + 2 \left( \frac{m^2 + \bar{m}^2}{k^2} \right) + \left( \frac{m^2 - \bar{m}^2}{k^2} \right)^2 \right]^{\frac{d-3}{2}} \\ &\quad \times \left\{ \Theta(k^2) \frac{1}{2\pi} \Gamma\left(\frac{3}{2} - \frac{d}{2}\right) \Gamma\left(\frac{d}{2} - \frac{1}{2}\right) \left( \frac{k^2}{(4\pi\mu)^2} \right)^{\frac{d-4}{2}} \right. \\ &\quad \left. + \Theta((\bar{m} - m)^2 + k^2) \Theta(-k^2) \left( \frac{-k^2}{(4\pi\mu)^2} \right)^{\frac{d-4}{2}} \right\} \end{aligned} \quad (\text{B.28})$$

Expanding around  $d = 4$  we get

$$\begin{aligned} B_{PP}(k) = B_{MM}(k) &= \frac{1}{8\pi} \left[ 1 + 2 \left( \frac{m^2 + \bar{m}^2}{k^2} \right) + \left( \frac{m^2 - \bar{m}^2}{k^2} \right)^2 \right]^{\frac{1}{2}} \\ &\quad \times \left\{ -\frac{1}{2} \Theta(k^2) + \Theta((\bar{m} - m)^2 + k^2) \Theta(-k^2) \right\} \end{aligned} \quad (\text{B.29})$$

where we have used  $B_{MM}(k) = B_{PP}(-k) = B_{PP}(k)$ . Taking  $m = \bar{m}$ , the second factor vanishes and we obtain

$$\boxed{B_{PP}(k) = B_{MM}(k) = \frac{[-\frac{1}{2} \Theta(k^2)]}{8\pi} \sqrt{1 + \frac{4m^2}{k^2}}} \quad (\text{B.30})$$

## B.4 Reduction of divergent integrals to $B_{RP}(k)$

We now turn to the ‘quarter-cut’ integrals  $B_{RP}(k), B_{RM}(k), B_{LP}(k)$  and  $B_{LM}(k)$  which also do not occur in the usual discussions of cutting rules in a unitary theory. They are also loop integrals peculiar to open QFTs. However, unlike the integrals considered in the last section, they do not evaluate to on-shell phase space for various processes. This off-shell nature means that they exhibit UV divergences and hence are crucial to the issue of renormalizability of open QFTs. When the open QFT is renormalisable, these diagrams contribute to  $\beta$  functions of an open QFT. As before, we will evaluate these integrals in various kinematic regimes and then put together the answers at the end.

We will consider the integral

$$B_{RP}(k) = \mu^{4-d} \int \frac{d^d p}{(2\pi)^{d_i}} \int \frac{d^d q}{(2\pi)^{d_i}} \frac{1}{p^2 + m^2 - i\varepsilon} 2\pi i \delta_+(q^2 + \bar{m}^2) (2\pi)^d \delta^d(p - q - k) \quad (\text{B.31})$$

This is the characteristic integral which leads to UV divergences in open QFT. Before analyzing this integral further, we will show that the other divergent integrals can be reduced to this integral. We start with

$$\begin{aligned} B_{RM}(k) &\equiv \mu^{4-d} \int \frac{d^d p}{(2\pi)^{d_i}} \int \frac{d^d q}{(2\pi)^{d_i}} \frac{1}{p^2 + m^2 - i\varepsilon} 2\pi i \delta_-(q^2 + \bar{m}^2) (2\pi)^d \delta^d(p - q - k) \\ &= B_{RP}(-k) \end{aligned} \quad (\text{B.32})$$

Similarly

$$\begin{aligned} B_{LP}(k) &\equiv \mu^{4-d} \int \frac{d^d p}{(2\pi)^{d_i}} \int \frac{d^d q}{(2\pi)^{d_i}} \frac{-1}{p^2 + m^2 + i\varepsilon} 2\pi i \delta_+(q^2 + \bar{m}^2) (2\pi)^d \delta^d(p - q - k) \\ &= [B_{RP}(k)]^* \\ B_{LM}(k) &\equiv \mu^{4-d} \int \frac{d^d p}{(2\pi)^{d_i}} \int \frac{d^d q}{(2\pi)^{d_i}} \frac{-1}{p^2 + m^2 + i\varepsilon} 2\pi i \delta_-(q^2 + \bar{m}^2) (2\pi)^d \delta^d(p - q - k) \\ &= [B_{RM}(k)]^* = [B_{RP}(-k)]^* \end{aligned} \quad (\text{B.33})$$

The integrals with the subscripts exchanged can be obtained by exchanging  $m$  and  $\bar{m}$  (thus exchanging  $p^\mu$  and  $q^\mu$ ) and reversing  $k^\mu$ . For example,  $B_{PR}(k) = B_{RP}(-k)|_{m \leftrightarrow \bar{m}}$  and similarly for other integrals :

$$\begin{aligned} B_{PR}(k) &= B_{RP}(-k)|_{m \leftrightarrow \bar{m}} , & B_{MR}(k) &= B_{RP}(k)|_{m \leftrightarrow \bar{m}} , \\ B_{PL}(k) &= B_{RP}(-k)^*|_{m \leftrightarrow \bar{m}} , & B_{ML}(k) &= B_{RP}(k)^*|_{m \leftrightarrow \bar{m}} . \end{aligned} \quad (\text{B.34})$$

It is convenient to define the following combination of integrals :

$$\begin{aligned} B_{RL}^+(k) &\equiv B_{RP}(k) + B_{ML}(k) = B_{RP}(k) + [B_{RP}(k)]_{m \leftrightarrow \bar{m}}^* \\ B_{RR}^+(k) &\equiv \Theta(m > \bar{m})(B_{RM}(k) - B_{ML}(k)) + \Theta(m < \bar{m})(B_{PR}(k) - B_{LP}(k)) \\ &= \Theta(m > \bar{m})(B_{RP}(-k) - B_{RP}(k)_{m \leftrightarrow \bar{m}}^*) + \Theta(m < \bar{m})(B_{RP}(-k)_{m \leftrightarrow \bar{m}} - B_{RP}(k)^*) \end{aligned} \quad (\text{B.35})$$

As we will see in next subsection, using these combinations, the rest of the divergent integrals can also be reduced to  $B_{RP}(k)$ .

### B.4.1 Time-like $k^\mu$ : reduction of divergent integrals

We will begin with the case of time-like  $k^\mu$  and move to the rest frame of  $k^\mu$  i.e., set  $k^\mu = (M, \vec{0})$ . Let us begin by evaluating

$$\begin{aligned}
B_{RP}(k) &= \mu^{4-d} \int \frac{d^d p}{(2\pi)^{d_i}} \int \frac{d^d q}{(2\pi)^{d_i}} \frac{1}{p^2 + m^2 - i\varepsilon} 2\pi i \delta_+(q^2 + \bar{m}^2) (2\pi)^d \delta^d(p - q - k) \\
&= \mu^{4-d} \int \frac{d^d p}{(2\pi)^{d_i}} \int \frac{d^{d-1} q}{(2\pi)^{d-1}(2\bar{\omega}_q)} \frac{1}{p^2 + m^2 - i\varepsilon} (2\pi)^d \delta^{d-1}(\vec{p} - \vec{q}) \delta(p^0 - \bar{\omega}_q - M) \\
&= \mu^{4-d} \int \frac{d^d p}{(2\pi)^{d_i}} \frac{1}{2\bar{\omega}_p} \frac{1}{p^2 + m^2 - i\varepsilon} 2\pi \delta(p^0 - \bar{\omega}_p - M) \\
&= \mu^{4-d} \int \frac{d^{d-1} p}{(2\pi)^{d-1} i} \frac{1}{2\bar{\omega}_p} \frac{1}{\omega_p^2 - (M + \bar{\omega}_p)^2 - i\varepsilon} \\
&= \frac{\mu^{4-d} \text{Vol}(\mathbb{S}^{d-2})}{2(2\pi)^{d-1} i} \int_{\bar{m}}^{\infty} d\bar{\omega}_p \frac{(\bar{\omega}_p^2 - \bar{m}^2)^{\frac{d-3}{2}}}{\omega_p^2 - (M + \bar{\omega}_p)^2 - i\varepsilon}
\end{aligned} \tag{B.36}$$

We will now show how the rest of the one-loop integrals can be reduced to  $B_{PR}(k)$  for time-like  $k^\mu$ . We have

$$\begin{aligned}
B_{RL}(k) &\equiv \mu^{4-d} \int \frac{d^d p}{(2\pi)^{d_i}} \int \frac{d^d q}{(2\pi)^{d_i}} \frac{1}{p^2 + m^2 - i\varepsilon} \frac{-1}{q^2 + \bar{m}^2 + i\varepsilon} (2\pi)^d \delta^d(p - q - k) \\
&= -\mu^{4-d} \int \frac{d^d p}{(2\pi)^{d_i} i^2} \frac{1}{p^2 + m^2 - i\varepsilon} \frac{1}{(p - k)^2 + \bar{m}^2 + i\varepsilon} \\
&= -\mu^{4-d} \int \frac{d^d p}{(2\pi)^{d_i} i^2} \frac{1}{(\omega_p - i\varepsilon)^2 - (p^0)^2} \frac{1}{(\bar{\omega}_p + i\varepsilon)^2 - (p^0 - M)^2} \times e^{i\delta \frac{p^0}{M}}
\end{aligned} \tag{B.37}$$

where in the last step, we have put  $\epsilon, \delta$  in different places to help in contour integration. Now we perform the contour integral by closing the contour in the upper half plane for  $M > 0$  and in the lower half plane for  $M < 0$ . This gives

$$\begin{aligned}
B_{RL}(k) &= \mu^{4-d} \int \frac{d^{d-1} p}{(2\pi)^{d-1} i} \left( \frac{1}{\omega_p^2 - (|M| + \bar{\omega}_p)^2 - i\varepsilon} \frac{1}{2\bar{\omega}_p} - \frac{1}{2\omega_p} \frac{1}{\bar{\omega}_p^2 - (|M| + \omega_p)^2 + i\varepsilon} \right) \\
&= \frac{\mu^{4-d} \text{Vol}(\mathbb{S}^{d-2})}{2(2\pi)^{d-1} i} \left( \int_{\bar{m}}^{\infty} d\bar{\omega}_p \frac{(\bar{\omega}_p^2 - \bar{m}^2)^{\frac{d-3}{2}}}{\omega_p^2 - (|M| + \bar{\omega}_p)^2 - i\varepsilon} - \int_m^{\infty} d\omega_p \frac{(\omega_p^2 - m^2)^{\frac{d-3}{2}}}{\bar{\omega}_p^2 - (|M| + \omega_p)^2 + i\varepsilon} \right) \\
&= \Theta(k^0) [B_{RP}(k) + B_{ML}(k)] + \Theta(-k^0) [B_{RM}(k) + B_{PL}(k)] \\
&= \Theta(k^0) \left( B_{RP}(k) + [B_{RP}(k)]_{m \leftrightarrow \bar{m}}^* \right) + \Theta(-k^0) \left( B_{RP}(-k) + [B_{RP}(-k)]_{m \leftrightarrow \bar{m}}^* \right) \\
&= \Theta(k^0) B_{RL}^+(k) + \Theta(-k^0) B_{RL}^+(-k)
\end{aligned} \tag{B.38}$$

where we have used the definition given in equation(B.35). Next, we turn to

$$\begin{aligned}
B_{LR}(k) &\equiv \mu^{4-d} \int \frac{d^d p}{(2\pi)^{d_i}} \int \frac{d^d q}{(2\pi)^{d_i}} \frac{-1}{p^2 + m^2 + i\varepsilon} \frac{1}{q^2 + \bar{m}^2 - i\varepsilon} (2\pi)^d \delta^d(p - q - k) \\
&= B_{RL}(k)_{m \leftrightarrow \bar{m}} = \Theta(k^0)[B_{MR}(k) + B_{LP}(k)] + \Theta(-k^0)[B_{PR}(k) + B_{LM}(k)] \\
&= \Theta(k^0) \left( B_{RP}(k)_{m \leftrightarrow \bar{m}} + [B_{RP}(k)]^* \right) + \Theta(-k^0) \left( B_{RP}(-k)_{m \leftrightarrow \bar{m}} + [B_{RP}(-k)]^* \right) \\
&= \Theta(k^0)[B_{RL}^+(k)]^* + \Theta(-k^0)[B_{RL}^+(-k)]^*
\end{aligned} \tag{B.39}$$

We then look at

$$\begin{aligned}
B_{RR}(k) &= \mu^{4-d} \int \frac{d^d p}{(2\pi)^{d_i}} \int \frac{d^d q}{(2\pi)^{d_i}} \frac{1}{p^2 + m^2 - i\varepsilon} \frac{1}{q^2 + \bar{m}^2 - i\varepsilon} (2\pi)^d \delta^d(p + q - k) \\
&= \mu^{4-d} \int \frac{d^d p}{(2\pi)^d i^2} \frac{1}{p^2 + m^2 - i\varepsilon} \frac{1}{(k - p)^2 + \bar{m}^2 - i\varepsilon} \\
&= \mu^{4-d} \int \frac{d^d p}{(2\pi)^d i^2} \frac{1}{(\omega_p - i\varepsilon)^2 - (p^0)^2} \frac{1}{(\bar{\omega}_p - i\varepsilon)^2 - (p^0 - M)^2}
\end{aligned} \tag{B.40}$$

We want to now write the answer of the contour integral with a definite  $\varepsilon$  prescription. An examination of the sign of resulting  $\varepsilon$ 's shows that the form depends now on the sign of  $M$  as well as  $m - \bar{m}$ . A careful examination of  $\varepsilon$ 's give

$$\begin{aligned}
&B_{RR}(k) \\
&= \Theta(m > \bar{m}) \mu^{4-d} \int \frac{d^{d-1} p}{(2\pi)^{d-1} i} \left( \frac{1}{2\omega_p} \frac{1}{\bar{\omega}_p^2 - (|M| + \omega_p)^2 + i\varepsilon} + \frac{1}{\omega_p^2 - (|M| - \bar{\omega}_p)^2 - i\varepsilon} \frac{1}{2\bar{\omega}_p} \right) \\
&+ \Theta(m < \bar{m}) \mu^{4-d} \int \frac{d^{d-1} p}{(2\pi)^{d-1} i} \left( \frac{1}{2\omega_p} \frac{1}{\bar{\omega}_p^2 - (|M| - \omega_p)^2 - i\varepsilon} + \frac{1}{\omega_p^2 - (|M| + \bar{\omega}_p)^2 + i\varepsilon} \frac{1}{2\bar{\omega}_p} \right)
\end{aligned} \tag{B.41}$$

Transcribing it into  $B_{RP}$  integrals, we obtain

$$\begin{aligned}
&B_{RR}(k) \\
&= \Theta(k^0) \left\{ \Theta(m > \bar{m})(B_{RP}(-k) - B_{RP}(k)_{m \leftrightarrow \bar{m}}^*) + \Theta(m < \bar{m})(B_{RP}(-k)_{m \leftrightarrow \bar{m}} - B_{RP}(k)^*) \right\} \\
&\quad + \Theta(-k^0) \left\{ \Theta(m > \bar{m})(B_{RP}(k) - B_{RP}(-k)_{m \leftrightarrow \bar{m}}^*) + \Theta(m < \bar{m})(B_{RP}(k)_{m \leftrightarrow \bar{m}} - B_{RP}(-k)^*) \right\} \\
&= \Theta(k^0) B_{RR}^+(k) + \Theta(-k^0) B_{RR}^+(-k)
\end{aligned} \tag{B.42}$$

It follows that

$$\begin{aligned}
&B_{LL}(k) = B_{RR}(k)^* \\
&= \Theta(k^0) \left\{ \Theta(m > \bar{m})(B_{RP}(-k)^* - B_{RP}(k)_{m \leftrightarrow \bar{m}}) + \Theta(m < \bar{m})(B_{RP}(-k)_{m \leftrightarrow \bar{m}}^* - B_{RP}(k)) \right\} \\
&\quad + \Theta(-k^0) \left\{ \Theta(m > \bar{m})(B_{RP}(k)^* - B_{RP}(-k)_{m \leftrightarrow \bar{m}}) + \Theta(m < \bar{m})(B_{RP}(k)_{m \leftrightarrow \bar{m}}^* - B_{RP}(-k)) \right\} \\
&= \Theta(k^0)[B_{RR}^+(k)]^* + \Theta(-k^0)[B_{RR}^+(-k)]^*
\end{aligned} \tag{B.43}$$

We will now turn to the case of space-like  $k^\mu$  to prove similar relations in that case.

### B.4.2 Space-like $k^\mu$ : reduction of divergent integrals

We will study  $B_{RP}(k)$  when  $k^\mu$  is space-like. We set  $k^\mu = \{0, Q = \sqrt{k^2}, \vec{0}_{d-2}\}$  where we can take  $Q > 0$  without loss of generality.

$$\begin{aligned}
B_{RP}(k) &= \mu^{4-d} \int \frac{d^d p}{(2\pi)^{d_i}} \int \frac{d^d q}{(2\pi)^{d_i}} \frac{1}{p^2 + m^2 - i\varepsilon} 2\pi i \delta_+(q^2 + \bar{m}^2) (2\pi)^d \delta^d(p - q - k) \\
&= \mu^{4-d} \int \frac{d^d p}{(2\pi)^{d_i}} \int \frac{d^d q}{(2\pi)^{d_i}} \frac{1}{p^2 + m^2 - i\varepsilon} 2\pi i \delta_+(q^2 + \bar{m}^2) \\
&\quad \times (2\pi)^d \delta(p^0 - q^0) \delta(p_{\parallel} - q_{\parallel} - Q) \delta(p_{\perp} - q_{\perp}) \\
&= \mu^{4-d} \int \frac{d^{d-1} q}{(2\pi)^{d-1_i}} \frac{1}{2\bar{\omega}_q} \frac{1}{q_{\perp}^2 + (Q + q_{\parallel})^2 + m^2 - \bar{\omega}_q^2 - i\varepsilon} \\
&= \mu^{4-d} \int \frac{d^{d-1} q}{(2\pi)^{d-1_i}} \frac{1}{2\bar{\omega}_q} \frac{1}{m^2 - \bar{m}^2 + Q^2 + 2Qq_{\parallel} - i\varepsilon} \\
&= \frac{\mu^{4-d}}{4Q} \int \frac{d^{d-1} q}{(2\pi)^{d-1_i}} \frac{1}{\bar{\omega}_q} \frac{1}{q_{\parallel}^* + q_{\parallel} - i\varepsilon}
\end{aligned} \tag{B.44}$$

where, we have defined

$$q_{\parallel}^* \equiv \frac{m^2 - \bar{m}^2 + Q^2}{2Q}.$$

Now, we move on to calculating  $B_{RL}(k)$ , given by

$$\begin{aligned}
B_{RL}(k) &= \mu^{4-d} \int \frac{d^d p}{(2\pi)^{d_i}} \int \frac{d^d q}{(2\pi)^{d_i}} \frac{1}{p^2 + m^2 - i\varepsilon} \frac{-1}{q^2 + \bar{m}^2 + i\varepsilon} (2\pi)^d \delta^d(p - q - k) \\
&= \mu^{4-d} \int \frac{d^d p}{(2\pi)^d} \frac{1}{p^2 + m^2 - i\varepsilon} \frac{1}{(p - k)^2 + \bar{m}^2 + i\varepsilon} \\
&= \mu^{4-d} \int \frac{d^d p}{(2\pi)^d} \frac{1}{\omega_p^2 - (p^0)^2 - i\varepsilon} \frac{1}{\bar{\omega}_{p_{\perp}}^2 + (Q - p_{\parallel})^2 - (p^0)^2 + i\varepsilon} \\
&= \mu^{4-d} \int \frac{d^{d-1} p}{(2\pi)^{d-1_i}} \left( -\frac{1}{2\omega_p} \frac{1}{\bar{m}^2 - m^2 + Q^2 - 2Qp_{\parallel} + i\varepsilon} \right. \\
&\quad \left. + \frac{1}{m^2 - \bar{m}^2 - Q^2 + 2Qp_{\parallel} - i\varepsilon} \frac{1}{2\bar{\omega}_{p-k}} \right)
\end{aligned} \tag{B.45}$$

Now, we take  $p = -q$  in the first integral and  $p = k + q$  for the second integral to write

$$\begin{aligned}
B_{RL}(k) &= \mu^{4-d} \int \frac{d^{d-1} q}{(2\pi)^{d-1_i}} \left( -\frac{1}{2\omega_q} \frac{1}{\bar{m}^2 - m^2 + Q^2 + 2Qq_{\parallel} + i\varepsilon} \right. \\
&\quad \left. + \frac{1}{m^2 - \bar{m}^2 + Q^2 + 2Qq_{\parallel} - i\varepsilon} \frac{1}{2\bar{\omega}_q} \right) \\
&= B_{RP}(k)^*|_{m \leftrightarrow \bar{m}} + B_{RP}(k) = B_{RL}^+(k)
\end{aligned} \tag{B.46}$$

Similarly,

$$B_{LR}(k) = B_{RL}(k)|_{m \leftrightarrow \bar{m}} = B_{RP}(k)|_{m \leftrightarrow \bar{m}} + B_{RP}(k)^* = [B_{RL}^+(k)]^* \tag{B.47}$$

Let us now do the  $B_{RR}(k)$  integral for space-like  $k^\mu$  :

$$\begin{aligned}
B_{RR}(k) &= \mu^{4-d} \int \frac{d^d p}{(2\pi)^d i} \int \frac{d^d q}{(2\pi)^d i} \frac{1}{p^2 + m^2 - i\varepsilon} \frac{1}{q^2 + \bar{m}^2 - i\varepsilon} (2\pi)^d \delta^d(p + q - k) \\
&= \mu^{4-d} \int \frac{d^d p}{(2\pi)^d i^2} \frac{1}{p^2 + m^2 - i\varepsilon} \frac{1}{(k-p)^2 + \bar{m}^2 - i\varepsilon} \\
&= \mu^{4-d} \int \frac{d^d p}{(2\pi)^d i^2} \frac{1}{\omega_p^2 - (p^0)^2 - i\varepsilon} \frac{1}{\bar{\omega}_{p_\perp}^2 + (Q - p_\parallel)^2 - (p^0)^2 - i\varepsilon} \\
&= \mu^{4-d} \int \frac{d^{d-1} p}{(2\pi)^{d-1} i} \left( \frac{1}{2\sqrt{\omega_{p_\perp}^2 + p_\parallel^2}} \frac{1}{\bar{m}^2 - m^2 + Q^2 - 2Qp_\parallel - i\varepsilon \operatorname{sgn}(\bar{\omega}_{p_\perp} - \omega_{p_\perp})} \right. \\
&\quad \left. + \frac{1}{m^2 - \bar{m}^2 - Q^2 + 2Qp_\parallel - i\varepsilon \operatorname{sgn}(\omega_{p_\perp} - \bar{\omega}_{p_\perp})} \frac{1}{2\sqrt{\bar{\omega}_{p_\perp}^2 + (Q - p_\parallel)^2}} \right)
\end{aligned} \tag{B.48}$$

Now, we take  $p_\parallel = -q_\parallel$  in the first integral and  $p_\parallel = Q + q_\parallel$  in the second, to get

$$\begin{aligned}
B_{RR}(k) &= \mu^{4-d} \int \frac{d^{d-1} q}{(2\pi)^{d-1} i} \left( \frac{1}{2\sqrt{\omega_{q_\perp}^2 + q_\parallel^2}} \frac{1}{\bar{m}^2 - m^2 + Q^2 + 2Qq_\parallel - i\varepsilon \operatorname{sgn}(\bar{\omega}_{p_\perp} - \omega_{p_\perp})} \right. \\
&\quad \left. + \frac{1}{m^2 - \bar{m}^2 + Q^2 + 2Qq_\parallel - i\varepsilon \operatorname{sgn}(\omega_{q_\perp} - \bar{\omega}_{q_\perp})} \frac{1}{2\sqrt{\bar{\omega}_{q_\perp}^2 + q_\parallel^2}} \right) \\
&= \Theta(m > \bar{m}) \mu^{4-d} \int \frac{d^{d-1} q}{(2\pi)^{d-1} i} \left( \frac{1}{m^2 - \bar{m}^2 + Q^2 - 2Qq_\parallel - i\varepsilon} \frac{1}{2\bar{\omega}_q} \right. \\
&\quad \left. + \frac{1}{2\omega_q} \frac{1}{\bar{m}^2 - m^2 + Q^2 + 2Qq_\parallel + i\varepsilon} \right) \\
&+ \Theta(m < \bar{m}) \mu^{4-d} \int \frac{d^{d-1} q}{(2\pi)^{d-1} i} \left( \frac{1}{2\omega_q} \frac{1}{\bar{m}^2 - m^2 + Q^2 - 2Qq_\parallel - i\varepsilon} \right. \\
&\quad \left. + \frac{1}{m^2 - \bar{m}^2 + Q^2 + 2Qq_\parallel + i\varepsilon} \frac{1}{2\bar{\omega}_q} \right) \\
&= \Theta(m > \bar{m}) (B_{RP}(-k) - B_{RP}(k)_{m \leftrightarrow \bar{m}}^*) + \Theta(m < \bar{m}) (B_{RP}(-k)_{m \leftrightarrow \bar{m}} - B_{RP}(k)^*) \\
&= B_{RR}^+(k)
\end{aligned} \tag{B.49}$$

Here, in the penultimate step, we have done some variable redefinitions to obtain an answer similar to the time-like case. We can finally compute

$$B_{LL}(k) = B_{RR}(k)^* = [B_{RR}^+(k)]^* . \tag{B.50}$$

### B.4.3 Summary of divergent integrals

We can now put together various cases and write

$$\begin{aligned}
B_{RL}(k) &= \Theta(k^0)\Theta(-k^2)B_{RL}^+(k) + \Theta(-k^0)\Theta(-k^2)B_{RL}^+(-k) + \Theta(k^2)B_{RL}^+(k) \\
B_{LR}(k) &= \Theta(k^0)\Theta(-k^2)[B_{RL}^+(k)]^* + \Theta(-k^0)\Theta(-k^2)[B_{RL}^+(-k)]^* + \Theta(k^2)[B_{RL}^+(k)]^* \\
B_{RR}(k) &= \Theta(k^0)\Theta(-k^2)B_{RR}^+(k) + \Theta(-k^0)\Theta(-k^2)B_{RR}^+(-k) + \Theta(k^2)B_{RR}^+(k) \\
B_{LL}(k) &= \Theta(k^0)\Theta(-k^2)[B_{RR}^+(k)]^* + \Theta(-k^0)\Theta(-k^2)[B_{RR}^+(-k)]^* + \Theta(k^2)[B_{RR}^+(k)]^* .
\end{aligned} \tag{B.51}$$

where

$$\begin{aligned}
B_{RL}^+(k) &\equiv B_{RP}(k) + B_{ML}(k) = B_{RP}(k) + [B_{RP}(k)]_{m \leftrightarrow \bar{m}}^* \\
B_{RR}^+(k) &\equiv \Theta(m > \bar{m})(B_{RM}(k) - B_{ML}(k)) + \Theta(m < \bar{m})(B_{PR}(k) - B_{LP}(k)) \\
&= \Theta(m > \bar{m})(B_{RP}(-k) - B_{RP}(k)_{m \leftrightarrow \bar{m}}^*) + \Theta(m < \bar{m})(B_{RP}(-k)_{m \leftrightarrow \bar{m}} - B_{RP}(k)^*)
\end{aligned} \tag{B.52}$$

This is apart from the other divergent integrals :

$$\begin{aligned}
B_{RM}(k) &= B_{RP}(-k) , \\
B_{LP}(k) &= [B_{RP}(k)]^* , \quad B_{LM}(k) = [B_{RP}(-k)]^* , \\
B_{PR}(k) &= B_{RP}(-k)|_{m \leftrightarrow \bar{m}} , \quad B_{MR}(k) = B_{RP}(k)|_{m \leftrightarrow \bar{m}} , \\
B_{PL}(k) &= B_{RP}(-k)^*|_{m \leftrightarrow \bar{m}} , \quad B_{ML}(k) = B_{RP}(k)^*|_{m \leftrightarrow \bar{m}} .
\end{aligned} \tag{B.53}$$

We note that all these integrals can be written in terms of  $B_{RP}(k)$  as advertised.

### B.4.4 Reduction and identities due to largest time equations

A further reduction is possible using largest time equations and their concomitant cutting rules :

$$\begin{aligned}
B_{RR}(k) + B_{RL}(k) &= B_{RP}(k) + B_{RM}(k) \\
B_{LR}(k) + B_{LL}(k) &= B_{LP}(k) + B_{LM}(k) \\
B_{PR}(k) + B_{PL}(k) &= B_{PP}(k) + B_{MM}(k) \\
B_{MR}(k) + B_{ML}(k) &= B_{MP}(k) + B_{RM}(k)
\end{aligned} \tag{B.54}$$

From applying these identities, we can conclude that  $\text{Re}[B_{RP}(k) + B_{RP}(-k)]$  and  $\text{Im}[B_{RP}(k) - B_{RP}(-k)]$  is symmetric under  $m \leftrightarrow \bar{m}$  exchange. Further, the real part (viz., the cut) of  $B_{RP}(k)$  integral is given by

$$\begin{aligned}
B_{RP}(k) + B_{RP}(k)^* &= \text{Re } B_{RL}^+(k) \\
&= \frac{\text{Vol}(\mathbb{S}^{d-2})}{32\pi^2} \left[ 1 + 2 \left( \frac{m^2 + \bar{m}^2}{k^2} \right) + \left( \frac{m^2 - \bar{m}^2}{k^2} \right)^2 \right]^{\frac{d-3}{2}} \\
&\times \left\{ \Theta(k^2) \frac{1}{2\pi} \Gamma\left(\frac{3}{2} - \frac{d}{2}\right) \Gamma\left(\frac{d}{2} - \frac{1}{2}\right) \left( \frac{k^2}{(4\pi\mu)^2} \right)^{\frac{d-4}{2}} \right. \\
&\quad \left. + [\Theta(k^0)\Theta((\bar{m} - m)^2 + k^2) + \Theta(-k^0)]\Theta(-k^2) \left( \frac{-k^2}{(4\pi\mu)^2} \right)^{\frac{d-4}{2}} \right\}
\end{aligned} \tag{B.55}$$

These conditions in turn lead to the identities :

$$\begin{aligned}
B_{RP}(k) + B_{LP}(k) &= B_{MR}(k) + B_{ML}(k) \\
B_{RP}(k) + B_{LM}(k) &= B_{MR}(k) + B_{PL}(k) \\
B_{RP}(k) + B_{PR}(k) &= B_{RM}(k) + B_{MR}(k) \\
B_{PR}(k) + B_{PL}(k) &= B_{RM}(k) + B_{LM}(k) \\
B_{PR}(k) + B_{ML}(k) &= B_{RM}(k) + B_{LP}(k) \\
B_{LP}(k) + B_{PL}(k) &= B_{LM}(k) + B_{ML}(k)
\end{aligned} \tag{B.56}$$

From, these identities we get

$$\begin{aligned}
B_{RL}^+(k) &\equiv B_{RP}(k) + B_{ML}(k) = B_{RP}(k) + [B_{RP}(k)]_{m \leftrightarrow \bar{m}}^* \\
B_{RR}^+(k) &= B_{RP}(-k) - B_{RP}(k)_{m \leftrightarrow \bar{m}}^* = B_{RP}(-k)_{m \leftrightarrow \bar{m}} - B_{RP}(k)^*
\end{aligned} \tag{B.57}$$

which in turn obey

$$B_{RR}^+(k) + B_{RL}^+(k) = B_{RP}(k) + B_{RP}(-k) = B_{RP}(k) + B_{RM}(k) \tag{B.58}$$

Another implication is

$$\begin{aligned}
\text{Re } B_{RR}^+(k) &= \frac{\text{Vol}(\mathbb{S}^{d-2})}{32\pi^2} \left[ 1 + 2 \left( \frac{m^2 + \bar{m}^2}{k^2} \right) + \left( \frac{m^2 - \bar{m}^2}{k^2} \right)^2 \right]^{\frac{d-3}{2}} \\
&\times \frac{1}{2} [\Theta(k^0) - \Theta(-k^0)] \Theta(-(\bar{m} - m)^2 - k^2) \Theta(-k^2) \left( \frac{-k^2}{(4\pi\mu)^2} \right)^{\frac{d-4}{2}}
\end{aligned} \tag{B.59}$$

The following combination is symmetric under  $m \leftrightarrow \bar{m}$  as well as  $k \leftrightarrow -k$  exchange.

$$\begin{aligned}
&B_{RP}(k) + B_{RP}(k)^* + B_{PM}(k) \\
&= \frac{\text{Vol}(\mathbb{S}^{d-2})}{32\pi^2} \left[ 1 + 2 \left( \frac{m^2 + \bar{m}^2}{k^2} \right) + \left( \frac{m^2 - \bar{m}^2}{k^2} \right)^2 \right]^{\frac{d-3}{2}} \\
&\times \left\{ \Theta(k^2) \frac{1}{2\pi} \Gamma\left(\frac{3}{2} - \frac{d}{2}\right) \Gamma\left(\frac{d}{2} - \frac{1}{2}\right) \left( \frac{k^2}{(4\pi\mu)^2} \right)^{\frac{d-4}{2}} \right. \\
&\quad \left. + \Theta(-k^2) \left( \frac{-k^2}{(4\pi\mu)^2} \right)^{\frac{d-4}{2}} \right\}
\end{aligned} \tag{B.60}$$

## B.5 Evaluation of $B_{RP}(k)$

The basic integral  $B_{RP}(k)$  has the following form on the time-like case :

$$\begin{aligned}
B_{RP}(k) &= \frac{\mu^{4-d} \text{Vol}(\mathbb{S}^{d-2})}{2(2\pi)^{d-1} i} \int_{\bar{m}}^{\infty} d\bar{\omega}_p \frac{(\bar{\omega}_p^2 - \bar{m}^2)^{\frac{d-3}{2}}}{\omega_p^2 - (M + \bar{\omega}_p)^2 - i\varepsilon} \\
&= \frac{\mu^{4-d} \text{Vol}(\mathbb{S}^{d-2})}{2(2\pi)^{d-1} i} \int_{\bar{m}}^{\infty} d\bar{\omega}_p \frac{(\bar{\omega}_p^2 - \bar{m}^2)^{\frac{d-3}{2}}}{2M(\bar{\omega}_p^* - \bar{\omega}_p) - i\varepsilon}
\end{aligned} \tag{B.61}$$

with

$$\bar{\omega}_p^* \equiv \frac{m^2 - \bar{m}^2 - M^2}{2M} .$$



The same integral in the space-like case takes the form

$$B_{RP}(k) = \frac{\mu^{4-d}}{2Q} \int \frac{d^{d-1}q}{(2\pi)^{d-1}i} \frac{1}{2\bar{\omega}_q} \frac{1}{q_{||}^* + q_{||} - i\varepsilon} \quad (\text{B.62})$$

where, we have defined

$$q_{||}^* \equiv \frac{m^2 - \bar{m}^2 + Q^2}{2Q}.$$

Our aim in this subsection is to evaluate these integrals and extract out the appropriate divergences.

### B.5.1 Time-like $k^\mu$ : computation of divergences

We begin by setting  $\bar{\omega}_p = \bar{m} \cosh \eta$  in the time-like case to get

$$\begin{aligned} B_{RP}(k) &= \frac{\mu^{4-d} \text{Vol}(\mathbb{S}^{d-2}) \bar{m}^{d-3}}{4M(2\pi)^{d-1} i} \int_0^\infty d\eta \frac{\sinh^{d-2} \eta}{\bar{\gamma} - \cosh \eta} \\ &= \frac{\text{Vol}(\mathbb{S}^{d-2}) \bar{m}}{32\pi^2} \frac{\bar{m}}{M} \left( \frac{\bar{m}^2}{4\pi\mu^2} \right)^{\frac{d-4}{2}} \int_0^\infty \frac{d\eta}{i\pi^{d/2-1}} \frac{\sinh^{d-2} \eta}{\bar{\gamma} - \cosh \eta} \end{aligned} \quad (\text{B.63})$$

where we have defined

$$\bar{\gamma} = \frac{\bar{\omega}_p^*}{\bar{m}} \equiv \frac{m^2 - \bar{m}^2 - M^2 - i\varepsilon}{2M\bar{m}}. \quad (\text{B.64})$$

Thus, we have reduced our analysis to the integral

$$F(\bar{\gamma}) \equiv \int_0^\infty \frac{d\eta}{i\pi^{d/2-1}} \frac{\sinh^{d-2} \eta}{\bar{\gamma} - \cosh \eta} \quad (\text{B.65})$$

This integral can then analyzed in detail to study the analytic structure of this integral. But, for our purposes, it is sufficient to extract the divergences.

For our computation of  $\beta$  function, we need to extract out the divergent part of these integrals. Focusing on the large  $\bar{\omega}_p$  contribution, we can approximate  $B_{RP}(k)$  by

$$\begin{aligned} B_{RP}(k) &= \frac{\mu^{4-d} \text{Vol}(\mathbb{S}^{d-2})}{2(2\pi)^{d-1} i} \int_{\bar{m}}^\infty d\bar{\omega}_p (\bar{\omega}_p^2 - \bar{m}^2)^{\frac{d}{2}} \left[ -\frac{1}{2M\bar{\omega}_p^4} + \frac{M^2 + \bar{m}^2 - m^2}{4M^2\bar{\omega}_p^5} + O(\bar{\omega}_p^{-6}) \right] \\ &= \frac{i}{128\pi^2} \frac{\Gamma\left(\frac{d+2}{2}\right)}{\Gamma\left(\frac{d-1}{2}\right)} \left( \frac{\bar{m}^2}{4\pi\mu^2} \right)^{\frac{d-4}{2}} \left\{ \frac{16\bar{m}}{3M} \Gamma\left(\frac{3-d}{2}\right) - \sqrt{\pi} \Gamma\left(\frac{4-d}{2}\right) \frac{M^2 + \bar{m}^2 - m^2}{M^2} + \dots \right\} \end{aligned} \quad (\text{B.66})$$

Near  $d = 4$ , this gives

$$B_{RP}(k) = \frac{i}{(4\pi)^2} \left\{ -\frac{16\bar{m}}{3M} + \frac{M^2 + \bar{m}^2 - m^2}{2M^2} \left[ \frac{2}{d-4} + \ln\left(\frac{4\bar{m}^2}{4\pi\mu^2 e^{-\gamma_E}}\right) - \frac{1}{2} \right] + \dots \right\} \quad (\text{B.67})$$

so that

### B.5.2 Space-like $k^\mu$ : computation of divergences

In this subsection, we will consider the space-like case and confirm that the divergence structure is same in the space-like case. Let us first get the real part of  $B_{RP}(k)$ , which is given by

$$B_{RP}(k) = \frac{\mu^{4-d} \text{Vol}(\mathbb{S}^{d-2})}{2(2\pi)^{d-1} i} \int_{\bar{m}}^{\infty} d\bar{\omega}_p \frac{(\bar{\omega}_p^2 - \bar{m}^2)^{\frac{d-3}{2}}}{2M(\bar{\omega}_p^* - \bar{\omega}_p) - i\varepsilon} \quad (\text{B.68})$$

$$\begin{aligned} B_{RP}(k) &= \frac{\mu^{4-d}}{2Q} \int \frac{d^{d-1}q}{(2\pi)^{d-1} i} \frac{1}{2\bar{\omega}_q} \frac{1}{q_{||}^* + q_{||} - i\varepsilon} \\ &= \frac{\mu^{4-d}}{4Q(2\pi)^{d-1} i} \int_{\bar{m}}^{\infty} d\bar{\omega}_{q_\perp} \bar{\omega}_{q_\perp} (\bar{\omega}_{q_\perp}^2 - \bar{m}^2)^{\frac{d-4}{2}} \int_{-\infty}^{\infty} dq_{||} \frac{1}{\sqrt{\bar{\omega}_{q_\perp}^2 + q_{||}^2}} \frac{1}{q_{||}^* + q_{||} - i\varepsilon} \end{aligned} \quad (\text{B.69})$$

where, we have defined

$$q_{||}^* \equiv \frac{m^2 - \bar{m}^2 + Q^2}{2Q}.$$

Let us first get the real part of  $B_{RP}(k)$ , which is given by

$$\begin{aligned} &B_{RP}(k) \Big|_{\text{real part}} \\ &= \frac{\mu^{4-d}}{4Q(2\pi)^{d-1} i} \int_{\bar{m}}^{\infty} d\bar{\omega}_{q_\perp} \bar{\omega}_{q_\perp} (\bar{\omega}_{q_\perp}^2 - \bar{m}^2)^{\frac{d-4}{2}} \\ &\int_{-\infty}^{\infty} dq_{||} \frac{1}{\sqrt{\bar{\omega}_{q_\perp}^2 + q_{||}^2}} \left( \frac{1}{q_{||}^* + q_{||} - i\varepsilon} - \frac{1}{q_{||}^* + q_{||} + i\varepsilon} \right) \\ &= \frac{\mu^{4-d}}{4Q(2\pi)^{d-1} i} \int_{\bar{m}}^{\infty} d\bar{\omega}_{q_\perp} \bar{\omega}_{q_\perp} (\bar{\omega}_{q_\perp}^2 - \bar{m}^2)^{\frac{d-4}{2}} \int_{-\infty}^{\infty} dq_{||} \frac{1}{\sqrt{\bar{\omega}_{q_\perp}^2 + q_{||}^2}} 2\pi i \delta(q_{||}^* + q_{||}) \end{aligned} \quad (\text{B.70})$$

The above equation can easily be seen to be equal to  $B_{PP}(k)$  for the space-like case in (B.22). So, we have in the space-like case

$$B_{RP}(k) \Big|_{\text{real part}} = B_{PP}(k) \quad (\text{B.71})$$

Let us now get the imaginary part of  $B_{RP}(k)$ , which is also the divergent part. It is given by

$$B_{RP}(k) \Big|_{\text{imaginary part}} = \frac{i}{2(4\pi)^2} \frac{Q^2 + m^2 - \bar{m}^2}{Q^2} \left( \frac{2}{d-4} + \ln \frac{\bar{m}^2}{4\pi\mu^2 e^{-\gamma_E}} - 1 \right) + \dots \quad (\text{B.72})$$

when,  $m = \bar{m}$ , we get

$$B_{RP}(k) \Big|_{\text{imaginary part}} = \frac{i}{2(4\pi)^2} \left( \frac{2}{d-4} + \ln \frac{m^2}{4\pi\mu^2 e^{-\gamma_E}} - 1 \right) + \dots \quad (\text{B.73})$$

We see that these divergences are same as the time-like case.

### B.5.3 Summary of divergences

We now summarize the divergences in various integrals. We start with

$$\text{div}[B_{RP}] \Big|_{\overline{\text{MS}}} = \frac{i}{(4\pi)^2} \frac{k^2 - \bar{m}^2 + m^2}{2k^2} \left[ \frac{2}{d-4} + \ln\left(\frac{1}{4\pi e^{-\gamma_E}}\right) \right] \quad (\text{B.74})$$

and

$$\begin{aligned} \text{div}[B_{RL}^+] \Big|_{\overline{\text{MS}}} &= \frac{i}{(4\pi)^2} \frac{m^2 - \bar{m}^2}{k^2} \left[ \frac{2}{d-4} + \ln\left(\frac{1}{4\pi e^{-\gamma_E}}\right) \right] \\ \text{div}[B_{RR}^+] \Big|_{\overline{\text{MS}}} &= \frac{i}{(4\pi)^2} \left[ \frac{2}{d-4} + \ln\left(\frac{1}{4\pi e^{-\gamma_E}}\right) \right] \end{aligned} \quad (\text{B.75})$$

Thus,

$$\begin{aligned} \text{div}[B_{RP}] \Big|_{\overline{\text{MS}}} &= \text{div}[B_{RM}] \Big|_{\overline{\text{MS}}} = \frac{i}{(4\pi)^2} \frac{k^2 - \bar{m}^2 + m^2}{2k^2} \left[ \frac{2}{d-4} + \ln\left(\frac{1}{4\pi e^{-\gamma_E}}\right) \right] \\ \text{div}[B_{PR}] \Big|_{\overline{\text{MS}}} &= \text{div}[B_{MR}] \Big|_{\overline{\text{MS}}} = \frac{i}{(4\pi)^2} \frac{k^2 + \bar{m}^2 - m^2}{2k^2} \left[ \frac{2}{d-4} + \ln\left(\frac{1}{4\pi e^{-\gamma_E}}\right) \right] \\ \text{div}[B_{RL}] \Big|_{\overline{\text{MS}}} &= -\text{div}[B_{LR}] \Big|_{\overline{\text{MS}}} = \frac{i}{(4\pi)^2} \frac{m^2 - \bar{m}^2}{k^2} \left[ \frac{2}{d-4} + \ln\left(\frac{1}{4\pi e^{-\gamma_E}}\right) \right] \\ \text{div}[B_{RR}] \Big|_{\overline{\text{MS}}} &= -\text{div}[B_{LL}] \Big|_{\overline{\text{MS}}} = \frac{i}{(4\pi)^2} \left[ \frac{2}{d-4} + \ln\left(\frac{1}{4\pi e^{-\gamma_E}}\right) \right] \end{aligned} \quad (\text{B.76})$$

When  $m = \bar{m}$ , we can thus summarize the divergence of ‘quarter-cut’ integrals as

$$\begin{aligned} \text{div}[B_{RP}] \Big|_{\overline{\text{MS}}} &= \text{div}[B_{PR}] \Big|_{\overline{\text{MS}}} = \text{div}[B_{RM}] \Big|_{\overline{\text{MS}}} = \text{div}[B_{MR}] \Big|_{\overline{\text{MS}}} = \frac{i}{2(4\pi)^2} \left[ \frac{2}{d-4} + \ln\left(\frac{1}{4\pi e^{-\gamma_E}}\right) \right] \\ \text{div}[B_{LP}] \Big|_{\overline{\text{MS}}} &= \text{div}[B_{PL}] \Big|_{\overline{\text{MS}}} = \text{div}[B_{LM}] \Big|_{\overline{\text{MS}}} = \text{div}[B_{ML}] \Big|_{\overline{\text{MS}}} = -\frac{i}{2(4\pi)^2} \left[ \frac{2}{d-4} + \ln\left(\frac{1}{4\pi e^{-\gamma_E}}\right) \right] \end{aligned} \quad (\text{B.77})$$

This along with

$$\begin{aligned} \text{div}[B_{RR}] \Big|_{\overline{\text{MS}}} &= \frac{i}{(4\pi)^2} \left[ \frac{2}{d-4} + \ln\left(\frac{1}{4\pi e^{-\gamma_E}}\right) \right] \\ \text{div}[B_{LL}] \Big|_{\overline{\text{MS}}} &= -\frac{i}{(4\pi)^2} \left[ \frac{2}{d-4} + \ln\left(\frac{1}{4\pi e^{-\gamma_E}}\right) \right] \end{aligned} \quad (\text{B.78})$$

summarizes all the divergences needed in this work.

## B.6 UV divergences and symmetry factors

In this subsection, we will collect the UV divergences of various  $B$  type diagrams for the convenience of the reader.

$$\text{div}[B_{RR}(k)] \Big|_{\overline{\text{MS}}} = \frac{i}{(4\pi)^2} \left[ \frac{2}{d-4} + \ln\left(\frac{1}{4\pi e^{-\gamma_E}}\right) \right] \quad (\text{B.79a})$$

$$\text{div}[B_{LR}(k)] \Big|_{\overline{\text{MS}}} = 0 \quad (\text{B.79b})$$

$$\text{div}[B_{PP}(k)] \Big|_{\overline{\text{MS}}} = 0 \quad (\text{B.79c})$$

$$\text{div}[B_{PR}(k)] \Big|_{\overline{\text{MS}}} = \frac{1}{2} \text{div}[B_{RR}(k)] \Big|_{\overline{\text{MS}}} \quad (\text{B.79d})$$

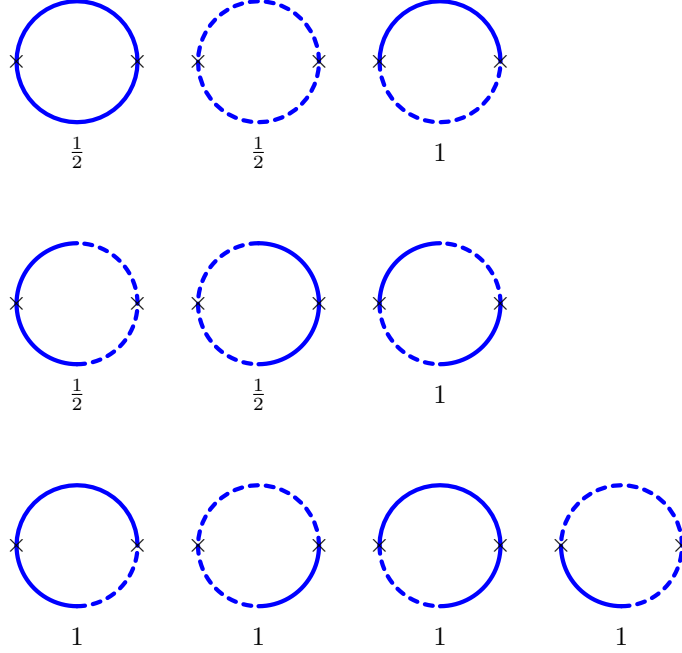
Further, we have

$$\text{div}[B_{RR}] \Big|_{\overline{\text{MS}}} = \text{div}[B_{LL}]^* \Big|_{\overline{\text{MS}}} \quad (\text{B.80a})$$

$$\text{div}[B_{LR}] \Big|_{\overline{\text{MS}}} = \text{div}[B_{PM}]^* \Big|_{\overline{\text{MS}}} = \text{div}[B_{MP}] \Big|_{\overline{\text{MS}}} = \text{div}[B_{PP}] \Big|_{\overline{\text{MS}}} = 0 \quad (\text{B.80b})$$

$$\text{div}[B_{PR}] \Big|_{\overline{\text{MS}}} = \text{div}[B_{MR}] \Big|_{\overline{\text{MS}}} = \text{div}[B_{PL}]^* \Big|_{\overline{\text{MS}}} = \text{div}[B_{ML}]^* \Big|_{\overline{\text{MS}}} = \frac{1}{2} \text{div}[B_{RR}] \Big|_{\overline{\text{MS}}} \quad (\text{B.80c})$$

We also give below the symmetry factors of the corresponding diagrams in figure 28. The divergences given above along with the symmetry factors provides a quick way to write down appropriate  $\beta$  functions for the open QFT. In the ensuing figure 29 and figure 30, we tabulate a set of useful diagrammatic identities which relate the various SK loop integrals.



**Figure 28:** Symmetry factors for all the ten one loop integrals

## C Passarino-Veltman diagrams in the average-difference basis

Let us now take a look at the Passarino-Veltman diagrams in average-difference basis. It's worth remembering here that only three out of the four propagators, in this basis, are non-vanishing: the ' $d$ ' propagator vanishes. This means that we have lesser number of non-vanishing diagrams in this basis. As a matter of fact, some of the non-vanishing diagrams (in average-difference basis) do not diverge. All these facts add up to give only a few divergent one loop diagrams - only one  $A$  type and two  $B$  type integrals. Thus, computations for the beta functions greatly simplifies in this basis. We will not try to evaluate the PV integrals from scratch. We will express the integrals in the average-difference basis in terms of the integrals in the  $\phi_R$ - $\phi_L$  basis and then, use the results from the previous sections to determine the former.

$$\begin{aligned}
& B_{RR}(k) + B_{LL}(k) + 2B_{LR}(k) \\
& = B_{PM}(k) + B_{MP}(k) + 2B_{MM}(k)
\end{aligned}$$

**Figure 29:** Cutting identity of one loop integrals

### C.1 Passarino-Veltman $A$ type integral in the average-difference basis

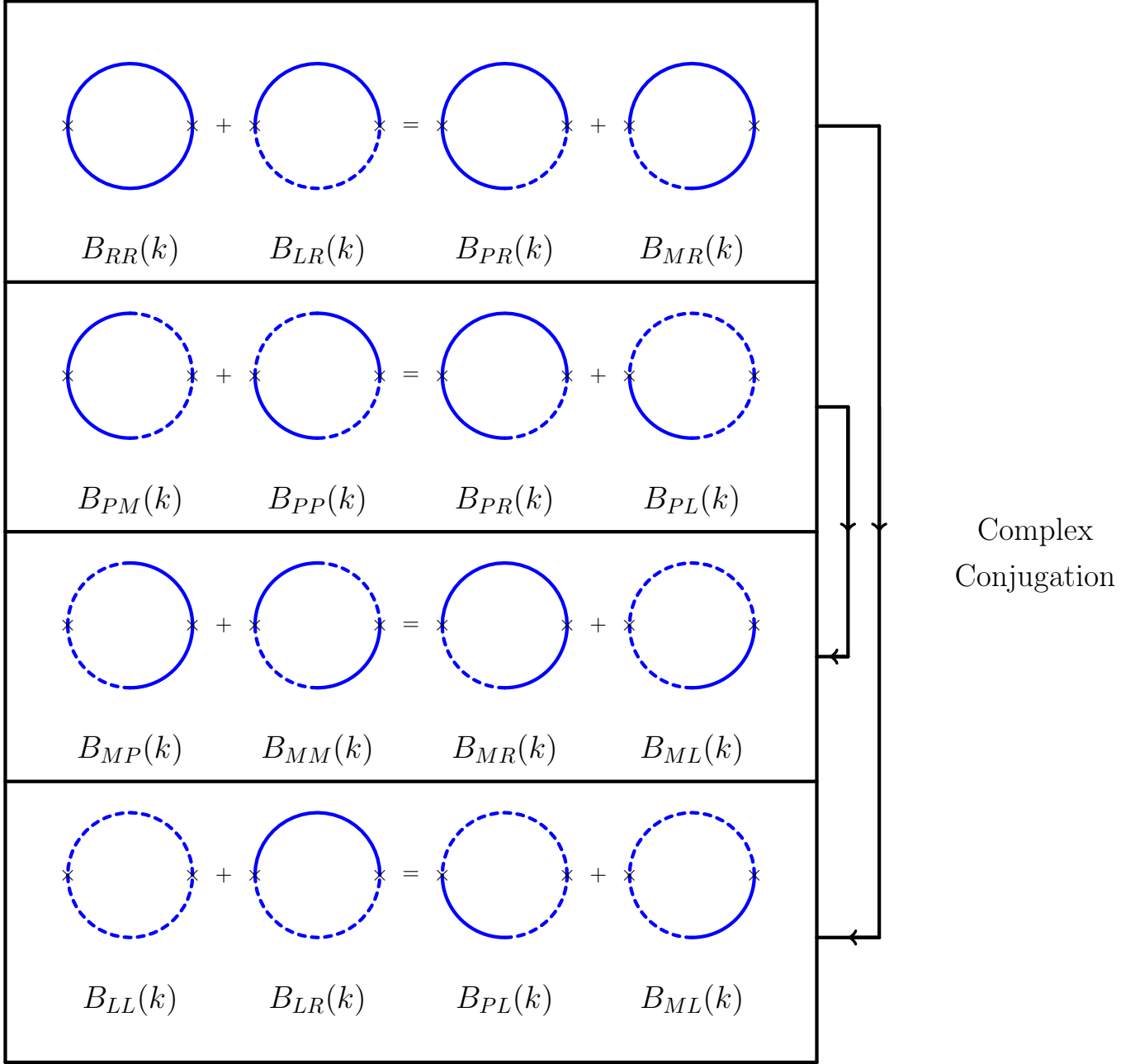
There are two  $A$  type PV integrals in this basis:  $A_a$  and  $A_b = A_f$ . Using the relations in equation (4.3) and equation (B.3)-(B.4), it's easy to check that we get

$$\begin{aligned}
A_a &= \frac{1}{2}(A_R + A_L) = \frac{1}{(4\pi)^2} \left[ \frac{2}{(d-4)} + \ln\left(\frac{m^2}{4\pi\mu^2 e^{-\gamma_E}}\right) - 1 \right] m^2 \\
A_b &= A_R - A_M = 0 \\
A_f &= A_R - A_P = 0
\end{aligned} \tag{C.1}$$

### C.2 Passarino-Veltman $B$ type integral in the average-difference basis

There are six PV  $B$  type integrals in this basis:  $B_{aa}$ ,  $B_{af}$ ,  $B_{ab}$ ,  $B_{bf}$ ,  $B_{fb}$  and  $B_{ff} = B_{bb}$ . Using the relations given in equation (4.3), it is easy to check that

$$\begin{aligned}
B_{aa} &= \frac{1}{4}(B_{RR} + B_{RL} + B_{LR} + B_{LL}) \\
B_{af} &= \frac{1}{2}(B_{RR} - B_{RP} + B_{LR} - B_{LP}) \\
B_{ab} &= \frac{1}{2}(B_{RR} - B_{RM} + B_{LR} - B_{LM}) \\
B_{fb} &= B_{RR} - B_{RM} - B_{PR} + B_{PM} \\
B_{bf} &= B_{RR} - B_{RP} - B_{MR} + B_{MP} \\
B_{ff} &= B_{bb} = B_{RR} - B_{RP} - B_{PR} + B_{PP}
\end{aligned} \tag{C.2}$$



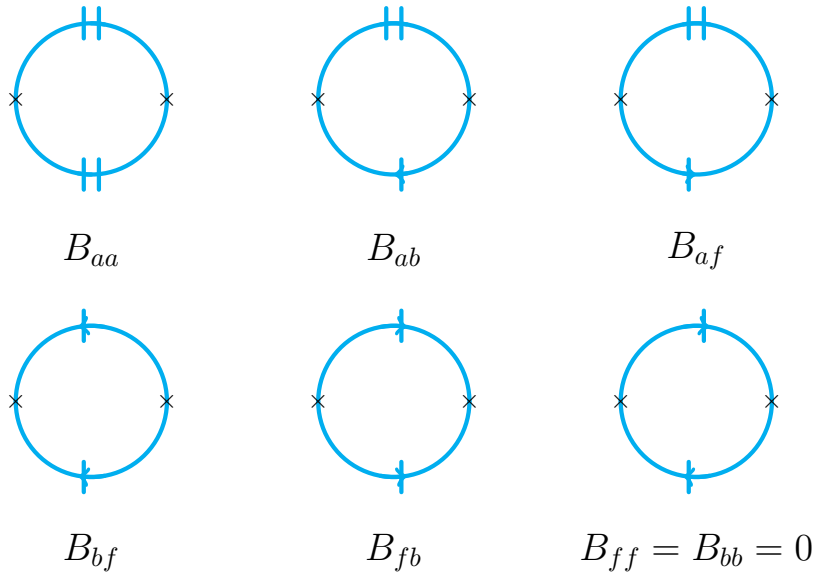
**Figure 30:** Identities between the ten one loop  $B$  type integrals

To compute the divergences for the above-mentioned integrals, we use the results given in equations (B.79a)-(B.80c) in section B.6. So, we have

$$\begin{aligned}
\operatorname{div}[B_{aa}] \Big|_{\overline{\text{MS}}} &= 0 \\
\operatorname{div}[B_{af}] \Big|_{\overline{\text{MS}}} &= \frac{1}{2} \operatorname{div}[B_{RR}] \Big|_{\overline{\text{MS}}} = \frac{i}{2(4\pi)^2} \left[ \frac{2}{d-4} + \ln \left( \frac{1}{4\pi e^{-\gamma_E}} \right) \right] \\
\operatorname{div}[B_{ab}] \Big|_{\overline{\text{MS}}} &= \frac{1}{2} \operatorname{div}[B_{RR}] \Big|_{\overline{\text{MS}}} = \frac{i}{2(4\pi)^2} \left[ \frac{2}{d-4} + \ln \left( \frac{1}{4\pi e^{-\gamma_E}} \right) \right] \\
\operatorname{div}[B_{fb}] \Big|_{\overline{\text{MS}}} &= 0 \\
\operatorname{div}[B_{bf}] \Big|_{\overline{\text{MS}}} &= 0 \\
\operatorname{div}[B_{ff}] \Big|_{\overline{\text{MS}}} &= \operatorname{div}[B_{bb}] \Big|_{\overline{\text{MS}}} = 0
\end{aligned} \tag{C.3}$$



**Figure 31:** PV one loop  $A$  type integrals in the average-difference basis



**Figure 32:** PV one loop  $B$  type integrals in the average-difference basis

We shall use these results for the computations in section 4 and in the next section.

## D Computations in the average-difference basis

In section 4, we have already computed the beta functions for the Lindblad violating combinations in the average-difference basis and we found that it matches with our computations in the  $\phi_R$ - $\phi_L$  basis. For the sake of completion, we calculate the beta function for rest of the mass terms and the rest of the coupling constants in this basis. This computation enables one to verify the beta functions computed in  $\phi_R$ - $\phi_L$  basis. We shall start off by providing the set of Feynman rules in this basis.

The propagators in this basis are given in equation (4.3). The vertex factors in this basis are given by

Vertex	Factor
$\phi_d^3$	$\frac{(-i)}{4}(\text{Re } \lambda_3 - 3 \text{ Re } \sigma_3)(2\pi)^d \delta(\sum p)$
$\phi_a^3$	$2(\text{Im } \lambda_3 + 3 \text{ Im } \sigma_3)(2\pi)^d \delta(\sum p)$
$\phi_d^2 \phi_a$	$\frac{1}{2}(\text{Im } \lambda_3 - \text{Im } \sigma_3)(2\pi)^d \delta(\sum p)$
$\phi_d \phi_a^2$	$(-i)(\text{Re } \lambda_3 + \text{Re } \sigma_3)(2\pi)^d \delta(\sum p)$
$\phi_d^4$	$\frac{1}{8}(\text{Im } \lambda_4 - 4 \text{ Im } \sigma_4 - 3\lambda_\Delta)(2\pi)^d \delta(\sum p)$
$\phi_a^4$	$2(\text{Im } \lambda_4 + 4 \text{ Im } \sigma_4 - 3\lambda_\Delta)(2\pi)^d \delta(\sum p)$
$\phi_d^3 \phi_a$	$\frac{(-i)}{4}(\text{Re } \lambda_4 - 2 \text{ Re } \sigma_4)(2\pi)^d \delta(\sum p)$
$\phi_d \phi_a^3$	$(-i)(\text{Re } \lambda_4 + 2 \text{ Re } \sigma_4)(2\pi)^d \delta(\sum p)$
$\phi_d^2 \phi_a^2$	$\frac{1}{2}(\text{Im } \lambda_4 + \lambda_\Delta)(2\pi)^d \delta(\sum p)$

## D.1 Beta functions for the mass terms

In order to compute the beta functions of the masses  $\text{Re } m^2$ ,  $\text{Im } m^2$  and  $m_\Delta^2$ , we need to compute three different correlators. As usual, we omit all the finite terms which are irrelevant for beta function computation.

We have chosen the following three correlators:

### D.1.1 $\phi_a^2$ vertex

First we consider  $\phi_a \rightarrow \phi_a$  via  $\phi_a^2$  vertex. There are three divergent one loop contribution, as depicted in the first row of the figure 34. The total contribution is given by

$$\begin{aligned}
& 2(\text{Im } m^2 - m_\Delta^2) + (2 \text{ diagrams}) \times 2(\text{Im } \lambda_3 + 3 \text{ Im } \sigma_3) \\
& \quad \times (-i)(\text{Re } \lambda_3 + \text{Re } \sigma_3) \frac{i}{2(4\pi)^2} \left( \frac{2}{d-4} + \ln \frac{1}{4\pi e^{-\gamma_E}} \right) \\
& \quad + 2(\text{Im } \lambda_4 + 4 \text{ Im } \sigma_4 - 3\lambda_\Delta) \frac{\text{Re } m^2}{2(4\pi)^2} \left( \frac{2}{d-4} + \ln \frac{1}{4\pi e^{-\gamma_E}} \right)
\end{aligned} \tag{D.1}$$

where, the first term is from tree level contribution and the rest are from loop level. Thus, from equation (D.1), the beta function for  $(\text{Im } m^2 - m_\Delta^2)$  is given by




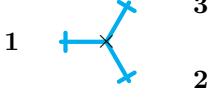
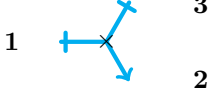
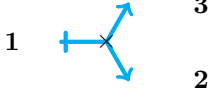
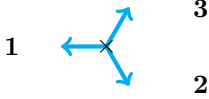





$$\frac{d}{d \ln \mu} (\text{Im } m^2 - m_\Delta^2) = \frac{2}{(4\pi)^2} (\text{Im } \lambda_3 + 3 \text{ Im } \sigma_3) (\text{Re } \lambda_3 + \text{Re } \sigma_3) + \frac{\text{Re } m^2}{(4\pi)^2} (\text{Im } \lambda_4 + 4 \text{ Im } \sigma_4 - 3\lambda_\Delta) \tag{D.2}$$

### D.1.2 $\phi_a \phi_d$ vertex

Next we consider  $\phi_a \rightarrow \phi_a$  via  $\phi_a \phi_d$  vertex. It has same divergent diagrams as that of (D.1), but with different vertex factors. The corresponding Feynman diagrams are depicted in the second row of the figure 34. The total contribution is given by

$$\begin{aligned}
& (-i)\text{Re } m^2 + (-i)(\text{Re } \lambda_3 + \text{Re } \sigma_3) \times (-i)(\text{Re } \lambda_3 + \text{Re } \sigma_3) \frac{i}{2(4\pi)^2} \left( \frac{2}{d-4} + \ln \frac{1}{4\pi e^{-\gamma_E}} \right) \\
& \quad + 2(\text{Im } \lambda_3 + 3 \text{ Im } \sigma_3) \times \frac{1}{2}(\text{Im } \lambda_3 - \text{Im } \sigma_3) \frac{i}{2(4\pi)^2} \left( \frac{2}{d-4} + \ln \frac{1}{4\pi e^{-\gamma_E}} \right) \\
& \quad + (-i)(\text{Re } \lambda_4 + 2 \text{ Re } \sigma_4) \frac{\text{Re } m^2}{2(4\pi)^2} \left( \frac{2}{d-4} + \ln \frac{1}{4\pi e^{-\gamma_E}} \right)
\end{aligned} \tag{D.3}$$



		
$2(\text{Im } m^2 - m_\Delta^2)$	$(-i)\text{Re } m^2$	$\frac{1}{2}(\text{Im } m^2 + m_\Delta^2)$
		
$2(\text{Im } \lambda_3 + 3 \text{Im } \sigma_3)$	$(-i)(\text{Re } \lambda_3 + \text{Re } \sigma_3)$	$\frac{1}{2}(\text{Im } \lambda_3 - \text{Im } \sigma_3)$
		
	$\frac{-i}{4}(\text{Re } \lambda_3 - 3 \text{Re } \sigma_3)$	
		
$2(\text{Im } \lambda_4 + 4 \text{Im } \sigma_4 - 3\lambda_\Delta)$	$(-i)(\text{Re } \lambda_4 + 2 \text{Re } \sigma_4)$	$\frac{1}{2}(\text{Im } \lambda_4 + \lambda_\Delta)$
		
$\frac{(-i)}{4}(\text{Re } \lambda_4 - 2 \text{Re } \sigma_4)$	$\frac{1}{8}(\text{Im } \lambda_4 - 4 \text{Im } \sigma_4 - 3\lambda_\Delta)$	

**Figure 33:** Feynman rules in the average-difference basis

Again, the first term is the tree level and the rest are the one loop contributions. Thus, from (D.3) the beta function for  $(\text{Re } m^2)$  is as follows

$$\begin{aligned} \frac{d}{d \ln \mu} \text{Re } m^2 &= \frac{1}{(4\pi)^2} (\text{Re } \lambda_3 + \text{Re } \sigma_3)^2 - \frac{1}{(4\pi)^2} (\text{Im } \lambda_3 + 3 \text{Im } \sigma_3)(\text{Im } \lambda_3 - \text{Im } \sigma_3) \\ &\quad + \frac{\text{Re } m^2}{(4\pi)^2} (\text{Re } \lambda_4 + 2 \text{Re } \sigma_4) \end{aligned} \quad (\text{D.4})$$

### D.1.3 $\phi_d^2$ vertex

The Feynman diagrams for  $\phi_a \rightarrow \phi_a$  via  $\phi_d^2$  vertex are depicted in the third row of the figure 34. The tree level and one loop contributions are given by

$$\begin{aligned} & \frac{1}{2}(\text{Im } m^2 + m_\Delta^2) + (2 \text{ diagrams}) \times \frac{1}{2}(\text{Im } \lambda_3 - \text{Im } \sigma_3) \\ & \quad \times (-i)(\text{Re } \lambda_3 + \text{Re } \sigma_3) \frac{i}{2(4\pi)^2} \left( \frac{2}{d-4} + \ln \frac{1}{4\pi e^{-\gamma_E}} \right) \\ & \quad + \frac{1}{2}(\text{Im } \lambda_4 + \lambda_\Delta) \frac{\text{Re } m^2}{2(4\pi)^2} \left( \frac{2}{d-4} + \ln \frac{1}{4\pi e^{-\gamma_E}} \right) \end{aligned} \quad (\text{D.5})$$

From this equation we obtain the beta function for  $(\text{Im } m^2 + m_\Delta^2)$

$$\frac{d}{d\ln \mu}(\text{Im } m^2 + m_\Delta^2) = \frac{2}{(4\pi)^2}(\text{Im } \lambda_3 - \text{Im } \sigma_3)(\text{Re } \lambda_3 + \text{Re } \sigma_3) + \frac{\text{Re } m^2}{(4\pi)^2}(\text{Im } \lambda_4 + \lambda_\Delta) \quad (\text{D.6})$$

### D.1.4 Final $\beta$ function

The beta functions of  $m^2$  ( $= \text{Re } m^2 + i \text{Im } m^2$ ) and  $m_\Delta^2$  can be obtained from the equations (D.2), (D.4) and (D.6)

$$\begin{aligned} \frac{dm^2}{d\ln \mu} &= \frac{1}{(4\pi)^2}(\lambda_3 + \sigma_3^*)(\lambda_3 + \sigma_3 + 2i \text{Im } \sigma_3) + \frac{m^2}{(4\pi)^2}[\lambda_4 + 2\sigma_4 - i\lambda_\Delta] \\ \frac{dm_\Delta^2}{d\ln \mu} &= -\frac{4}{(4\pi)^2}\text{Im } \sigma_3 (\text{Re } \lambda_3 + \text{Re } \sigma_3) + \frac{2}{(4\pi)^2}\text{Re}[m^2(\lambda_\Delta + i\sigma_4)] \end{aligned} \quad (\text{D.7})$$

## D.2 Beta functions for the cubic couplings

We have four cubic coupling constants and the corresponding vertices are  $\phi_a^3$ ,  $\phi_a^2\phi_d$ ,  $\phi_a\phi_d^2$ ,  $\phi_d^3$  and we need to compute four correlators. In each case, we will keep only the divergent parts as before.

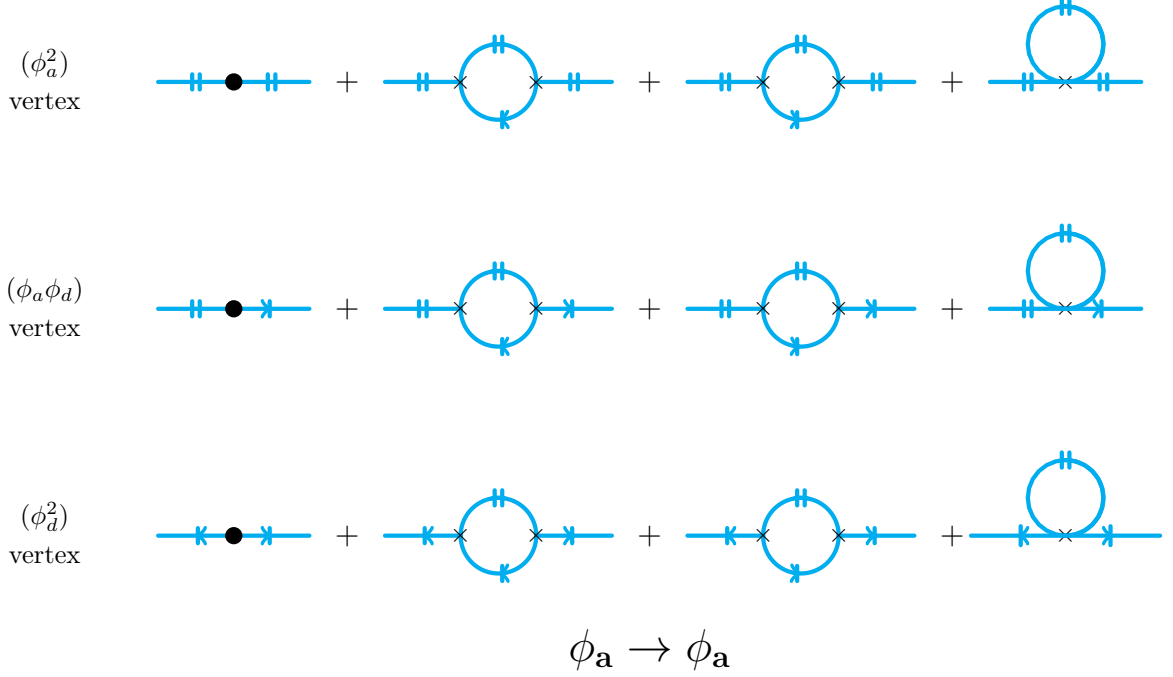
### D.2.1 $\phi_a^3$ vertex

The tree level and one loop Feynman diagram for  $\phi_d \rightarrow \phi_d\phi_d$  via  $\phi_a^3$  vertex is depicted in the first row of the figure 35. These contributions are given by

$$\begin{aligned} & 2(\text{Im } \lambda_3 + 3 \text{Im } \sigma_3) \\ & \quad + (3 \text{ channels}) \times 2(\text{Im } \lambda_3 + 3 \text{Im } \sigma_3) \times (-i)(\text{Re } \lambda_4 + 2 \text{Re } \sigma_4) \times \frac{i}{2(4\pi)^2} \left( \frac{2}{d-4} + \ln \frac{1}{4\pi e^{-\gamma_E}} \right) \\ & \quad + (3 \text{ channels}) \times 2(\text{Im } \lambda_4 + 4 \text{Im } \sigma_4 - 3\lambda_\Delta) \times (-i)(\text{Re } \lambda_3 + \text{Re } \sigma_3) \times \frac{i}{2(4\pi)^2} \left( \frac{2}{d-4} + \ln \frac{1}{4\pi e^{-\gamma_E}} \right) \end{aligned} \quad (\text{D.8})$$

and from this equation we determine the beta function for  $\text{Im } \lambda_3 + 3 \text{Im } \sigma_3$

$$\begin{aligned} \frac{d}{d\ln \mu}(\text{Im } \lambda_3 + 3 \text{Im } \sigma_3) &= \frac{3}{(4\pi)^2}(\text{Im } \lambda_3 + 3 \text{Im } \sigma_3)(\text{Re } \lambda_4 + 2 \text{Re } \sigma_4) \\ & \quad + \frac{3}{(4\pi)^2}(\text{Im } \lambda_4 + 4 \text{Im } \sigma_4 - 3\lambda_\Delta)(\text{Re } \lambda_3 + \text{Re } \sigma_3) \end{aligned} \quad (\text{D.9})$$



**Figure 34:** Mass renormalization in the average-difference basis

### D.2.2 $\phi_a^2 \phi_d$ vertex

Now we compute  $\phi_d \rightarrow \phi_a \phi_a$  via  $\phi_a^2 \phi_d$  vertex. The relevant tree level and one loop Feynman diagrams are shown in the second row of the figure 35 and these contributions are given by

$$\begin{aligned}
& (-i)(\text{Re } \lambda_3 + \text{Re } \sigma_3) \\
& + (3 \text{ diagrams}) \times (-i)(\text{Re } \lambda_3 + \text{Re } \sigma_3) \times (-i)(\text{Re } \lambda_4 + 2 \text{Re } \sigma_4) \times \frac{i}{2(4\pi)^2} \left( \frac{2}{d-4} + \ln \frac{1}{4\pi e^{-\gamma E}} \right) \\
& + (1 \text{ diagram}) \times 2(\text{Im } \lambda_4 + 4 \text{Im } \sigma_4 - 3\lambda_\Delta) \times \frac{1}{2}(\text{Im } \lambda_3 - \text{Im } \sigma_3) \times \frac{i}{2(4\pi)^2} \left( \frac{2}{d-4} + \ln \frac{1}{4\pi e^{-\gamma E}} \right) \\
& + (2 \text{ diagram}) \times \frac{1}{2}(\text{Im } \lambda_4 + \lambda_\Delta) \times 2(\text{Im } \lambda_3 + 3 \text{Im } \sigma_3) \times \frac{i}{2(4\pi)^2} \left( \frac{2}{d-4} + \ln \frac{1}{4\pi e^{-\gamma E}} \right)
\end{aligned} \tag{D.10}$$

This implies that the beta function for  $(\text{Re } \lambda_3 + \text{Re } \sigma_3)$  is given by

$$\begin{aligned}
\frac{d}{d \ln \mu} (\text{Re } \lambda_3 + \text{Re } \sigma_3) &= \frac{3}{(4\pi)^2} (\text{Re } \lambda_3 + \text{Re } \sigma_3) (\text{Re } \lambda_4 + 2 \text{Re } \sigma_4) \\
& - \frac{1}{(4\pi)^2} (\text{Im } \lambda_4 + 4 \text{Im } \sigma_4 - 3\lambda_\Delta) (\text{Im } \lambda_3 - \text{Im } \sigma_3) \\
& - \frac{2}{(4\pi)^2} (\text{Im } \lambda_4 + \lambda_\Delta) (\text{Im } \lambda_3 + 3 \text{Im } \sigma_3)
\end{aligned} \tag{D.11}$$

### D.2.3 $\phi_a\phi_d^2$ vertex

The contribution (upto one loop) to  $\phi_a \rightarrow \phi_a\phi_a$  via  $\phi_a\phi_d^2$  vertex is given by

$$\begin{aligned}
& \frac{1}{2}(\text{Im } \lambda_3 - \text{Im } \sigma_3) \\
& + (3 \text{ diagrams}) \times (-i)(\text{Re } \lambda_3 + \text{Re } \sigma_3) \times \frac{1}{2}(\text{Im } \lambda_4 + \lambda_\Delta) \times \frac{i}{2(4\pi)^2} \left( \frac{2}{d-4} + \ln \frac{1}{4\pi e^{-\gamma_E}} \right) \\
& + (2 \text{ diagrams}) \times (-i)(\text{Re } \lambda_4 + 2 \text{Re } \sigma_4) \times \frac{1}{2}(\text{Im } \lambda_3 - \text{Im } \sigma_3) \times \frac{i}{2(4\pi)^2} \left( \frac{2}{d-4} + \ln \frac{1}{4\pi e^{-\gamma_E}} \right) \\
& + \frac{(-i)}{4}(\text{Re } \lambda_4 - 2 \text{Re } \sigma_4) \times 2(\text{Im } \lambda_3 + 3 \text{Im } \sigma_3) \times \frac{i}{2(4\pi)^2} \left( \frac{2}{d-4} + \ln \frac{1}{4\pi e^{-\gamma_E}} \right)
\end{aligned} \tag{D.12}$$

The corresponding Feynman diagram can be found in the third row of the figure 35. Hence the beta function for  $(\text{Im } \lambda_3 - \text{Im } \sigma_3)$  is as follows

$$\begin{aligned}
\frac{d}{d\ln \mu}(\text{Im } \lambda_3 - \text{Im } \sigma_3) &= \frac{3}{(4\pi)^2}(\text{Re } \lambda_3 + \text{Re } \sigma_3)(\text{Im } \lambda_4 + \lambda_\Delta) \\
& + \frac{2}{(4\pi)^2}(\text{Re } \lambda_4 + 2 \text{Re } \sigma_4)(\text{Im } \lambda_3 - \text{Im } \sigma_3) \\
& + \frac{1}{(4\pi)^2}(\text{Re } \lambda_4 - 2 \text{Re } \sigma_4)(\text{Im } \lambda_3 + 3 \text{Im } \sigma_3)
\end{aligned} \tag{D.13}$$

### D.2.4 $\phi_d^3$ vertex

The tree level and the one loop Feynman diagrams for  $\phi_a \rightarrow \phi_a\phi_a$  via  $\phi_d^3$  vertex is depicted in the fourth row of the figure 35 and the contribution from these diagrams are given by

$$\begin{aligned}
& \frac{-i}{4}(\text{Re } \lambda_3 - 3 \text{Re } \sigma_3) \\
& + (3 \text{ channels}) \times (-i)(\text{Re } \lambda_3 + \text{Re } \sigma_3) \times \frac{(-i)}{4}(\text{Re } \lambda_4 - 2 \text{Re } \sigma_4) \times \frac{i}{2(4\pi)^2} \left( \frac{2}{d-4} + \ln \frac{1}{4\pi e^{-\gamma_E}} \right) \\
& + (3 \text{ channels}) \times \frac{1}{2}(\text{Im } \lambda_4 + \lambda_\Delta) \times \frac{1}{2}(\text{Im } \lambda_3 - \text{Im } \sigma_3) \times \frac{i}{2(4\pi)^2} \left( \frac{2}{d-4} + \ln \frac{1}{4\pi e^{-\gamma_E}} \right)
\end{aligned} \tag{D.14}$$

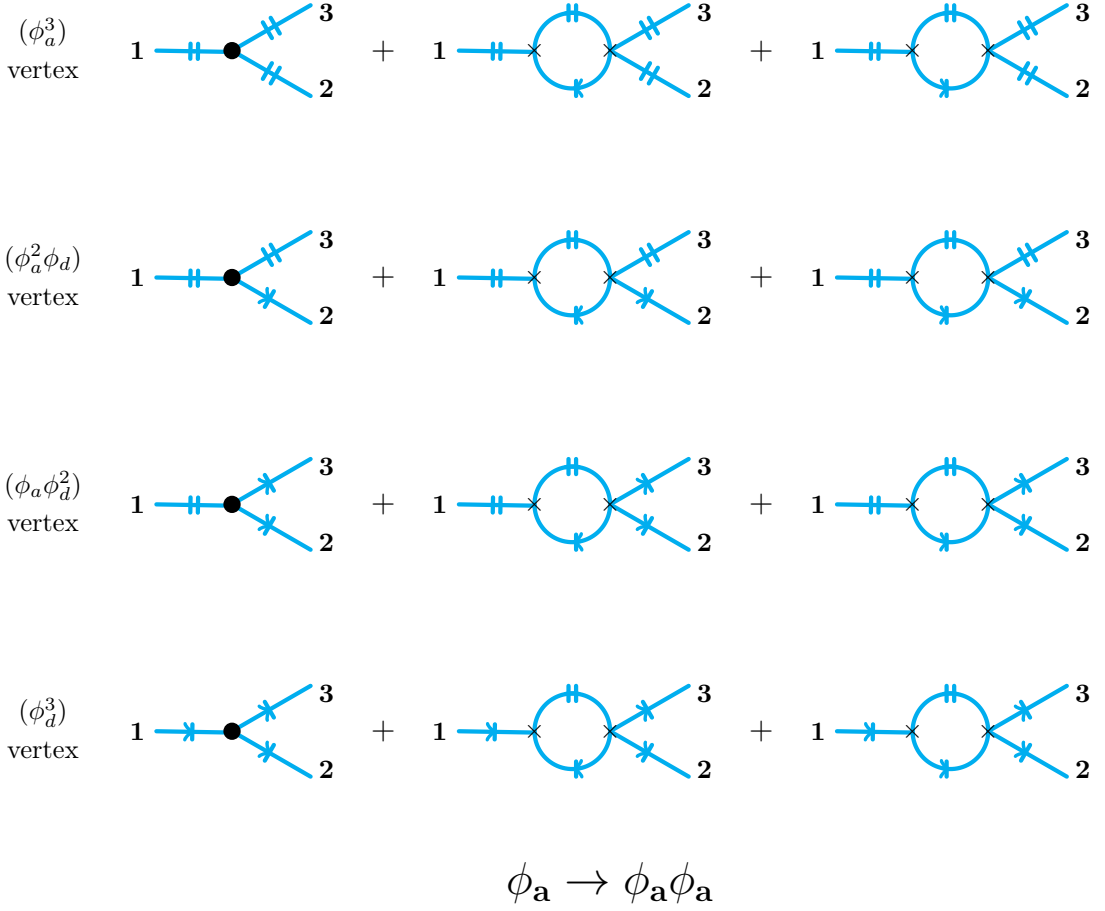
which leads to the following beta function for  $(\text{Re } \lambda_3 - 3 \text{Re } \sigma_3)$

$$\begin{aligned}
\frac{d}{d\ln \mu}(\text{Re } \lambda_3 - 3 \text{Re } \sigma_3) &= \frac{3}{(4\pi)^2}(\text{Re } \lambda_3 + \text{Re } \sigma_3)(\text{Re } \lambda_4 - 2 \text{Re } \sigma_4) \\
& - \frac{3}{(4\pi)^2}(\text{Im } \lambda_4 + \lambda_\Delta)(\text{Im } \lambda_3 - \text{Im } \sigma_3)
\end{aligned} \tag{D.15}$$

### D.2.5 Final $\beta$ function

From the equations (D.9), (D.11), (D.13) and (D.15) we can compute the beta functions of  $\lambda_3$ ,  $\sigma_3$

$$\begin{aligned}
\frac{d\lambda_3}{d\ln \mu} &= \frac{3}{(4\pi)^2} \left[ \lambda_4(\lambda_3 + \sigma_3) + \sigma_4(\lambda_3 + \sigma_3^*) + i\lambda_\Delta(\sigma_3 - \sigma_3^*) \right] \\
\frac{d\sigma_3}{d\ln \mu} &= \frac{1}{(4\pi)^2} \left[ (\lambda_4 + 2\sigma_4^*)(\sigma_3 - \sigma_3^*) + \sigma_4(\lambda_3^* + 2\lambda_3 + 3\sigma_3) - i\lambda_\Delta(\lambda_3^* + 2\lambda_3 + 3\sigma_3^*) \right]
\end{aligned} \tag{D.16}$$



**Figure 35:** Renormalization of the cubic couplings in the average-difference basis

### D.3 Beta functions for the quartic couplings

In this subsection we compute the beta functions for the quartic couplings in the average-difference basis. There are five different quartic coupling constants: these are the coupling constants multiplying the operators  $\phi_a^4$ ,  $\phi_a^3\phi_d$ ,  $\phi_a^2\phi_d^2$ ,  $\phi_a\phi_d^3$ ,  $\phi_d^4$ . For all these couplings there are two distinct divergent diagrams (similar to the cubic coupling constants). As in the last subsection, we keep only the divergent terms from the one loop contributions.

#### D.3.1 $\phi_a^4$ vertex

We start by computing  $\phi_d\phi_d \rightarrow \phi_d\phi_d$  via  $\phi_a^4$  vertex. The Feynman diagrams are depicted in the first row of the figure 36 and the corresponding contributions are given by

$$\begin{aligned}
& 2(\text{Im } \lambda_4 + 4 \text{Im } \sigma_4 - 3\lambda_\Delta) \\
& + (2 \text{ diagrams})(3 \text{ channels}) \times 2(\text{Im } \lambda_4 + 4 \text{Im } \sigma_4 - 3\lambda_\Delta) \\
& \times (-i)(\text{Re } \lambda_4 + 2 \text{Re } \sigma_4) \times \frac{i}{2(4\pi)^2} \left( \frac{2}{d-4} + \ln \frac{1}{4\pi e^{-\gamma_E}} \right)
\end{aligned} \tag{D.17}$$

Thus the beta function for  $(\text{Im } \lambda_4 + 4 \text{ Im } \sigma_4 - 3\lambda_\Delta)$  is given by

$$\frac{d}{d\ln \mu}(\text{Im } \lambda_4 + 4 \text{ Im } \sigma_4 - 3\lambda_\Delta) = \frac{6}{(4\pi)^2}(\text{Im } \lambda_4 + 4 \text{ Im } \sigma_4 - 3\lambda_\Delta)(\text{Re } \lambda_4 + 2\text{Re } \sigma_4) \quad (\text{D.18})$$

### D.3.2 $\phi_a^3\phi_d$ vertex

Next we compute  $\phi_d\phi_d \rightarrow \phi_a\phi_d$  via  $\phi_a^3\phi_d$  vertex, which is depicted in the second row of the figure 36. The tree level and one loop contributions from these Feynman diagrams are given by

$$\begin{aligned} \frac{d}{d\ln \mu}(\text{Re } \lambda_4 + 2 \text{ Re } \sigma_4) &+ (3 \text{ channels}) \times 2(\text{Im } \lambda_4 + 4 \text{ Im } \sigma_4 - 3\lambda_\Delta) \\ &\times \frac{1}{2}(\text{Im } \lambda_4 + \lambda_\Delta) \times \frac{i}{2(4\pi)^2} \left( \frac{2}{d-4} + \ln \frac{1}{4\pi e^{-\gamma_E}} \right) \\ &+ (3 \text{ channels}) \times (-i)(\text{Re } \lambda_4 + 2 \text{ Re } \sigma_4) \\ &\times (-i)(\text{Re } \lambda_4 + 2 \text{ Re } \sigma_4) \times \frac{i}{2(4\pi)^2} \left( \frac{2}{d-4} + \ln \frac{1}{4\pi e^{-\gamma_E}} \right) \end{aligned} \quad (\text{D.19})$$

we can determine the beta function for  $(\text{Re } \lambda_4 + 2 \text{ Re } \sigma_4)$  -

$$\frac{d}{d\ln \mu}(\text{Re } \lambda_4 + 2 \text{ Re } \sigma_4) = \frac{3}{(4\pi)^2} \left[ (\text{Re } \lambda_4 + 2 \text{ Re } \sigma_4)^2 - (\text{Im } \lambda_4 + 4 \text{ Im } \sigma_4 - 3\lambda_\Delta)(\text{Im } \lambda_4 + \lambda_\Delta) \right] \quad (\text{D.20})$$

### D.3.3 $\phi_a^2\phi_d^2$ vertex

The tree level and one loop Feynman diagrams for  $\phi_a\phi_a \rightarrow \phi_a\phi_a$  via  $\phi_a^2\phi_d^2$  vertex, which is depicted in the third row of the figure 36, contributes as follows

$$\begin{aligned} &\frac{1}{2}(\text{Im } \lambda_4 + \lambda_\Delta) \\ &+ (3 \text{ channels}) \times \frac{1}{2}(\text{Im } \lambda_4 + \lambda_\Delta) \times (-i)(\text{Re } \lambda_4 + 2 \text{ Re } \sigma_4) \times \frac{i}{2(4\pi)^2} \left( \frac{2}{d-4} + \ln \frac{1}{4\pi e^{-\gamma_E}} \right) \\ &+ (2 \text{ channels}) \times \frac{1}{2}(\text{Im } \lambda_4 + \lambda_\Delta) \times (-i)(\text{Re } \lambda_4 + 2 \text{ Re } \sigma_4) \times \frac{i}{2(4\pi)^2} \left( \frac{2}{d-4} + \ln \frac{1}{4\pi e^{-\gamma_E}} \right) \\ &+ 2(\text{Im } \lambda_4 + 4 \text{ Im } \sigma_4 - 3\lambda_\Delta) \times \frac{(-i)}{4}(\text{Re } \lambda_4 - 2 \text{ Re } \sigma_4) \times \frac{i}{2(4\pi)^2} \left( \frac{2}{d-4} + \ln \frac{1}{4\pi e^{-\gamma_E}} \right) \end{aligned} \quad (\text{D.21})$$

From this equation we evaluate the beta function for  $(\text{Im } \lambda_4 + \lambda_\Delta)$ ,

$$\begin{aligned} \frac{d}{d\ln \mu}(\text{Im } \lambda_4 + \lambda_\Delta) &= \frac{1}{(4\pi)^2} \left[ 5(\text{Im } \lambda_4 + \lambda_\Delta)(\text{Re } \lambda_4 + 2 \text{ Re } \sigma_4) \right. \\ &\left. + (\text{Im } \lambda_4 + 4 \text{ Im } \sigma_4 - 3\lambda_\Delta)(\text{Re } \lambda_4 - 2 \text{ Re } \sigma_4) \right] \end{aligned} \quad (\text{D.22})$$

### D.3.4 $\phi_a\phi_d^3$ vertex

Here we determine the tree level and one loop contribution to  $\phi_a\phi_a \rightarrow \phi_a\phi_a$  via  $\phi_a\phi_d^3$  vertex. The Feynman diagrams can be found in the fourth row in figure 36 and the corresponding

contributions are

$$\begin{aligned}
& \frac{(-i)}{4}(\text{Re } \lambda_4 - 2 \text{ Re } \sigma_4) \\
& + (3 \text{ channels}) \times \frac{1}{2}(\text{Im } \lambda_4 + \lambda_\Delta) \times \frac{1}{2}(\text{Im } \lambda_4 + \lambda_\Delta) \times \frac{i}{2(4\pi)^2} \left( \frac{2}{d-4} + \ln \frac{1}{4\pi e^{-\gamma_E}} \right) \\
& + (3 \text{ channels}) \times \frac{(-i)}{4}(\text{Re } \lambda_4 - 2 \text{ Re } \sigma_4) \\
& \times (-i)(\text{Re } \lambda_4 + 2 \text{ Re } \sigma_4) \times \frac{i}{2(4\pi)^2} \left( \frac{2}{d-4} + \ln \frac{1}{4\pi e^{-\gamma_E}} \right)
\end{aligned} \tag{D.23}$$

The beta function for  $(\text{Re } \lambda_4 - 2 \text{ Re } \sigma_4)$  is given by

$$\frac{d}{d \ln \mu} (\text{Re } \lambda_4 - 2 \text{ Re } \sigma_4) = \frac{3}{(4\pi)^2} \left[ (\text{Re } \lambda_4 - 2 \text{ Re } \sigma_4)(\text{Re } \lambda_4 + 2 \text{ Re } \sigma_4) - (\text{Im } \lambda_4 + \lambda_\Delta)^2 \right] \tag{D.24}$$

### D.3.5 $\phi_d^4$ vertex

The last computation of this section is  $\phi_a \phi_a \rightarrow \phi_a \phi_a$  via  $\phi_d^4$  vertex, which is depicted in the fifth row in figure 36. The tree level and one loop contribution to this process is given by

$$\begin{aligned}
& \frac{1}{8}(\text{Im } \lambda_4 - 4 \text{ Im } \sigma_4 - 3\lambda_\Delta) \\
& + (2 \text{ diagrams})(3 \text{ channels}) \times \frac{1}{2}(\text{Im } \lambda_4 + \lambda_\Delta) \\
& \times \frac{(-i)}{4}(\text{Re } \lambda_4 - 2 \text{ Re } \sigma_4) \times \frac{i}{2(4\pi)^2} \left( \frac{2}{d-4} + \ln \frac{1}{4\pi e^{-\gamma_E}} \right)
\end{aligned} \tag{D.25}$$

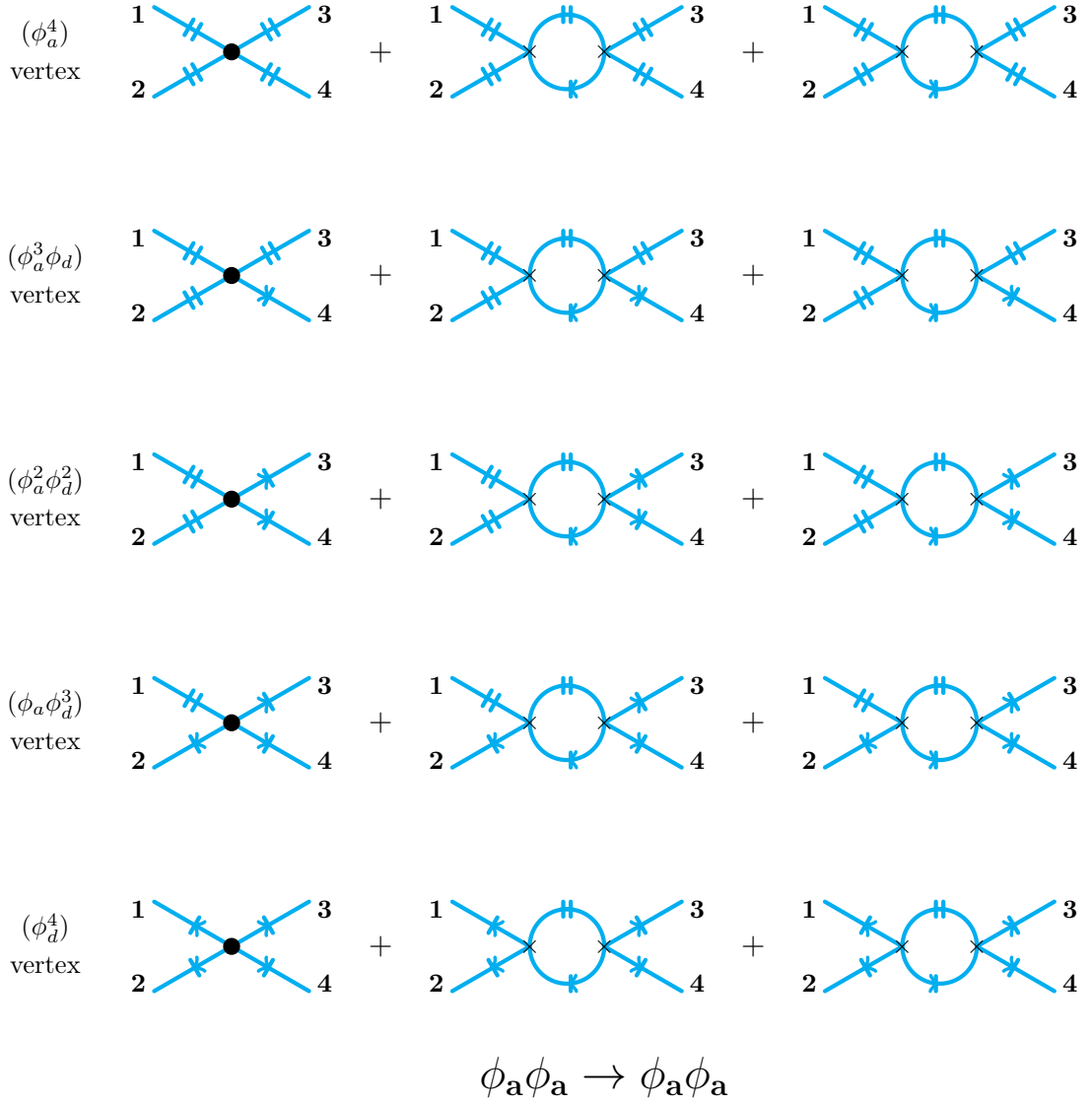
this equation determines the the beta function for  $(\text{Im } \lambda_4 - 4 \text{ Im } \sigma_4 - 3\lambda_\Delta)$  and it is given by

$$\frac{d}{d \ln \mu} (\text{Im } \lambda_4 - 4 \text{ Im } \sigma_4 - 3\lambda_\Delta) = \frac{6}{(4\pi)^2} (\text{Im } \lambda_4 + \lambda_\Delta) \times (\text{Re } \lambda_4 - 2 \text{ Re } \sigma_4) \tag{D.26}$$

### D.3.6 Final $\beta$ functions

From the five equations - (D.18), (D.20), (D.22), (D.24) and (D.26) we can determine the beta functions of  $\lambda_4$  ( $= \text{Re } \lambda_4 + i \text{ Im } \lambda_4$ ),  $\sigma_4$  ( $= \text{Re } \sigma_4 + i \text{ Im } \sigma_4$ ) and  $\lambda_\Delta$  and they are given by

$$\begin{aligned}
\frac{d\lambda_4}{d \ln \mu} &= \frac{3}{(4\pi)^2} \left[ \lambda_4^2 + 2 \sigma_4 (\lambda_4 + i\lambda_\Delta) + \lambda_\Delta^2 \right] = \frac{3}{(4\pi)^2} (\lambda_4 + 2 \sigma_4 - i\lambda_\Delta) (\lambda_4 + i\lambda_\Delta) \\
\frac{d\sigma_4}{d \ln \mu} &= \frac{3}{(4\pi)^2} \left[ \sigma_4^2 + (\lambda_4 + \sigma_4^*) (\sigma_4 - i\lambda_\Delta) + \lambda_\Delta^2 \right] = \frac{3}{(4\pi)^2} (\lambda_4 + \sigma_4 + \sigma_4^* + i\lambda_\Delta) (\sigma_4 - i\lambda_\Delta) \\
\frac{d\lambda_\Delta}{d \ln \mu} &= \frac{1}{(4\pi)^2} i \left[ \lambda (\sigma_4^* + i\lambda_\Delta) - 2\sigma_4^2 + 5i\sigma_4\lambda_\Delta - \lambda_4^* (\sigma_4 - i\lambda_\Delta) + 2(\sigma_4^*)^2 + 5i\sigma_4^*\lambda_\Delta \right] \\
&= \frac{1}{(4\pi)^2} i \left[ (\lambda_4 + 2\sigma_4^*) (\sigma_4^* + i\lambda_\Delta) + 3i\sigma_4\lambda_\Delta - c.c. \right]
\end{aligned} \tag{D.27}$$



**Figure 36:** Renormalization of the quartic couplings in the average-difference basis

## E Tadpoles

In this appendix we compute various one loop tadpoles in this theory.

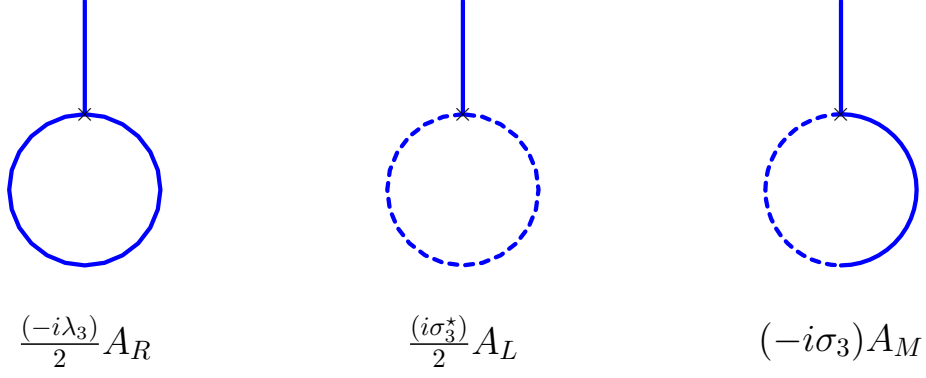
**$\phi_{\mathbf{R}}$  1 loop tadpole** The Feynman diagrams contributing to one loop tadpole of  $\phi_{\mathbf{R}}$  is being drawn in figure 37. The sum of the contribution from all the Feynman diagrams is given by

$$i\mathcal{M} = +\frac{(-i\lambda_3)}{2}A_R + \frac{(i\sigma_3^*)}{2}A_L + (-i\sigma_3)A_M \quad (\text{E.1})$$

Now using result from appendix B we get the following divergent contribution

$$= \frac{-i\text{Re } m^2}{(4\pi)^2} \left[ \frac{\lambda_3 - \sigma_3^* + 2\sigma_3}{2} \right] \left( \frac{2}{d-4} + \ln \frac{1}{4\pi\mu^2 e^{-\gamma_E}} \right) \quad (\text{E.2})$$





**Figure 37:** 1 loop tadpole to  $\phi_R$

This can be removed a counter-term of the form

$$\kappa = \frac{-i \text{Re } m^2}{(4\pi)^2} \left[ \frac{\text{Re } \lambda_3 + \text{Re } \sigma_3 + i(\text{Im } \lambda_3 + 3 \text{Im } \sigma_3)}{2} \right] \left( \frac{2}{d-4} + \ln \frac{1}{4\pi\mu^2 e^{-\gamma_E}} \right) \quad (\text{E.3})$$

**Checking lindblad condition** Now we want to check whether the counter-terms that were added to remove the tadpoles satisfy the Lindblad condition or not.

$$i[\kappa - \kappa^*] = \frac{-1}{(4\pi)^2} [\text{Im } \lambda_3 + 3 \text{Im } \sigma_3] \left( \frac{2}{d-4} + \ln \frac{1}{4\pi\mu^2 e^{-\gamma_E}} \right) \text{Re } m^2 \quad (\text{E.4})$$

So, the counter-terms obey Lindblad condition if there is no Lindblad violating cubic couplings.

## References

- [1] J. S. Schwinger, “Brownian motion of a quantum oscillator,” *J. Math. Phys.* **2** (1961) 407–432.
- [2] L. V. Keldysh, “Diagram technique for nonequilibrium processes,” *Zh. Eksp. Teor. Fiz.* **47** (1964) 1515–1527. [Sov. Phys. JETP20,1018(1965)].
- [3] R. P. Feynman and F. L. Vernon, Jr., “The Theory of a general quantum system interacting with a linear dissipative system,” *Annals Phys.* **24** (1963) 118–173. [Annals Phys.281,547(2000)].
- [4] F. L. Vernon, Jr., *The theory of a general quantum system interacting with a linear dissipative system*. Dissertation (Ph.D.), California Institute of Technology, 1959.  
[http://thesis.library.caltech.edu/737/1/Vernon\\_fl\\_1959.pdf](http://thesis.library.caltech.edu/737/1/Vernon_fl_1959.pdf).
- [5] R. E. Cutkosky, “Singularities and discontinuities of Feynman amplitudes,” *J. Math. Phys.* **1** (1960) 429–433.
- [6] M. J. G. Veltman, “Unitarity and causality in a renormalizable field theory with unstable particles,” *Physica* **29** (1963) 186–207.
- [7] G. ’t Hooft and M. J. G. Veltman, “Diagrammar,” *NATO Sci. Ser. B* **4** (1974) 177–322.  
<http://cds.cern.ch/record/186259/files/?ln=en>.
- [8] V. Gorini, A. Kossakowski, and E. C. G. Sudarshan, “Completely Positive Dynamical Semigroups of N Level Systems,” *J. Math. Phys.* **17** (1976) 821.
- [9] G. Lindblad, “On the Generators of Quantum Dynamical Semigroups,” *Commun. Math. Phys.* **48** (1976) 119.
- [10] H. P. Breuer and F. Petruccione, *The theory of open quantum systems*. Oxford, UK: Univ. Pr. (2002) 625 p, 2002. <https://global.oup.com/academic/product/the-theory-of-open-quantum-systems-9780198520634?cc=us&lang=en&>.
- [11] U. Weiss, *Quantum Dissipative Systems*. Series in modern condensed matter physics. World Scientific, 2008. <https://books.google.co.in/books?id=4NfnaEsbQq4C>.
- [12] H. Carmichael, *An Open Systems Approach to Quantum Optics: Lectures Presented at the Université Libre de Bruxelles, October 28 to November 4, 1991*. Lecture Notes in Physics Monographs. Springer Berlin Heidelberg, 2009.  
[https://books.google.co.in/books?id=uor\\_CAAAQBAJ](https://books.google.co.in/books?id=uor_CAAAQBAJ).
- [13] Á. Rivas and S. Huelga, *Open Quantum Systems: An Introduction*. SpringerBriefs in Physics. Springer Berlin Heidelberg, 2011. <https://books.google.co.in/books?id=FGCuYsIZAAOC>.
- [14] G. Schaller, *Open Quantum Systems Far from Equilibrium*. Lecture Notes in Physics. Springer International Publishing, 2014. <https://books.google.co.in/books?id=deS5BQAAQBAJ>.
- [15] A. Kamenev, *Field Theory of Non-Equilibrium Systems*. Cambridge University Press, Cambridge, 1985. <http://www.cambridge.org/us/academic/subjects/physics/condensed-matter-physics-nanoscience-and-mesoscopic-physics/field-theory-non-equilibrium-systems?format=HB&isbn=9780521760829>.
- [16] U. Täuber, *Critical Dynamics: A Field Theory Approach to Equilibrium and Non-Equilibrium Scaling Behavior*. Cambridge University Press, 2014. <http://www.cambridge.org/us/academic/subjects/physics/condensed-matter-physics-nanoscience-and-mesoscopic-physics/critical-dynamics-field-theory-approach-equilibrium-and-non-equilibrium-scaling-behavior?format=HB&isbn=9780521842235>.

- [17] R. D. Jordan, “Effective Field Equations for Expectation Values,” *Phys. Rev.* **D33** (1986) 444–454.
- [18] E. Calzetta and B. L. Hu, “Closed Time Path Functional Formalism in Curved Space-Time: Application to Cosmological Back Reaction Problems,” *Phys. Rev.* **D35** (1987) 495.
- [19] S. Weinberg, “Quantum contributions to cosmological correlations,” *Phys. Rev.* **D72** (2005) 043514, [arXiv:hep-th/0506236](https://arxiv.org/abs/hep-th/0506236) [hep-th].
- [20] E. A. Calzetta and B.-L. B. Hu, *Nonequilibrium Quantum Field Theory*. Cambridge University Press, 2008. <http://www.cambridge.org/mw/academic/subjects/physics/theoretical-physics-and-mathematical-physics/nonequilibrium-quantum-field-theory?format=AR>.
- [21] M. Gell-Mann, “The interpretation of the new particles as displaced charge multiplets,” *Nuovo Cim.* **4** no. S2, (1956) 848–866.
- [22] Avinash, C. Jana, R. Loganayagam, and A. Rudra, “ work in progress ”.
- [23] K.-C. Chou, Z.-B. Su, B.-l. Hao, and L. Yu, “Equilibrium and Nonequilibrium Formalisms Made Unified,” *Phys. Rept.* **118** (1985) 1.
- [24] F. M. Haehl, R. Loganayagam, and M. Rangamani, “Schwinger-Keldysh formalism I: BRST symmetries and superspace,” [arXiv:1610.01940](https://arxiv.org/abs/1610.01940) [hep-th].
- [25] A. Kamenev and A. Levchenko, “Keldysh technique and nonlinear sigma-model: Basic principles and applications,” *Adv. Phys.* **58** (2009) 197, [arXiv:0901.3586](https://arxiv.org/abs/0901.3586) [cond-mat.other].
- [26] L. M. Sieberer, M. Buchhold, and S. Diehl, “Keldysh Field Theory for Driven Open Quantum Systems,” *Rept. Prog. Phys.* **79** no. 9, (2016) 096001, [arXiv:1512.00637](https://arxiv.org/abs/1512.00637) [cond-mat.quant-gas].
- [27] F. M. Haehl, R. Loganayagam, P. Narayan, and M. Rangamani, “Classification of out-of-time-order correlators,” [arXiv:1701.02820](https://arxiv.org/abs/1701.02820) [hep-th].
- [28] A. I. Larkin and Y. N. Ovchinnikov, “Quasiclassical method in the theory of superconductivity,” *Sov.Phys.JETP* **28** no. 6, (1969) 1200–1205.
- [29] M. J. G. Veltman, “Diagrammatica: The Path to Feynman rules,” *Cambridge Lect. Notes Phys.* **4** (1994) 1–284.
- [30] R. P. Feynman, “Closed Loop and Tree Diagrams (Talk),”.
- [31] K. Symanzik, “A field theory with computable large-momenta behaviour,” *Lettere al Nuovo Cimento (1971-1985)* **6** no. 2, (1973) 77–80. <http://dx.doi.org/10.1007/BF02788323>.
- [32] D. Poulin and J. Preskill, “Diagrammatics for the field theoretic Lindblad equation,” *Un-published note* (2014) .
- [33] G. ’t Hooft and M. J. G. Veltman, “Scalar One Loop Integrals,” *Nucl. Phys.* **B153** (1979) 365–401.
- [34] G. Passarino and M. J. G. Veltman, “One Loop Corrections for e+ e- Annihilation Into mu+ mu- in the Weinberg Model,” *Nucl. Phys.* **B160** (1979) 151–207.